Tomas Bata University in Zlín
Faculty of Technology

Doctoral Thesis

Epoxy-silicone filled nanocomposites: Study of mechanical and electrical properties.

Nanokompozity na bázi plněného epoxid-silikonu: Studium mechanických a elektrických vlastností.

Author: **Ing. Lenka Kutějová**

Study programme**:** P2808 Chemistry and Materials Technology
2808V006 Technology of Macromolecular Substances

Supervisor: doc. Ing. Jarmila Vilčáková, Ph.D.

Opponents**:** 1. Ing. Mária Omastová, Dr.Sc.
2. Prof. RNDr. Miroslav Raab, CSc.
3. doc. Ing. et Ing. Ivo Kuřitka, Ph.D. et Ph.D.

Zlín, November, 2017

Vydala **Univerzita Tomáše Bati ve Zlíně** v edici **Doctoral Thesis**.
Publikace byla vydána v roce 2017

Klíčová slova: *vícefázový polymerní systém, vodivé kompozity, saze, uhlíkové nanotuby, plniva, fyzikálně- mechanické vlastnost, elektrické vlastnosti.*

Key words: *multiphase polymer system, conductive composites, carbon black, carbon nanotubes, physico-mechanical properties, electrical properties.*

The full version of the Doctoral thesis may be found at the Central Library TBU in Zlín.

ABSTRACT

The work is focused on the modification of the brittle epoxy matrix by silicone elastomer with a view to improve the toughness characteristics without significant reduction of modulus, glass transition temperature and interfacial adhesion, and, to obtain conductive nanocomposites. The emphasis has been put on the preparation technology of epoxy-silicone polymer system with controlled morphology and mechanical properties. To this end, epoxy resins based on diglycidyl ether bisfenol A and different types and content of polydimethylsiloxanes were mixed. Curing was carried out using diethylentriamine hardener and dicumyl peroxides as compatibilizator. These polymer blends were subsequently filled with carbon black or carbon nanotubes to obtain electroconductive systems. It has been established that mechanical properties of such nanocomposites are influenced by the microstructure of the multiphase epoxy-silicone polymer system, which in turn is determined by the presence or absence of interphase compatibility between two polymer phases. The electrical properties of nanocomposites heavily depend on filler aspect ratio, filler content, and, to some extent, on polymer matrix composition. Aforementioned types of conductive materials can be used as conductive adhesives, electromagnetic interference (EMI) isolation materials, antistatic coatings, etc.

SHRNUTÍ

Práce je zaměřena na modifikaci křehké epoxidové matrice silikonovým elastomerem s cílem zlepšit houževnatost bez významného snížení modulu, teploty skelného přechodu a mezifázové adheze a získání elektricky vodivých nanokompozitů. Důraz byl kladen na technologii přípravy epoxid-silikonového polymerního systému s řízenou morfologií a fyzikálně-mechanickými vlastnostmi. Za tímto účelem byla smíchána epoxidová pryskyřice na bázi diglycidyl ether bisphenol A s různým podílem a typy polydimethylsiloxanů. Síťování bylo provedeno za použití diethylentriaminu a dikumyl peroxidu jako kompatibilizátoru. Tyto polymerní směsi byly následně naplněny sazemi nebo uhlíkovými nanotrubkami, aby se získaly elektrovodivé systémy. Bylo zjištěno, že mechanické vlastnosti takových nanokompozitů jsou ovlivňovány mikrostrukturou vícefázového systému epoxid-silikonového polymeru, který je zase určován přítomností nebo nepřítomností mezifázové kompatibility mezi dvěma polymerními fázemi. Elektrické vlastnosti nanokompozitů velmi závisí na štíhlostním poměru plniva, koncentraci plniva a do určité míry na složení

polymerní matrice. Výše uvedené typy vodivých materiálů mohou být použity jako vodivá lepidla, izolační materiály pro elektromagnetickou interferenci (EMI), antistatický povlak, atd.

CONTENTS

ACKNOWLEDGMENTS

I am very grateful to my supervisor Assoc. Prof. Jarmila Vilčáková. I would like to thank Jarmila for her patience, kindness, time, support, encouragement and motivation. I am also grateful to my consultants Assoc. Prof. Natalia Kazantseva, and Dr. Robert Moučka for sharing their professional advice. I would like to thank Prof. Petr Saha, Rector of Tomas Bata University in Zlín for providing excellent facilities for the research activities. I am also pleased to express my gratitude to colleagues from Tomas Bata University in Zlín for their collaboration, especially to Dr. Vladimir Babayan, Dr. Ilona Smolkova.

I would like to thank my mother and father and whole my family for their love and support.

INTRODUCTION

Multiphase polymers systems (MPS) such as polymer blends and polymer composites are of particular interest from both the fundamental point of the view and that of applications. Different properties of the particular components can be combined in such systems. Moreover, new properties not inherent to the components may emerge because of synergy. High resistance to crack growth [1,2,3,] characterizes rubber-modified epoxy resin. To this end, epoxy resin generally can be modified by rubber: natural liquid [4], hydroxyl terminated polybutadiene [5, 6], carboxyl-terminated copolymer of acrylonitrile liquid rubber etc. [7, 8]. When elastomer is added to the uncured epoxy resins and after the cross-linking reactions, the elastomer modified epoxy resins exhibited a two-phase microstructure consisting of relatively small rubber particles dispersed in a matrix of epoxy. This microstructure resulted in the material possessing a higher toughness than the unmodified one with only a minimal reduction in other important properties, such as modulus. As the content to the minor component increases to a critical value the morphology of multicomponent, mixture changes into a co-continuous structure [9]. Generally, the study of cure kinetics of epoxy is usually carried out by calorimetric technique (DSC) and dynamic mechanical analyse (DMA). Moreover, the usage of multiphase polymers systems as a matrix of polymer composites filled with conductive and magnetic fillers can bring the new set of properties (for example, enhanced total conductivity). For instance, the electrical conductivity of composites depends significantly on the geometric parameters of the filler particles (aspect ratio), the quality of their contacts, the interaction between the matrix and the filler as well as on the dispersion state of conductive particles in composites. Different types of filler can influenced the value of electrical percolation threshold, significantly. With increasing, the value of filler aspect ratio is value of percolation threshold shift to lower value. Multiphase systems exploit the structural percolation of one of the phases in the other with percolated phase filled with conductive filler. This due to morphological reasons consequently lowers the required amount of filler i.e. percolation threshold in the multiphase systems compared to a standard filler/matrix composite. Therefore, the formation of conductive network is affected not only by the filler volume fraction, but also by the processing technology and different affinity of filler to each polymer in the system; thus, it is selectively dispersed in one of the two phases [10-11]. For example, the percolation value in such multicomponent system is governed by the percolation of the carbon black (CB) rich phase and

the continuity of this phase in the system.

In current work we introduce methodology that can significantly reduce the percolation threshold and enhance the total conductivity of polymer composites and simultaneously to modify the brittle behaviour of epoxy resin by elastomers and to develop conductive nanocomposites with different types of fillers (nickel, carbon black, carbon nanotubes, carbonyl iron etc.).

1 STATE OF ART

1.1 Conductive polymer composites

Polymer composite is defined as a multicomponent material comprising multiple different (nongaseous) phase domains in which at least one type of phase domain is a continuous phase. Conductive polymer matrix composite (CPC) [12] consists from a nonconductive polymer matrix (with electrical conductivity, $\sigma < 10–11$ S cm^{-1}) and conductive fillers: inorganic (metal) or organic (carbon black, carbon nanotubes, graphene or fullerene). Total electrical conductivity of CPC is affected by: 1) volume fraction of filler, 2) interface between matrix and filler, at which these are chemically and mechanically combined and 3) processing conditions. These materials have many potential applications, including antistatic materials, electrostatic discharge, electromagnetic interference shielding etc. [13].

1.1.1. Polymer matrix

The matrix is a continuous phase in CPC and plays several important roles: it holds the filler in place, acts as a path for stress transfer between fillers, and protects the reinforcements from an adverse environment. The matrix has a major influence on composite processing characteristics. Generally, polymer matrixes are classified as thermoplastic or thermosetting polymers and their blends. Thermoplastics consist of linear or branched chain molecules having strong intramolecular bonds but weak intermolecular bonds. They can be reshaped by application of heat and pressure and are either semicrystalline or amorphous in structure. Examples include polyethylene, polypropylene, polystyrene, nylons, polycarbonate, polyacetals, polyamide-imides, polyether ether ketone, polysulfone, polyphenylene sulfide, polyether imide. Thermosets have cross-linked or network structures with covalent bonds with all molecules. They do not soften but decompose on heating. Once solidified by cross-linking process they cannot be reshaped. Common examples are epoxies, polyesters, phenolics, ureas, melamine resins, and silicone [14]. In this work we used epoxy resin and silicone elastomer as a modifier for preparation of matrix, which was filled with conductive filler commonly and widely used industrial applications.

Epoxy resin

Epoxy resins (ER) are a class of polymers with molecules containing an epoxide group (oxirane) consisting of an oxygen atom attached to two connected

carbon atoms (Fig.1). While the presence of this functional group defines the molecule as an epoxide, the molecular base to which it is attached can vary widely, yielding various classes of epoxy resins.

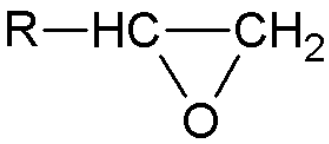

Fig. 1 General structure of epoxy resin

Epoxy resins are produced from base molecules containing an unsaturated carbon-carbon bond. There are two processes that can be used to convert this double bond into an oxirane ring: (i.) dehydrohalogenation of a halohydrin intermediate and (ii.) epoxidation. Epoxy resin has unique properties, such as high strength, excellent adhesion, chemical and solvent resistance, superior dimensional stability, good resistance to heat and electrical properties. However not all properties products of epoxy resin are favourable .Epoxy resin can be devided into 2 groups: a) glycidyl (2,3 – epoxy propyl) which is used extensively in the technologies as filament winding, pultrusion or some adhesives and b) glycidylamine, where the typical reprezentant of group is tetraglycidyl methylene dianiline (TGMDA), also known as tetraglycidyl- 4,4"-diaminodiphenylmethane (TGDDM), which is used for a large number of the commercial an high-tech composite matrix systems in aircraft. In my study I concentrated on ER of glycidyl group - diglycidyl ether of bisphenol – A (DGEBA), which is formed by the alcalic condensation between epichlorhydrin and a phenol group in the presence of sodium hydroxide [15]. Subsequently hydrochloric breaks away while epoxy groups are created, as can be seen in Fig. 2. The most outstanding property of this resin is its excellent adhesion, which is due in part to secondary hydroxyl group located along the molecular chain. The term curing is used to describes the process by which one or more kinds of reactants, i.e., an epoxide and curing agent, are transformed from low molecular weight materials to a highly crosslinked network. The network is composed of segments involving only the epoxide or both the epoxide and the crosslinking agent. The major classes of epoxy curing agents are aliphatic amines [16], acid [17], anhydrides [18], and amines [19].

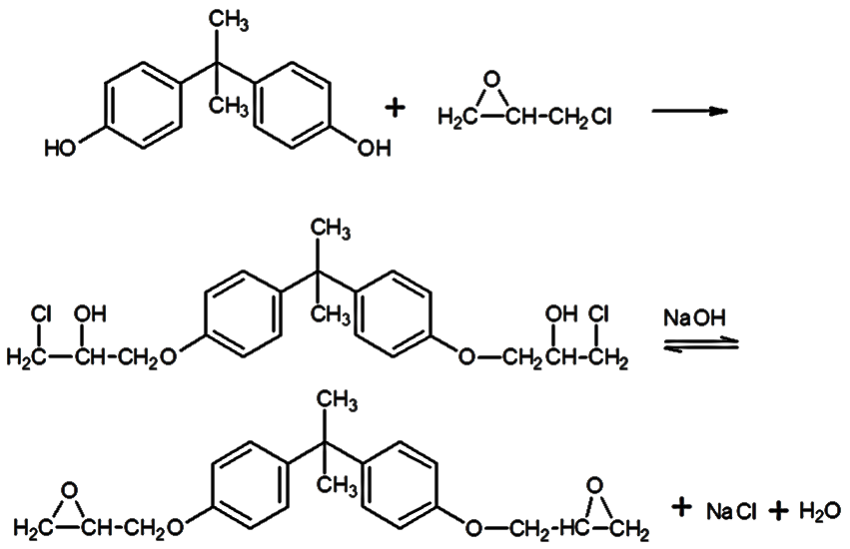

Fig. 2 The synthesis of a bisphenol A based epoxy resin [20]

Aliphatic amines are the hardeners used in adhesive systems capable of curing at normal or slightly elevated temperature. The most widely used aliphatic curing agents are diethylenetriamine (DETA), triethylenetetramine (TETA) and diethylaminopropylamine (DEAPA). Diglycidyl ether bisphenol A and amines are normally used for preparation of composites and cycloaliphatics are used extensively in electrical applications or as a minor epoxy in composite matrix systems. In my study DETA was used as curing agent for epoxy resin composite for its low viscosity, easy mixing, and relatively fast curing at room temperature. Its disadvantages comprise high volatility, toxicity, short pot life and temperature limit of 80°C. The reactivity of the amine increases with its nucleophilic character.

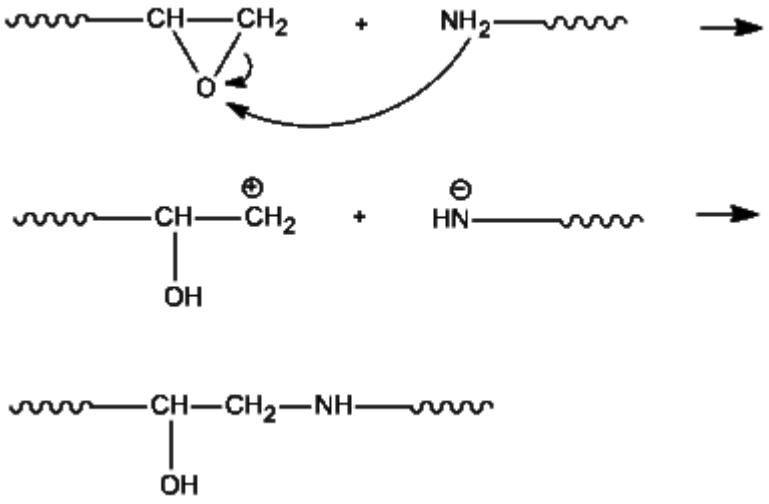

Fig. 3 Scheme of the reaction between an amine and an epoxy resin [18]

The reaction proceeds of the oxirane ring through a nucleophilic addition reaction can we see on Fig.3. During the curing reaction, two epoxy rings react with a primary amine. The amines react with the epoxy group through the active amine hydrogen. Each primary amine group is theoretically capable of reacting with two epoxide groups, and each secondary amine group is capable of reacting with one epoxide group. The curing is a process in which the linear resins in presence of proper hardener of curing agent are converted into three-dimensional thermoset network. In this process, resin and curing agents are mixed together, once this mixing has occurred, a point of no return has been reached, cure begins and proceeds at a rate dependent upon factors such as temperature and reactivates of the resins. The isothermal curing reaction of an epoxy resin is complex as a consequence of the interaction of the chemical curing with other physical processes, such as gelation and vitrification, causing important changes in the physical properties of the reacting system [18]. Gelation is a sudden and irreversible transformation of the system from a viscous liquid to an elastic gel. It corresponds to the incipient formation of an infinite network at the first stage of curing, causing changes in the macroscopic properties of a system. Its occurrence depends on the functionality of the epoxy resin and stoichiometry of the components but not on the experimental conditions such as curing temperature. Vitrification involves a physical transformation from a liquid or rubbery state to a glassy state as a result of an increase in the crosslinking density of the material.

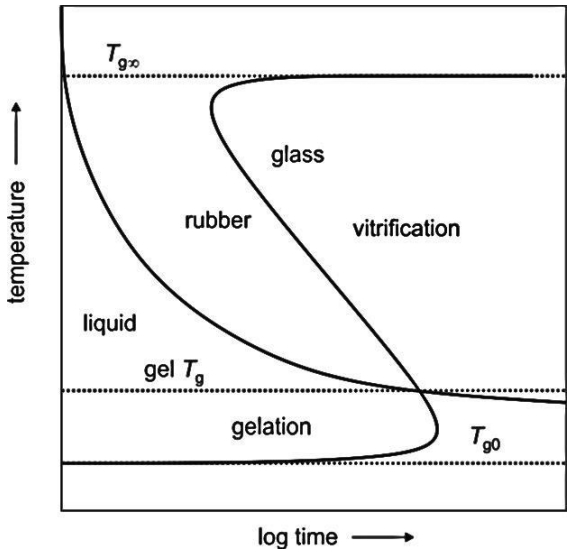

Fig. 4 Schematic TTT curve diagram [21]

This phenomenon occurs when the glass transition temperature (T_g) becomes

equal to the curing temperature (T_c). The vitrification point marks a change in the reaction mechanism passing from chemically, kinetically controlled to diffusion controlled one. From that point the reaction becomes slow and finally stops [19].

The time-temperature-transformation (TTT) isothermal cure diagram introduced and developed by Gillham and co-workers [20] for epoxy systems is based on phenomenological changes that take place during cure, such as gelation and vitrification (Fig. 4). The curing agent, which becomes an integral part of the cured epoxy resin, has a marked effect on its thermal stability. The proper choice of resin and curing agent depends on the application and on their characteristics (viscosity, gel time). The point gelation can be determined by different method based on rheology.

Polysiloxane

Silicones are mixed inorganic–organic polymers with the chemical formula $[R_2SiO]_n$, where R is an organic group such as methyl, ethyl, or phenyl, which are also known as polymerized siloxanes or polysiloxanes. Silicone consists of an inorganic silicon-oxygen backbone chain (…-Si-O-Si-OSi-O-…) with organic side groups attached to the silicon atoms, which are tetravalent. The (-Si O-) repeat unit is called as the "siloxane" bond. Since the polymer backbone is "inorganic" in nature, while the substituents attached to the silicon atom are generally "organic" radicals, silicones form an important bridge between inorganic and organic polymers. Silicones are frequently used for preparation of silicone containing copolymers and silicone-modified networks. High demand of these materials is due to the interesting combination of properties offered, which include extremely high backbone flexibility and very low glass transition temperatures (T_g), around −120 °C, good thermal and oxidative stability, high gas permeability, excellent dielectric properties and physiological inertness or biocompatibility [21-22]. Silicone polymers display an unusual combination of physical and chemical properties when compared with homologous carbon-based polymers. The differences between the atomic radii and the electro negativities of carbon and silicon atoms are the main reasons that lead to the remarkable differences in the physicochemical properties of (-C-O-) and (-Si-O-) bonds. The siloxane bond displays an ionic character due to the large electronegativity difference between silicon and oxygen atoms. At the same time, the siloxane bond has partially double bond character, due to pπ–dπ interaction between the silicon and oxygen atoms. This partial double bond character results in a large bond angle and in reduced energy barrier for the

rotation of the organic groups attached to the silicon atom thus providing substantial flexibility to the silicone polymer backbone. Another very interesting property of the (-Si-O-) bond is its very high bond dissociation energy of 460 kJ/mole, when compared with the (-C-O-) (345 kJ/mole) bond. The double bond character also plays a critical role in such a high bond dissociation energy. Unusual thermal stability of silicone polymers is a direct result of such a high (-Si-O-) bond dissociation energy. The partial ionic nature of the (-Si-O-) bond also provides great flexibility to synthetic chemists for the preparation of a wide range of siloxane backbone compositions through so-called "equilibration" or "redistribution" reactions, using strong acid or base catalysts. One of the major advantages offered by the flexible chemistry of silicone polymers is the possibility of introducing a wide selection of substituents onto the silicon atom in the backbone (Fig. 5). These substituents can be inert, such as methyl, phenyl and 3,3,3-trifluoropropyl or reactive such as vinyl, hydrogen, epoxy or amino groups. For the preparation of silicone containing block copolymers inert backbones are preferred. On the other hand, for crosslinked systems silicone backbones with reactive substituents may be more suitable [23].

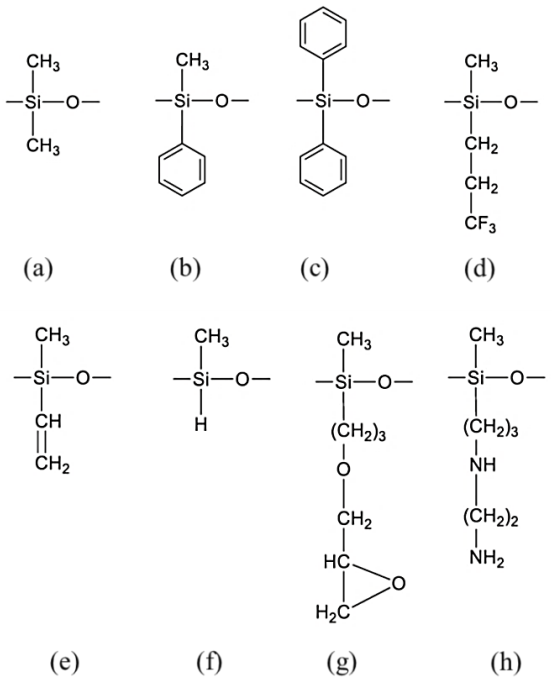

Fig. 5 Chemical structures of some important silicone polymer backbones with non-reactive substituents: (a) dimethylsiloxane, (b) methylphenylsiloxane, (c) diphenylsiloxane, and (d) 3,3,3 trifluoropropylmethylsiloxane. And silicone polymer backbones with chemically reactive substituents: (e) methylvinylsiloxane, (f) methylhydrogensiloxane, (g) methylglycidoxypropylsiloxane, and (h) methylaminosiloxane [24]

Organofunctionally terminated silicone oligomers and silicone containing copolymers are used as impact modifiers for epoxy, novolac and bismaleimide resins [25]. Due to its simple curing chemistry and wide range of applications, most of the work has been carried out on epoxy resin toughening. It is well documented that in order to obtain optimum toughening in epoxy resins, the additive should preferably be miscible with the resin before curing and microphase separate into discrete domains during curing [26]. Although low molecular weight silicones (< 500 g/mole) are miscible, high molecular weight, PDMS is quite immiscible with the epoxy resins. In order to improve the compatibility, functionally terminated PDMS oligomers are first reacted with the epoxy resin before adding the curing agent. For example, hydroxyl terminated PDMS oligomers with molecular weights in 650–24,000 g/mole range were used as modifiers for epoxy resins [27]. As expected modified networks displayed microphase separated morphologies and silicone rich surfaces. Low molecular weight amine terminated silicones were also used as a curing agent and modifier for epoxy resins. Initial mixture and the cured networks were transparent and homogenous. Impact strengths of the networks increased linearly with the amount of silicone additive [28].

1.1.2. Polymer blends

Polymer blends can be divided into three categories: miscible, partially miscible and immiscible. An immiscible polymer blend represents a multiphase system. The reasons for incompatibility are high interfacial tension and poor interfacial adhesion [29]. Generally, one polymer is dispersed in another, and the multicomponent mixture forms a sea-island microstructure. As the content of the minor component increases to a critical value the morphology of multicomponent mixture changes into a co-continuous structure. Utracki [30] defines the polymer blend as a mixture of at least two polymers or copolymers comprising more than 2 wt. % of each macromolecular component. Depending on the sign of the free energy of mixing, the components of the blends are miscible and immiscible. An immiscible polymer blend is associated with positive value of the Gibbs free energy of mixing (eq.1), upper curve. Complete miscibility in a mixture of two polymers requires that the following condition was fulfilled

$$Gm = \Delta H_m - T\Delta S_m < 0 \quad [1]$$

where ΔG_m, ΔH_m and ΔS_m are Gibss free energy, the enthalphy and entropy of mixing at temperature T [K^{-1}]. Miscible polymer blend is homogenous down to the molecular level associated with negative value of the free energy of mixing

and the domain size is comparable to the dimensions of the macromolecular statistical segment. The value of $T\Delta S_m$ is positive since there is increase in the entropy on mixing. Therefore, the sign of ΔG_m depends on the value of the enthalpy of mixing ΔH_m. The polymer pairs mix to form a single phase only if the entropic contribution to free energy exceeds the enthalpic contribution and is valid ($\Delta H_m < T\Delta S_m$). Blends can be classified as either *homogeneous* or *heterogeneous* systems. The homogeneous system can be depicted as a solution with a single phase or single glass-transition temperature (T_g). A heterogeneous blend has both continuous and dispersed phases, each retaining its own distinctive T_g. Until recently, blending was either restricted to polymers that had an inherent physical affinity for each other or else a third component, called a compatibilizer, was employed. These constraints severely limited the types of polymers that could be blend without sacrificing their good physical properties. The incompatible polymers produce a heterogeneous blend with poor physical properties. In details, a system is thermodynamically stable if its formation is accompanied by a decrease ΔG_m, in morphological terms of homogenous domains size is presented. The ΔG_m decreases to a definite equilibrium value, which does not change subsequently with time. Performance of polymer blends depends on the properties of polymer components as well, how they are arranged in space. The mixing of polymers at elevated temperatures and of amorphous polymers can be considered a mixing of two liquids [32]. The polymer blends opens up the possibility of effectively producing advanced multicomponent polymeric matrices with new properties. The properties of polymer blends are intimately tied to their morphology, which depends on the miscibility of the components and the mechanism and kinetics of phase separation. For some applications, phase-separated morphologies are required for improving electrical properties, mechanical properties such as impact toughness, while in other instances, a miscible blend is desired, e.g. for improving processability or extending an expensive material with a cheaper one.

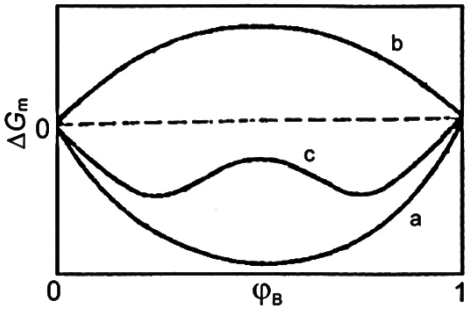

Fig. 6 Plots of Gibbs free energy of mixing (ΔG_m) for a) miscible b) immiscible c) partly miscible blends [31].

For either a single phase or two-phase blend, the development of the optimum morphology and properties requires knowledge of the phase diagram (Fig. 6) and the characteristic of the phase separation process [33]. The interactions between two components of polymer are modelled by a mean field approach. This leads to a relatively simple form for the (excess) Helmholtz free energy ΔF of a bimodal polymer blend (eq. 2):

$$\frac{\Delta F}{kT} = \frac{1}{N_A}\varphi_A \ln\varphi_A + \frac{1}{N_B}\varphi_B \ln\varphi_B + \chi\varphi_A\varphi_B \quad [2]$$

Here, $N_{A,B}$ and $\varphi_{A,B}$ denote the number of segments and the monomer concentration of species A and B, respectively. In the above notation of the ΔF , the monomer concentration φ is to be understood as a segment number density. Flory-Huggins thermodynamic interaction parameter is the γ. One way to describe the interaction between two polymers is through their interaction parameter, $\chi'_{1,2}$. The interaction parameter is a thermodynamic term which encompasses the entropic and enthalpic effects associated with creating a blend. The number of segments interacting with any one segment provides us with a coordination number, *z*. By knowing the coordination number and the strength of interaction between any two segments a and b ($\varepsilon_{a,b}$), we can determine the interaction parameter. Huggins-Flory binary interaction parameter $\chi_{1,2}$ (eq. 3)

$$\chi = \chi_{A,B} = \frac{z(\epsilon_{A,A}+\epsilon_{B,B}-2\epsilon_{A,B})}{2kT} \quad [3]$$

For binary systems the Flory-Huggins equation can be expressed in the following form (eq. 4),

$$\Delta G_m = RT\left(\frac{\varphi_A}{N_A} ln\varphi_A + \frac{\varphi_B}{N_B} ln\varphi_A + \chi\varphi_A\varphi_B\right) \quad [4]$$

where R [$J \cdot K^{-1} \cdot mol^{-1}$] is the universal gas constant, and T [K^{-1}] is the absolute temperature. Miscibility can only be achieved when χ is negative. χ depends on such quantities as temperature, concentration, pressure, molar mass, molar mass distribution of components. For polymers, the miscibility can only be achieved

when $\chi < \chi_c$. The χ parameter at the critical point χ_c is given by (eq.5)

$$\boldsymbol{\chi_c = \frac{1}{2}\left(\frac{1}{\sqrt{N_A}} + \frac{1}{\sqrt{N_B}}\right)^2} \text{ [5]}$$

where N_i is the number of polymer segments (which is proportional to the degree of polymerization) [34]. The polymer blends have been classified into twelve major groups depending on the type of the resin family they are based on polyolefin, styrenic, vinyl, acrylic, elastomeric, polyamide, polycarbonate, poly(oxymethylene), polyphenyleneether, thermoplastic polyester, special polymers, and thermoset blends.

Physical compatibilization methods of multiphase polymer composites

Most polymers are immiscible and need to be compatibilized. Compatibilized blends are characterized by the presence of a finely dispersed phase, good adhesion between blend phases, strong resistance to phase coalescence, and technologically desirable properties [35]. Physical compatibilization includes the addition of pre-synthesized copolymer, block (di-,tri-or tapered) copolymer, graft copolymer, random copolymer, gradient copolymer into the immiscible blend. One of the disadvantages of the physical compatibilization is the tendency of the added copolymers to form micelles, which reduces the compatibilizing efficiency, increases the blend viscosity and may worsen the mechanical properties [36]. Physical compatibilization can be provided by:

1) addition of block and graft copolymer, where significant amounts of the copolymer are expected to locate at the interface between immiscible blend phases, reducing the interfacial tension between blend components, reducing the resistance to minor phase breakup during melt mixing thus reducing the size of the dispersed phase [37-39] or by 2) addition of low molecular weight coupling agents provide compatibilization of polymer blends through copolymer formation. Recent examples of interest in this category include the compatibilization of PPS/PET, PA/PPE, PET/PPE blends by bis(2-oxazolines); PE/PP , PS/PE, PS/EPDM, HIPS/PP , PP/PA , PE/PA [40], blends by peroxides and coagents, PBT/PA66, PA6/PPE, PET/LCP, PET/PA6 , PET/PPE, PET/EVAL blends by multifunctional epoxy monomers; PPE/PA6,6 blends by organosilanes [41]. The use of a low molecular weight reagent or a mixture of low molecular weight coreagents to obtain interfacial reaction between the polymer

components for compatibilization is goal in this work. The purpose of using peroxide in a process of in situ compatibilization of polymers blends is to trigger the polymer modification, taking advantage of the high sensitivity (and reactivity) of polymers to free radicals [42]. Methyl ethyl ketone peroxide, benzoyl peroxide are used as initiators for radical polymerization of some resins, e.g. polyester, epoxy and silicone. Peroxides serve as accelerators, activators, cross-linking agents, curing and vulcanization agents, hardeners and polymerization initiators [43]. Peroxides or azo compounds generate free radicals. These radicals form he active grafting sites on the polymer and then initiate compatibilization of two components [44]. Peroxides are commonly used as the sources of radicals and upon decomposition; they generate free radicals in linear silicones. Peroxides are classified in two classes: (i) vinyl group specific catalyst, (ii) vinyl group non-specific catalysts. The dialkyl ones that are unable to crosslink polydimethylsiloxane (PDMS) if they do not contain any vinyl groups on the chain mainly constitute the first class of peroxides. The second group corresponds to the family of diaroyl peroxides because they can be used to crosslink PDMS with vinyl group. Use of dicumyl peroxide (DCP) as modifier to optimize the properties of epoxy resin modified by silicone elastomer is proposed to be investigated in this work.

Toughness improvement of epoxy resin by rubber

Epoxy resin was toughened by using reactive liquid rubber synthesized by company BF Goodrig Co., USA in 1965. For improvement of epoxy resin properties was used carboxyl terminated butadiene acrylonitrile copolymers (CTBN), amine terminated butadiene acrylonitrile copolymers (ATBN) and hydroxyl terminated butadiene acrylonitrile copolymers (HTBN). Most of the studies were confirmed to CTBN as it provided the ideal morphology needed for effective toughening (Tab. 1). Garina Tripathi et al. [45] have reported the toughening effect of CTBN in ER increases initially very rapidly with increasing CTBN concentration. The fracture energy of modified resins will reach a maximum, and then begin to decrease with further increase in CTBN. Raju Thomas [46] meantioned the critical concentration of CTBN in ER was 15 wt. %. When the CTBN phase attains a level between 20 to 25 wt. %, a state of cocontinuity is attained and further increase in the concentration leads to phase inversion. CTBN has two active hydrogens in its end groups so that the resin underwent chain extension and was precipitated as spherical rubbery particles in a glassy epoxy matrix. ATBN has four active hydrogens hence it acted as an

additional curative and provided a different morphology. Horiuchi [47] mentioned that addition of rubbery materials to epoxy resins enhance their fracture toughness while lowering glass transition temperature (T_g) and thermal and solvent stability. Mathew [48] investigated morphology and mechanical properties of DGEBA with hydroxylated liquid natural rubber.

Tab. 1 Mechanical properties of CTBN and PDMS modified epoxy resin

Modifier [in phr]	Flexural modulus [GMPa]	Modifier [in phr]	Flexural modulus [GMPa]
CTBN (5)	2.69	PDMS (5)	2.29
CTBN (10)	2.23	PDMS (10)	2.42
CTBN (15)	1.63	PDMS (15)	1.51
CTBN (20)	1.61		

The toughening of epoxy resin is an important subject in epoxy technology, where polydimethylsiloxane (PDMS) is uses as a perspective elastomer. As the prevention of macro-phase separation in epoxy and PDMS blends, different methods have been proposed, such as: (a) using silane-based compatibilizer (triethoxysilane, aminosilane), (b) copolymerizing (dimethyl siloxane with diphenyl) siloxane and (c) reactive groups into PDMS chains to bond with epoxy resins (hyperbranched polymers, polyhedral oligomeric) [50]. ER and PDMS blends are initially immiscible; however, chemically bonding of epoxy to the PDMS chain by the reaction between their reactive groups such as hydroxyl, oxirane and amine lead to partial compatibilization. An alternative to this approach is to use of peroxide-initiated functionalization leading to grafting or crosslinking reactions. Procedures that have been used for introducing such active sites include treatment of polymer backbone with an organic compound that is capable of generating radicals. These radicals form the active grafting sites on the polymer and then initiate polymerization of monomer as was presented in [51] for this polymer and this compatibilizator. The modification of silicone are much better for T_g of PDMS that is -120°C compared with around -50°C for CTBN [52]. The maximum level of silicone that could be added was about 15 wt. % beyond this lack of solubility of the hardener in the blend was suspected. The optimum performance was observed at the 10 wt. % level of PDMS, the fracture toughness of modified epoxy resins increases dramatically with only slight reduction in the glass transition temperature and the modulus.

The mechanical properties of modified epoxy resins by PDMS depend on the method of modification [53]. Miwa [54] introduced that volume fraction of silicone rubber particles (5-10 wt. %) and temperature appears to be the most suitable for obtaining a blend with epoxy resin in which the decrease in Young´s modulus and tensile strength is relatively low. Sobhani et al. [61] presented that epoxy modified by hydroxyl – terminated PDMS by 10 % showed the highest value of elongation at break (i.e. 3, 55) and the highest fracture energy (i.e. 150 J) belonged to the sample containing 5 wt. % PDMS. The aim was to prepare of polymer composites, and one of the important methods to form carrier path in an insulating blends, is the incorporation of conductive fillers.

1.1.3 Conductive filler

Filler is a crucial component of the composite material not only improving composite is stiffness but in the case of electric filler rendering it electroconductive. Electrically conductive filler, such as metal powder [55], fibers [56], carbon black [57-60] and carbon nanotubes [61] are used to prevent heat loss and achieve high electrical conductivity of the composite. Filler type and shape, aspect ratio, and dispersion degree of filler in polymer matrix influence the total electrical conductivity significantly. In my work I focused on the following types of filler: carbon black, carbon nanotubes.

Carbon black (CB)

CB is an amorphous form of carbon with a structure similar to disordered graphite. CB is a form of paracrystalline carbon that has a high surface area to volume ratio. When aromatic hydrocarbons are subjected to incomplete combustion at high temperature, their molecules will dissociate through the rupture of C-H bonds. CB is typically a pyrolysis product of hydrocarbon such as oil subjected to very high temperature. It may be partially graphitic with onionskin structure, each layer being graphitic (hexagonal organization of carbon atoms). Subsequently, carbon atoms and aromatic radicals react to form layer structures composed of hexagonal carbon rings, which tend to stack in three to four layers, forming crystallographic structures. Domain structures of CB are particle (~ 50 μm), aggregate (~ 1 μm) and agglomerate (~10 μm). Crystallites then form primary particles, which further fuse into primary aggregates. Van der Waals forces cause these aggregates to join in more loosely assembled agglomerates. There are five types of CB manufactured in the CB industry: furnace black, thermal black, lamp black, channel black, and acetylene

black (Fig.7 a). Over 90% of the CBs currently produced are made by the furnace process, in which oil is thermally decomposed to form CB particles. Electrical conductivity of dry compressed CB is of the order 10^4 S/cm [62] with density in the range (1.7-1.9 g/cm^3). As far as the CB particles are concerned the aggregate structure, morphology and micro porosity of particles affect the electrical conductivity of composite material and percolation threshold. CB have great potential in the application sphere as: electromagnetic interference shielding, electrostatic and heat dissipation [63].

Carbon nanotubes (CNT)

CNT represent the youngest allotropic form of carbon having a high degree of constitutional organization. They exist in two fundamental forms, single-wall (SWNT) and multi-wall (MWNT) Fig. 7 b. SWNT consist of a single tube of graphene, whereas MWNT are composed of several concentric tubes of graphene fitted one inside the other. Carbon nanotubes can be produced using a variety of methods. There are the three main methods for production: Arc discharge, laser ablation, and chemical-vapour deposition (CVD), which is produced on industrial scale and has recently, become relatively inexpensive. This efficient behaviour is caused by excellent electrical properties and very high aspect ratios p (p=L/D, where L= length, 1-50 μm and d-diameter,
1-50 nm) of the CNT, which was discovered in 1991 by Iijima [64]. They have electrical conductivity of 100- 101 S.cm^{-1}, low apparent density, high surface area, porosity, gas permeability and excellent mechanical properties: the high tensile strength (13-53 GPa) and Young's modulus (1000-5000 GPa). However, the effective utilization of the properties of nanotube composites depends on the quality of their dispersion and the level of interfacial boxing of nanocomposites [65]. Uniform dispersion and distribution of carbon nanotubes throughout the matrix is difficult to obtain due to the tendency to form agglomerates during synthesis because of strong van der Waals attraction among individual tubes.

Methods for CNT dispersion

There are two distinct approaches for dispersing carbon nanotubes: the mechanical method and methods that are designed to alter the surface energy of the solids, either physically (non-covalent treatment) or chemically (covalent treatment). Mechanical dispersion methods, such as ultrasonication and high shear mixing, separate nanotubes from each other, but can also fragments the nanotubes, decreasing their aspect ratio [66]. Non-covalent treatment is

particularly attractive because of the possibility of adsorbing various groups on CNT surface without disturbing the π system of the graphene sheets. In the last few years, the non-covalent surface treatment by surfactants or polymers has been widely used in the preparation of both aqueous and organic solutions to obtain high weight fraction of individually dispersed nanotubes. Chemical methods use surface functionalization of CNT to improve their chemical compatibility with the target medium (solvent or polymer solution/melt), that is to enhance wetting or adhesion characteristics and reduce their tendency to agglomerate. However, aggressive chemical functionalization, such as the use of neat acids at high temperatures, might introduce structural defects resulting in inferior properties for the tubes [67]. Surfactants are classified according to the sign of the charge on a surfactant molecule when it is dissolved in water. Generally, there are two groups of surfactants–non-ionic, with no charge in its head, and ionic: cationic, anionic and zwitterionic. Ionic surfactants can be used with water soluble polymers such as polyvinyl alcohol (PVA) [68]. In our work we used an anionic surfactant– dodecylbenzenesulfonic acid (DBSA), which forms a negative charge when dissolved in water, a cationic surfactant, cetyltrimethylammonium bromide (CTAB) – forming a positive charge when dissolved in water. Surfactant can also cause the non-covalent modification of the CNT surface, which is helpful for dispersion of this kind of filler in polymeric matrix. However, pristine carbon nanotubes cannot be homogeneously dispersed in most solvents. CNT are poorly soluble in nearly all classical solvents, with the exception of amide solvents such as N, N dimethylformamide (DMF) or N-methyl-2-pyrrolidone (NMP). In several studies, it has been demonstrated that it is possible to disperse considerable amounts of pristine CNT in bulk NMP (i.e. without adding any dispersing agents). Wong [69] found out that a single layer of NMP raises a big barrier between carbon nanotube interactions in CNT-NMP dispersion, preventing their aggregation into bundles [70]. The most promising organic solvent appears to be NMP with a reported dispersion limit of 0.01–0.02 g L^{-1} [71]. In the polymer nanocomposite these agglomerations decrease the surface area and disturb the formative network structure which is essential to improve electrical properties. In a typical dispersion procedure, after the surfactant has been adsorbed on the nanotube surface, ultrasonication for minutes or hours (with ultrasonication tip or bath, respectively) may help a surfactant to debundle nanotubes by steric or electrostatic repulsions. Carbon nanotubes have been attracting great interest due to their wide scope of possible applications, such as composite reinforcement material, hydrogen containers, field emission sources, super-capacitors,

molecular sensors.

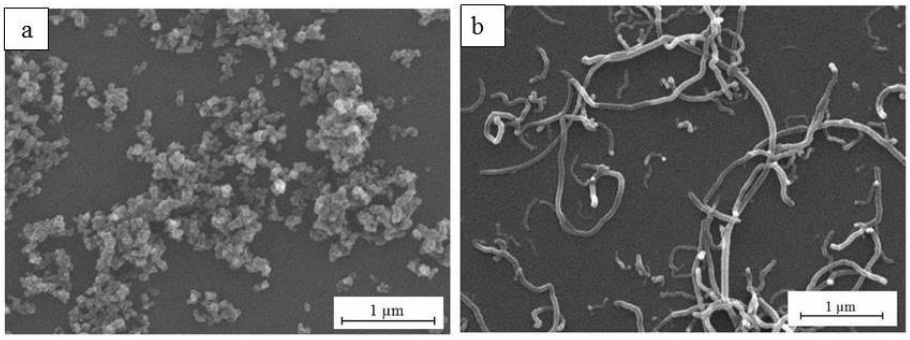

Fig. 7. SEM photographs of the of fillers: a) CB (acethylene blacks, Cabot, USA), b) CNTs (MWNT–2040, Conyuan Biochemical Technology, Taipei, Taiwan

1.2 Factors influencing the electrical properties of CPC

The main feature of the CPC is a drastic difference between electrical conductivity of polymer matrix and the filler reaching a factor of 10^{22} in terms of conductivity. This is due to the important specific feature – direct current (DC) can flow along such materials only through continuous chains of filler (if the possibility of quantum-mechanical tunnelling is not taken into account). Probability of forming such a structure depends on a variety of factors, namely: volume fraction, type and shape of filler, aspect ratio, distribution of lengths and orientation, degree of dispersion and processing. The electrical conductivity of CPC can be described by using abstract model of percolation theory.

Percolation theory

The majority of polymers are typical insulators, the probability of transfer of current carriers between two conductive points isolated from each other by and interlayer of the polymer decreases exponentially with the growth of gap $i_{tunnelling}$ (the tunnel effect) and is other than zero only for $i_{tunnelling}$<10 nm [72]. For this reason, the transfer of current through macroscopic distance can be affected via the contacting particles chains. Calculation of the probability of the formation of such chains is the subject of the percolation theory. The main notion of the percolation theory is the socalled percolation threshold $\mathbf{p_c}$ – minimal concentration of conducting filler c in that a continuous conducting chain of macroscopic length appears in the system [73]. Shermam [74] described percolation threshold as the point at that a macroscopic – length continuous chain first appears. The highly conductive filler is added to the matrix to provide a three-dimensional network of filler particles through the component. The

situation is known as percolation and percolation threshold is characterised by a sharp drop of several orders of magnitude in conductivity. Percolation theories are frequently applied to describe the insulator-to-conductor transitions in composites made of conductive filler and an insulating matrix. It has been shown both experimentally and theoretically, that percolation threshold strongly depends on the aspect (length-to diameter) ration of the filler [75]. The change i-n conductivity (σ) above the percolation threshold (where $\varphi_f > \varphi_c$) can be expressed using percolation theory as

$$\boldsymbol{\sigma = \sigma_f(\varphi - \varphi_c)^t}[6]$$

where σ is conductivity of composites (S m^{-1}), σ_f is conductivity of filler, φ - volume fraction of filler (%) above percolation threshold,φ_c – volume fraction of filler at pc (%), t – critical exponent is depends on the dimensionality of space and value of t is around 2 for three-dimensional composite materials, where $\mathbf{p_c}$ represents the volume fraction of conductive filler at the percolation threshold and the critical exponent *t* governs the scaling behavior in the region of $\mathbf{p_c}$.

1.3 Relationship between the morphology and the electrical properties

Figure 8 presents the percolation curve of typical CPC material. The infinitely steep change in conductivity of the composites with a minor change in conductive phase at the percolation threshold is evident. The percolation threshold, as well as, varies considerably with the shape and agglomeration of the conductive component [76]. If the conductive component is in the form of particles and are spatially correlated in three dimensions, the observed percolation threshold can be reduced and critical exponent elevated, both valuable traits for achieving highly sensitive stimuli sensitive materials.

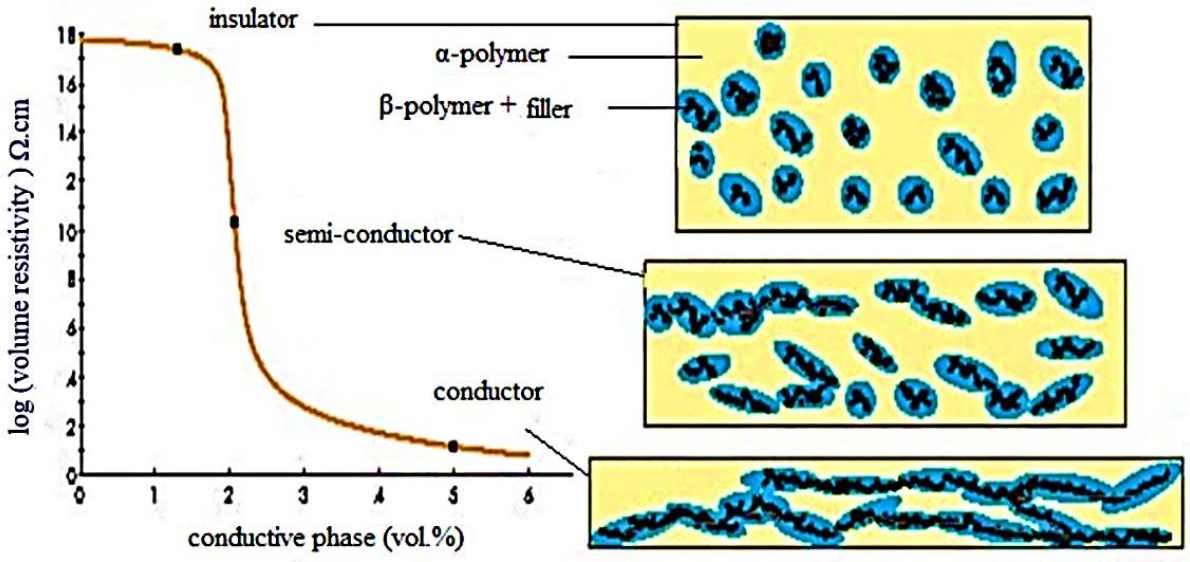

Fig. 8. Schematic of the variation in volume resistivity (ρ) of a multiple percolation composite and corresponding morphology

A reduction in the conductive element content required for percolation in CPC materials can be accomplished with a "percolation-within-percolation" approach and has been termed multiple percolation (Fig 8). It is possible to demonstrate the systematic reduction in conductive filler required for bulk conductivity resulting from this approach with an example of a ternary blend. We can identify two immiscible polymers, the α-polymer which is selectively filled with a conductive filler and the β-polymer which is to be filled with the conductive α-polymer blend. Denoting the critical fraction of the conductive filler required to insure conductivity in the α-polymer as p_α and the critical fraction of the α-phase required to insure connectivity of α in β as p_β, the critical fraction of the conductive filler in the total ternary blend [77] is

$$p_c = p_\alpha \cdot p_\beta \, [7]$$

Extending the approach to higher levels of percolation

$$p_c = p_\alpha \cdot p_\beta \cdot p_n \, [8]$$

where p_n is the threshold of co-continuity of the (*n-1*)-polymer blend in the n-polymer. A multiple percolation approach allows, at least theoretically, for the feasibility to obtain a CPC material with as low a level of conductive material as desired. In accordance with Eq. (7), for example the CB will be selectively blended into the polyolefin and this binary blend, which is designated the minor

phase α-polymer, will be incorporated into the polar polymer and is designated the major phase β-polymer. The two polymers in the system under investigation will have a structural similarity in the sense that the former will be a completely nonpolar polyolefin while the latter will differ only by the random insertion of the polar group (e.g., ethylene vinyl acetate) in the chain backbone [78] This phenomenon was described by Sumita [78] For instance, Gubbles et al. [3] Showed the localization of filler influenced electrical percolation of the blend system polyethylene/polystyrene/carbon black and electrical conductivity passes through a maximum when the particles are localized at the interface. In fact, filler selective localization in the polymer blends may cauce morphological changes, affecting the final properties at the performance of the material. Stabilization of domain size by addition of nanoparticles has been extensively reported [79]. The function of nanoparticles in reducing and coarsening has been explained by decrease in interfacial tension by localization of the filler at the interphase, coalescence suppression due to nanoparticles acting as barriers at the interface, increase of viscosity, elasticity of the phase contains nanoparticles or a combination of this parameters.

AIMS AND OBJECTIVES OF WORK

The aim of the work is to modify the brittle behaviour of epoxy resin by silicone elastomers and to develop on their base nanocomposites with high total conductivity.

The work that has been carried out within doctoral thesis entiled “Epoxy-silicone filled nanocomposites” can be summarized into following parts:

1. Development of technology for preparation of epoxy-silicone polymer system with improvement of mechanical properties.
2. Development of homogenous nanocomposites based on epoxy-silicone matrix filled with carbon black and carbon nanotubes.
3. Characterization of morphostructural, mechanical and electrical properties of polymer systems and nanocomposites.
4. Optimization of nanocomposites technology with a view ti improve their toughness and electrical properties.

2 METODOLOGY

2.1 Materials and preparation of epoxy polydimethylsiloxane blends

Materials

The epoxy resin (ER) used was a bisphenol A diglycidyl ether (DGEBA), D-3415, epoxide equivalent weight = 172–176 g, liquid, Sigma Aldrich, USA) with purity > 90%. The curing agent was an aliphatic amine, diethylenetriamine (DETA-D93856, Sigma Aldrich, USA) with purity > 90%. Liquid silicone-epoxy resin, Silikopon EF (SEF, Tego, Evonik, GE), this commercial product was used as a comparison sample. Dicumyl peroxide (DCP, Sigma Aldrich, USA) with purity >90% was used as a free radical initiator. In this study, two kinds of PDMS were studied: vinyl-terminated PDMS (VT-PDMS, Sigma Aldrich, USA) with purity >90% supplied in the liquid form and PDMS (PDMS – base A, Dow Corning, USA) were used.

ER and ER /DCP

The first set of ER samples was prepared without DCP, whereas the second set consisted of epoxy with DCP in concentration varying from 0 to 3 wt. %. DGEBA was mixed in a 50-mL beaker using a mechanical stirrer (MM-1000, Biosan, Germany) for 30 min. The appropriate amount of DETA was added, and the mixture was stirred for further 10 min at 80°C. All polymer blends were prepared from a stoichiometric mixture of DGEBA and DETA with molar ratio of 100:12. Rectangle-shaped samples with 3-mm thickness were produced by cast moulding into vacuum desiccators, where air bubbles were removed. Then, the form was closed and placed into a drying oven, where the where the material was cured for 2 h at 80 °C.

ER/VT-PDMS or ER/PDMS

The second set of *ER/VT-PDMS* and the fourth set of *ER/PDMS* polymer blends with varying concentrations of polysiloxane PDMS (5, 10, 15 wt. %) were prepared according to the recipes shown in Table 2 (in attachment) as follows: DGEBA was solved in acetone and mixed with PDMS and VT-PDMS at 80°C in vacuum at 300 rpm for 1 h. The reaction mixture was cooled to room temperature, and amino curing agent DETA was added and stirred for 10 minutes. The curing process was carried out in the same manner as in Section *ER and ER /DCP.*

ER/VT-PDMS/DCP or ER/PDMS/DCP blends

The fifth and sixth sets of samples were prepared in a 50-mL beaker using DGEBA and a varying amount of DCP (1-3 wt. %). Both components were stirred at 300 rpm for 1 h under reduced pressure at 80°C. Subsequently, PDMS (VT-PDMS or PDMS) was added in an amount in the range of 5-15 wt.%, and the mixture was stirred for 2 h at 80°C. After cooling to 25°C, the stochiometric amount of DETA was added. The curing process was carried out in the same manner as described in Section *ER and ER /DCP.* The composition of prepared blends are listed in Table 2 (in attachment).

2.2 Materials and preparation of epoxy polydimethylsiloxane composites filled with conductive filler

Materials

For preparation of conductive polymer composite were used polymer matrix presented in chapter 2.1. As conductive filler were used carbon black (CB), Carbon black used in the study was high structure Vulcan (CABOT XC- 72R Cabot, USA). Commercially available multiwall CNTs (MWNT-2040, purity ≥ 95 %, diameter of 20–40 nm, length 5–15μm, specific area of 40–300 m2 g–1, and density of 1.8 g cm–1) were purchased from Conyuan Biochemical Technology (Taipei, Taiwan). NMP with purity ≥ 99 % was used to modify CNTs (Sigma Aldrich, Saint Luis, MO, USA) Acetone (Sigma Aldrich, Saint Luis, MO, USA) and distilled water were used without further purification.

PDMS/CNT composite - Mechanical mixing

The first set of composites consisted of several samples with CNTs concentration varying from 0 to 3.4 vol. %. were prepared. Calculated amounts of CNTs and PDMS were placed into a beaker and stirred using mechanical mixer (IKA Labortechnik, Staufen, Germany) at 100 rpm for 1hr. Then a curing agent was added and subsequently stirred at 100 rpm for 5 min. After that, the mixture was filled into the mold and placed into the vacuum desiccators where air bubbles were removed. Finally, the mold was closed and placed into drying oven where material cured at 70 C for 12 hrs.

PDMS/CNT-acetone composite – Sonication

Several sets of nanocomposites filled by CNT with polymer matrix PDMS were prepared. CNTs were sonicated in acetone by using ultrasonic treatment (1

hr, at frequency 24 kHz and power 400 W). Then the beaker with the mixture was placed into the dish with hot oil (60°C) and mixed using magnetic stirrer until evaporation of whole acetone. Prepared mixture was subsequently filled into the mold and placed into the vacuum desiccators for the removal of air bubbles. Finally, the mold was closed and placed into drying oven where material cured at 70°C for 12 hrs.

PDMS/CNT-NMP composite - Sonication

Several composites of different filler concentrations (0, 1, 2.2, 2.8, 4 and 4.5 vol. %) were prepared. The certain amount of CNT-NMP, 15 ml of acetone and PDMS were placed into 50 ml beaker and sonicated by an UP 400s ultraprobe. The sonication frequency, power and time were 24 kHz, 400 W and 5 minutes, respectively. Then the beaker with the mixture was placed into the dish with hot oil (60°C) and mixed using magnetic stirrer until evaporation of whole acetone. Prepared mixture was subsequently filled into the mold and placed into the vacuum desiccators for the removal of air bubbles. Finally, the mold was closed and placed into drying oven where material cured at 70°C for 12 hrs.

PDMS/CB composite - Mechanical mixing

As comparative systems, PDMS filled with different concentration of carbon black (1, 3, 5, 7, 8, 9 and 12 vol. %) were used. Calculated amount of carbon black and S 184 were placed into a beaker and stirred mechanically (IKA Labortechnik, Staufen, Germany) at 100 rpm for 1hr. The curing agent was further added to the mixture and the latter was additionally stirred at 100 rpm for 5 min. The obtained mixture was then poured into the mold, evacuated and cured under the same conditions as in previous cases.

ER/CNT, PDMS/CNT and SEF/CNT

The three sets of nanocomposites filled by CNT with polymer matrix (ER, PDMS and SEF) sample were prepared. CNTs were sonicated in acetone by using ultrasonic treatment (1 hr, at frequency 24 kHz and power 400 W). ER was mixed in a 50-mL beaker using a mechanical stirrer (MM-1000, Biosan, Germany) for 30 min then CNT mixture was added and ultrasonic bath was applied for 20 min. In order to remove acetone the mixture was dried at 58 °C for 2 days. Then the appropriate amount of DETA was added and the mixture was stirred for further 10 min at 80°C. All polymer composites were prepared from stoichiometric mixture of the ER and the DETA (100:6) molar ratio.

Three -mm-thick rectangle-shaped samples were produced by cast moulding in

vacuum desiccators, where air bubbles were removed. Then, the form was closed and placed into a drying oven, where the material was cured for 6h at 80 °C. The post curing process was carried for 4 h at 80 °C.

ER/VT-PDMS/CNT and ER/SEF/CNT

The set of ER/VT-PDMS and set of ER/SEF multicomponent polymer composite with varying concentration of VT- PDMS and SEF from 5 to 40 vol. % were prepared. ER was solved in acetone and mechanically mixed with VT-PDMS or SEF at temperature of 80°C, in vacuum at 300 rpm for 2 hours. The dispergation of CNTs and curing process were carried out in the same manner as in Section: *ER/CNT, PDMS/CNT and SEF/CNT* (Table 3 in attachment).

ER/VT-PDMS/CB and ER/VT-PDMS/DCP2/CB

Preparation of polymer matrix was describe in chapter 2. 2.,where different concentration CB (0,5-10 wt. %) was used as a conductive filler. Calculated amount of carbon black and VT-PDMS were placed into a beaker and stirred mechanically (IKA Labortechnik, Staufen, Germany) at 100 rpm for 1hr. The curing process was carried out in the same manner as described in Chapter 2.1. The compostion of prepared composites is listed in Table 4 (in attachment).

2.3 Characterization of epoxy-polydimethylsiloxane blends and composites

2.3.1 Structure analysis

Nuclear Magnetic Resonance Spectroscopy (NMR)

NMR happens when certain atomic nuclei situated in a static magnetic field are exposed to another oscillating magnetic field. The nuclei possess spin angular momentum due to the protons and neutrons inside, and thus experience different energy levels when placed in the magnetic field. A nucleus can have three spin values (I= ½, 1, or 0) based on the net spin of the nucleons and in the external field its energy level splits according to their spin values. For example, a nucleus with ½ spin has two orientations and energy levels ± ½. In the absence of an external field, the orientations have equal energy whereas in the presence of the field, the energy levels vary with the lower level highly populated. An electromagnetic radiation (radio waves) of specific frequency is irradiated on a

nucleus in a particular situation and it starts flipping from the spin-aligned low energy state to the spin-opposed high-energy state. The energy required for this transition depends on the applied magnetic field strength.

The spin angular momentum (L) of the nucleus is expressed by Eqn (9). L is also proportional to the nucleus' intrinsic magnetic momentum.

$$L = mh \text{ [9]}$$

where *m* is the spin quantum number with (2I + 1) possible values (m= -I, -I+1... I - 1, I) and *h* is Planck's constant. For a given nucleus, the magnetic moment (μ) along the field direction z is related to the gyromagnetic ratio (γ):

$$\mu z = \gamma L \text{ [10]}$$

and thus Eqn (11) can be written as

$$\mu z = \gamma mh \text{ [11]}$$

In the presence of a magnetic field of strength H_0, the spinning nucleus undergoes a precessional motion with a frequency called the Larmor frequency *(ω)*:

$$\omega = 2\pi v = \gamma H_0 \text{ [12]}$$

The magnetic moment is also related to H_0 by Eqn (13):

$$E = -\mu z H_0 \text{ [13]}$$

This can also be written as:

$$E = -\gamma mh H_O \text{ [14]}$$

Considering the flipping of an electron between two consecutive energy levels, the energy difference is expressed as Eqn (15):

$$\Delta E = E_2 - E_1 = \gamma h H_0 \text{ [15]}$$

The NMR spectrum is usually taken at this level [86]. ΔE is also related to the population at higher (N_1) and lower energy states (N_0), as per the Boltzmann statistics (Eqn.16):

$$\frac{N+}{N-} = \exp(-\frac{\Delta E}{K_B T}) \text{ [16]}$$

where K_B, is the Boltzmann constant and *T* is the absolute temperature. NMR

spectra provide both qualitative and quantitative information. The connectivities of atoms or groups of atoms and their magnetic equivalence come under the qualitative parameters whereas J-coupling constant and cross-relaxation rates are useful to understand the conformation, distances, bond angle, and local mobility of atoms, and contribute the quantitative values [80].

Scanning electron microscopy

Scanning electron microscopy (SEM) is a type of electron microscopy that produces images of sample by scanning it with a focused beam of electrons. This is the most common technique for morphological analysis, chemical and crystallographic information. An SEM is composed of an electron gun that provides and electron probe with high intensity, a condenser lens system that generates a small p robe size, an objective lens for imaging, electron probe scanning coils, and a detector system for receiving images and spectra. The electron beam is formed by accelerating electrons generated from a filament set in a cathode held at a slightly negative or ground potential toward and anode whose potential is selectable. The cathode, filament, and anode are collectively referred to as the electron gun; the type, mode of operation, and cost of the filament depend on the brightness desired, its lifetime, and the vacuum level achievable in the electron gun chamber. The brightness β is defined as the current density per solid angle and can be calculated as

$$\beta = \frac{4I}{(\pi d_c \alpha_0)^2} \text{ [17]}$$

Where I is the beam current, d_c is the diameter of the beam at its crossover between the cathode and the anode, and α_0 is the divergence semi-angle of the beam as it emerges from crossover.

A scanning electron microscope (SEM) provides high-resolution 3-D images of a sample surface. The electrons hit the surface and are elastically scattered by atoms in the sample. The scattering process spreads the focused beam up to a few microns onto the surface of the sample leading to emission of electrons and x-rays. The principle of SEM is the following: 1. The lenses in an SEM are made of electromagnets with high voltages. 2. Electrons are made to strike the specimen vertically after being guided through these lenses and electromagnetic fields. 3. The signal produced by SEM depends upon the interaction of the incident radiation with the specimen surface. The signals include those from secondary electrons, back-scattered electrons, characteristic X-rays, specimen current and transmitted electrons. 4. Different signals are capable of providing

different information about the specimens that are analysed using detectors [81]

2.3.2 Electrical properties

Current-voltage characteristics

The current-voltage characteristics are basic parameters for calculation DC (direct current) electrical conductivity. Generally, the dependence between the current density J (A m^{-2}), and electric field intensity, E (V m^{-1}), is non-linear and can be described by the following relation (eq. 18):

$$J = \sigma E \text{ [18]}$$

where σ is the electrical conductivity (S m^{-1}). In practice it is usually calculated by the following (eq.21) derived from

$$\sigma = \frac{I}{U} \cdot \frac{l}{S} \text{ [18]}$$

where geometry of samples is given by *l* (m) is thickness and cross-section S (m^2). The measurement of electrical conductivity can be provided by the using two-point methods or four-point methods (Van der Pauw methods) [82]. A main advantage of four-point methods is the elimination of contact resistance against two-point methods. However, insulator and semiconductors are characterized by non-linear dependence due to the presence of no-ohmic phenomena (e.g. tunneling or hopping) and further conclusions can be drawn about the mechanism of charge transport across the gaps between conductive filler aggregates.

Dielectric spectroscopy

Dielectric spectroscopy is a method based on the principle of the interaction of electromagnetic waves with the electric dipole moment of the investigated material. The frequency range in dielectric spectroscopy is between 10^{-6} to 10^{10} Hz (for a solid polymeric systems with frequency range between 10^{-2} to 10^{7} Hz). Generally, polymers are dielectrics in which charge carries are not free, but bonded. In the presence of the applied field the movement of charge occurs through both additional polarization effects and, more importantly, through rotation of the polar molecule and its dipole to a position of minimum potential energy in the field [83]. When an electric field is applied across a parallel-plate capacitor containing a dielectric, various atomic and molecular charges that are present in the dielectric are displaced from their equilibrium positions and the material is said to be polarized.

The important electrical properties are the relative dielectric constant ε' (ω) and the relative dielectric loss ε" (ω). The term loss implies the conversion (or "loss") of electrical energy into heat, and the term relative means relative to free space. The complex relative permittivity ε* (ω) is given by the (Eq. 20)

$$\varepsilon^*(\omega) = \varepsilon'(\omega) + i\,\varepsilon''(\omega) \quad [19]$$

The relative dielectric constant ε'(ω) expresses the ability of the material to store electrical energy, and the relative dielectric loss ε" (ω) denotes the ability of the material to dissipate the electrical energy. These properties provide an indication of the electrical insulating ability of the material. The dielectric loss factor for the material, ε" (ω) which expresses the degree to which an externally applied electrical field will be converted to heat, is given by equation

$$\tan\delta = \frac{\varepsilon''(\omega)}{\varepsilon'(\omega)} = \frac{\sigma(\omega)}{\omega\varepsilon_0\varepsilon_r(\omega)} \quad [20]$$

where σ(ω) is alternating conductivity dependent on frequency ω (Hz), where ω=2πf. The loss tangent, tan δ, provides an indication of how well the material can be penetrated by an electrical field and how it dissipates electrical energy as heat.

2.3.3 Rheological analysis

Rheology involves measurements in controlled flow, mainly the viscometric flow in which the velocity gradients are nearly uniform in space. In these simple flows, there is an applied force where the velocity (or the equivalent shear rate) is measured, or vice versa. It is particularly concerned with the properties of matter that determine its behaviour when a mechanical force is exerted on it. Rheological properties have important implications in many and diverse applications. The applications of rheology are very important in the areas of industries involving metal, plastic, and many other materials. The rheological investigations will provide a mathematical description of the viscoelastic behaviour of material under study. The rheology of a material is very important in the processing of composites or determining the curing behaviour of the materials. The gained knowledge of study the behaviour of polymeric liquid in simple flows and for simple systems can be used in a complex flow pattern. They are called viscometric as they are used to define an effective shear viscosity η from the measurements,

$$\eta = \frac{\sigma_{xy}}{\dot{\gamma}} \quad [21]$$

where σ_{xy} is the shear stress (measured or applied) and is the shear rate (applied

or measured), Viscosity is measured in Pa s (Pascal second). Rheology is not just about viscosity, but also about another important property, namely the elasticity. Complex fluids also exhibit elastic behaviour. Similar to the viscosity defined above being similar to the definition of a Newtonian viscosity, the elasticity of a complex material can be defined similar to its idealised counterpart, the Hookean solid. The *modulus of elasticity* is defined as

$$G = \frac{\sigma_{xy}}{\gamma} \text{ [22]}$$

where γ is called the strain or the angle of the shearing deformation, G is measured in Pa (Pascal). G is one of the elastic moduli, known as the storage modulus, as it is related to the amount of recoverable energy stored by the deformation. G for most polymeric fluids is in the range 10–10^4 Pa, which is much smaller than that of solids (<10^{10} Pa). This is why complex fluids, of which polymeric fluids form a major part, are also known as soft matter, i.e. materials that exhibit weak elastic properties. Polymeric liquids have a microstructure that is like springs representing the linear chain. Restoration of these springs to their equilibrium state is through the elastic energy that is 'stored' during the deformation process. But polymeric fluids are not ideal elastic materials, and they also have a dissipative reaction to deformation, which is the viscous dissipation. For small deformations, the response of the system is linear, meaning that the response is additive: effect of sum of two small deformations is equal to the sum of the two individual responses. [84]

2.3.4 Mechanical properties

Dynamic Mechanical Analysis

The dynamic mechanical properties of multiphase polymer systems were determined using DMA. DMA is a material characterization technique that provides information on the about the mechanical properties by using oscillation as a function of time and temperature. The dynamic mechanical properties are determined as the dynamic storage (E') and loss moduli (E''). The dynamic storage and loss moduli are collectively referrers to as the complex modulus (E^*) of a material that is generally expressed as

$$E^* = E' + E'' \text{ [23]}$$

The complex modulus is a measure of the resistance of a material to deformation, and it encompasses both the elastic and viscous responses. Through dynamic testing, which measures the phase between the sinusoidal

force and displacement that the sample is experiencing, the stress can be deconvoluted into an elastic stress (in phase with the strain) and a viscous stress ($\pi/2$ out of phase with the strain). The elastic stress is used to calculate the elastic modulus, or storage modulus. Storage modulus is a measure of the recoverable stored strain energy. The viscous stress is used to calculate the viscous modulus, or loss modulus. Loss modulus is a measure of the energy dissipated, generally lost as heat. The loss modulus peak and tan δ (defined as the ratio of (E''/E') peaks are defined as the glass transition temperature, with the tan δ peak occurring at a higher temperature than the loss modulus peak. The tan δ peak is a good measure of the leather-like mid-point between the glassy and rubbery states. DMA is a powerful analytical instrument used to characterize material behaviour and to study material performance under specific conditions. Furthermore, data from DMA experiments can be mapped to a wide frequency range by the application of time–temperature superposition (TTS) [85].

Charpy impact strength analysis

Charpy impact strength of unmodified and modified epoxy resin was measured following the specification ISO 179/1eA. Impact strength of the samples described the energy required to break the specimen under sudden load. Test specimen is held as a simply supported beam and is impacted by a swinging pendulum. Impact strength is expressed in (kJ/m^2) and calculated by dividing impact energy in (J) by the cross section of sample (m^2). The magnitude of the impact strength reflects the ability of the sample to resist impact. Mechanical properties of multiphase polymer composites are a crucial indicator for its application. Impact strength is dependent not only on the phase structure, but also on morphological detail (for example, on the distribution and particle size) and adhesion between phases [86].

Adhesion properties

The lap shear strength of the cured specimens was investigated with the use of a Universal tensile instrument (Instron 5567, UK) according to ISO 4587:2003. The test was performed at a rate of 5 mm/min at room temperature. All adhesion values were averaged over five samples. The substrates used in this method were steel sheets.

3 RESULTS AND DISCUSSION

In the current work, the effect of siloxanes compatibilized with ERs by DCP on the mechanical properties of ER was investigated. The aim of the work is to determine the optimum composition of the epoxy-polydimehylsiloxane blend that results in improved toughness of the final composite.

3.1 Effect of DCP on the compatibilization of epoxy resin with polysiloxanes

In this study, glycidyl epoxies for which the best performance and the highest crosslinking degree is achieved when they are cured via an addition reaction with amines is studied. Epoxies can undergo ring opening reactions towards nucleophiles [96]. For the compatibilization between ER and, it is necessary to introduce peroxide in the compound (Fig. 9).

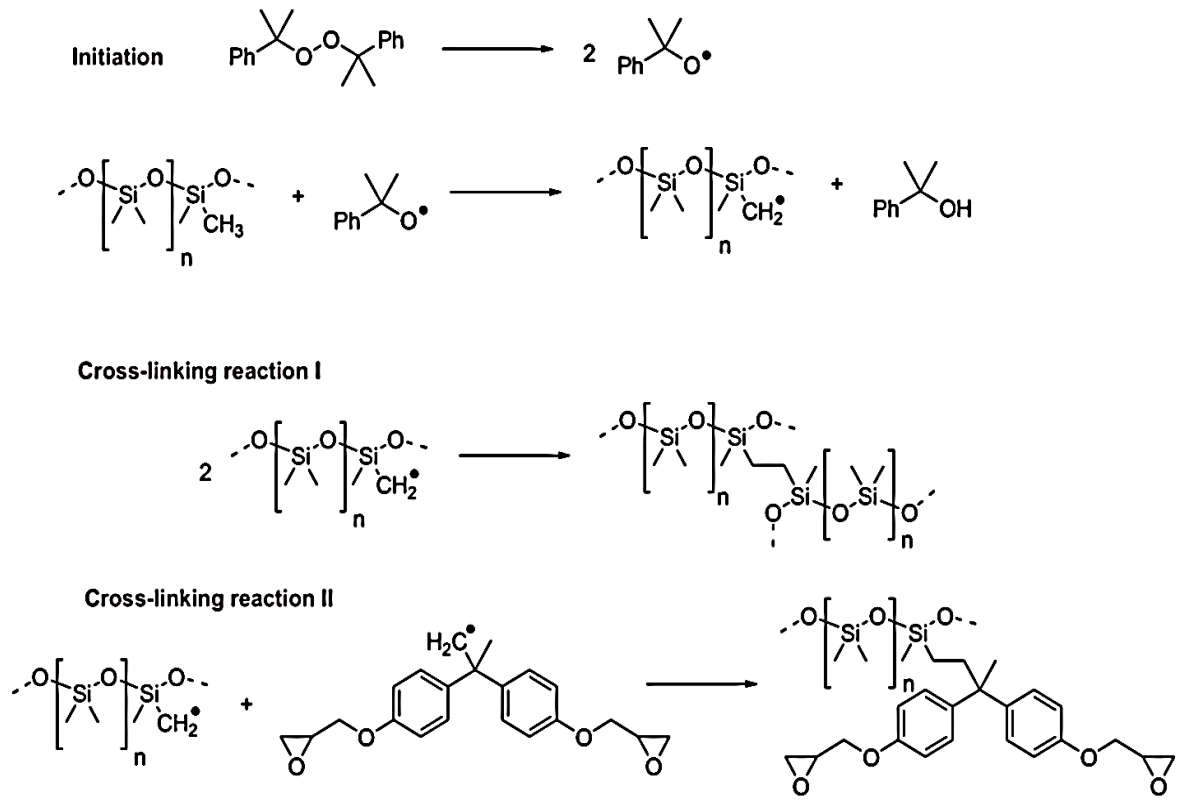

Fig. 9. Peroxides initiations and two possible chain scissions reactions. For the sake of transparency only middle parts of polysiloxane chains are depicted.

It is known that peroxides decompose to form free radicals, which abstract hydrogen atoms from polysiloxane. Hydrogen atom in macromolecules (ER or polysiloxane) is transferred to a reactive free radical (initiation stage). There are two possible essential models of crosslinking reactions: I) recombination reaction between two radicals of PDMS (curing of polysiloxane), and II) reaction between radicals of polysiloxane and DGEBA. There is approximately 800 of CH_3 groups [400 mers] and only 2 vinyl groups per one polysiloxane macromolecule [M_n 27.000]. Therefore, the probability of a reaction of radical with vinyl is very low compared to CH_3. Therefore, we do not consider that this reaction has any important role and we do not include it in the scheme 1.

3.1.1 NMR RESULTS

^{1}H NMR measurements of starting materials and prepared resins to shed light on the chemical behaviour during preparation of resins were performed. Initially, starting materials PDMS and (VT-PDMS) were characterized (Fig. 10 a, b). In the spectrum of a CDCl3 solution of VT-PDMS, the signals of methyl groups and terminal vinyl groups were clearly observed at 0.08 ppm and 5.72–6.17 ppm, respectively. Assuming that the VT-PDMS material is both-ends-vinyl-terminated polysiloxane, the average polymerization degree n to be of 300 can be calculated. The identity and purity of DGEBA, DCP and DETA were confirmed by 1H and 13C NMR.Due to the poor solubility of prepared resins, the NMR analysis of $CDCl_3$ extracts is focused. The sample preparation is described in section Preparation of epoxy-polysiloxane blends and it was proved that an increase in the extraction period had essentially no impact on the extract composition. In NMR spectra, no signals related to the DETA or low-weight products of reactions between mixture components in extracts of all of the tested samples have been detected. These results indicate that all of the DETA was consumed during resin formation and no unexpected compounds arose. In addition, the NMR data further suggest that DCP was quantitatively transformed into the corresponding alcohol, i.e., 2-phenylpropan-2-ol (PIP), under reaction conditions.

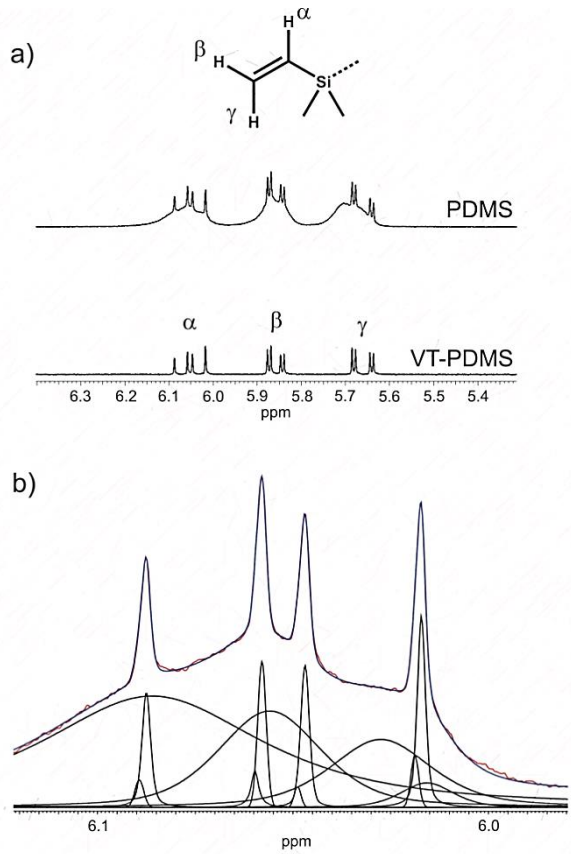

Fig. 10. a) Partial ^{1}H-NMR spectrum recorded at 500 MHz. Signals were assigned according to J(HH) values ($_{2}J(\beta\gamma)$=4.0Hz; $_{3}J(\alpha\beta)$=14.8Hz; $_{3}J(\alpha\gamma)$=20.5Hz); b) deconvolution of α–H signals of PDMS , contributing lines – black, simulated spectrum – blue, experimental spectrum - red.

As it can be seen in Fig. 11, there is a clear linear relationship between the starting molar ratio ER/DCP (*R*) and the ratio of the corresponding normalized NMR signals for samples where no siloxanes were used (Fig. 11, black squares). The *R* values for all of the examined samples are given in Table 5.

Tab. 5 Sample characteristics obtained by ^{1}H NMR spectroscopy.

Samples	*n*	*R*[a]
ER	n_a	n_a
ER /DCP1	n_a	0.27
ER /DCP2	n_a	0.52
ER /DCP3	n_a	0.78
ER /VT-PDMS10	160	n_a
ER /VT-PDMS5/DCP2	n_a	0.40
ER /VT-PDMS10/DCP2	50	0.28
ER /VT-PDMS15/DCP2	n_a	0.30
ER /PDMS10	70	n_a
ER /PDMS10/DCP2	80	0.42

n_a – compound under consideration was not taken into reaction
[a] a ratio of normalized signals of PIP(2-phenyl-propan-2-ol) and DGEBA expressing molar ratio (I_{PIP}/I_{DGEBA})

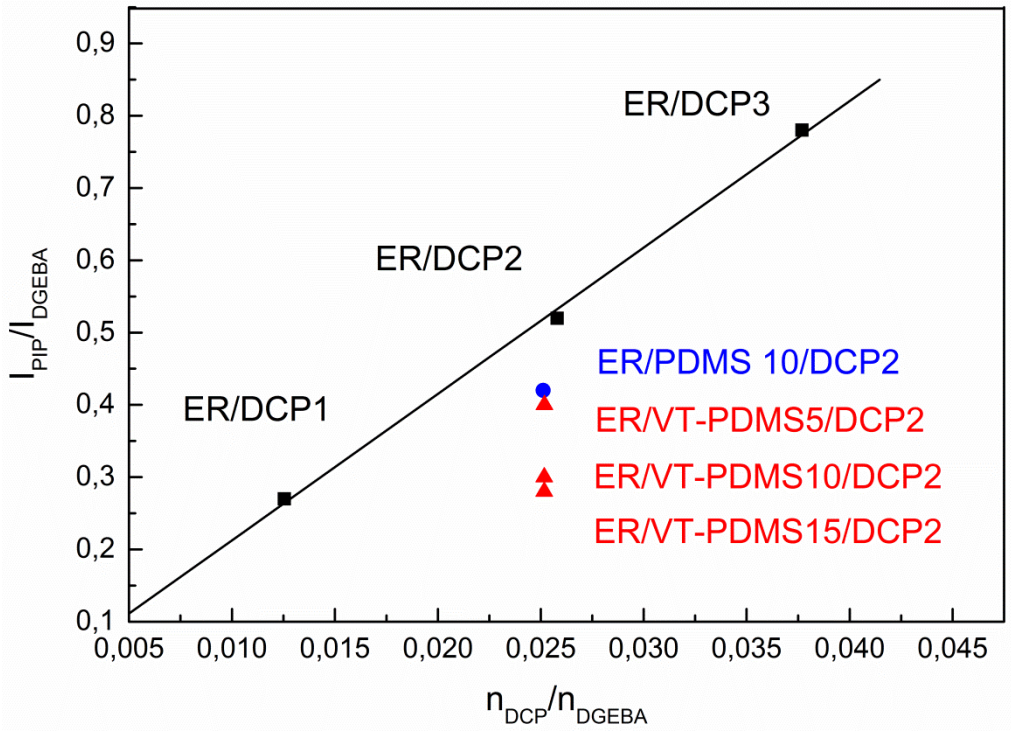

Fig. 11 Relationship between the initial molar ratio of DCP and DGEBA and normalized integral intensities of the corresponding NMR signals from resin extracts.

The value of the least-squares regression line slope of 20.3 correlates with the expected consumption of DGEBA during the resin formation process (in the case of no concentration changes, the slope should be 1). In contrast, the points related to samples containing siloxanes display significant deviation from the

expected line. This observation can be rationalized by decreasing the PIP amount in the extracts (some unexpected covalent and/or non-covalent incorporation into a resin) or by increasing the DGEBA amount (lower degree of incorporation to the resin). Finally, the changes in the averaged polymerization degree *n* of the siloxane component (all of the *n* values obtained are given in Table 2) were tested. In all of the examined samples of the resin extracts, we clearly detected NMR signals related to the vinyl-groups. This result indicates that not all of added amount of siloxane was bound into the resin structure. Interestingly, the *n* was significantly decreased in contrast to that for the starting siloxane. Since there is a lack of reasonable explanation for such low-weight siloxanes discrimination considering a chemical binding of siloxane, it is supposed that siloxane was incorporated into resin by physical means. Accordingly, a more rapid extraction of low-weight siloxanes gives an acceptable explanation for the observed decrease in *n*.

3.1.2 SEM morphology

Polysiloxane was added to uncured ERs, and, after cross-linking reactions, Elastomer modified ERs exhibited a two-phase microstructure consisting of relatively small (15-80 μm) elastomer particles dispersed in ERs due to its immiscible nature with the ER, which results in phase separation from the dominant epoxy component throughout the curing reaction (Fig. 12). Toughening of glassy polymers (such as thermosetting epoxy resin) with a soft low-modulus polymers occur when elastomer is introduced into the plastic [87-89]. The soft dispersed phase of elastomer, however, provides not only an increase in the toughness (due to the ability to dissipate impact energy), but also an increase in strength under uniaxial tension and with other types of deformation, which is especially effective when thermosetting polymers are filled with elastomer [90-99]. In these cases, the destruction of the material proceeds by the brittle fracture mechanism, as indicated by the small value of elongation at break. Usually, the neat epoxy resin fracture surface reveal a mostly smooth fracture surface, representative of brittle failure. In this case, both, impact and uniaxial tension leads to a high speed of the crack propagation. It is true that in highly cross-linked epoxy polymers, plastic shear deformation is considered the main energy absorbing process, as can be seen in our case for 5 and 10 % in both studied systems, where we can observe cracks propagating from rubber inclusions as these act as stress concentrators (Fig.12a, b, d, e). However, increase of the elastomer concentration up to 15 wt. % leads to a different mechanism of energy absorption as can be seen by absence of cracks

but appearance of damage zone around elastomer particles (Fig.12 f). Damage zone presence is manifested by stress whitening region around elastomer particle comprising small holes. The presence of such holes (see yellow arrows) is interpreted as caused by the dilatational deformation of the particles and the matrix [95, 96] that nucleates local shear yielding of the epoxy matrix causing a significant crack tip deformation. The synergic effects of localized cavitation at the elastomer/matrix interface and plastic shear yielding in the epoxy matrix are supposed to be responsible for deformation that results in energy dissipation process, which ultimately improves the impact strength values of the elastomer-modified epoxies.

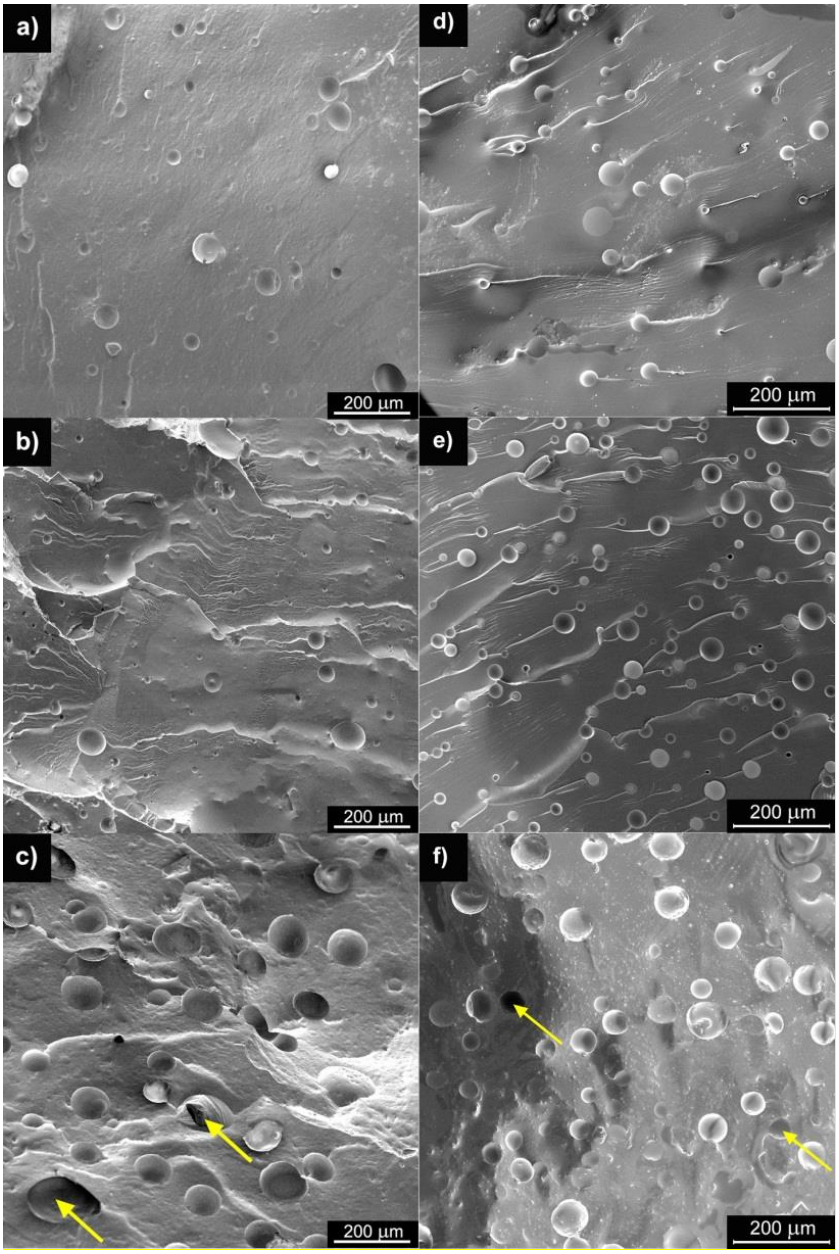

Fig. 12 SEM micrographs for epoxy modified PDMS: a) ER/PDMS5, b) ER/PDMS10, c) ER/PDMS15, d) ER/VT-PDMS5, e) ER/VT-PDMS10, and f) ER/VT-PDMS15.

Increase in elastomer concentration in the epoxy also leads to higher particle concentration per unit volume (e.g. Fig. 12 d, e) as well as the shift of particle size distribution towards slightly higher values such as in
VT-PDMS (Fig. 12 e, f).
Figure 13 shows a morphological comparison between modified ER/PDMS and ER/VT-PDMS by DCP. One can observe that DCP modification results in a more regular and homogenous distribution of the individual component in the blend. Upon addition of DCP, emulsification of ER and silicone elastomer take place, leading to a much finer dispersion and improved interfacial adhesion. The beneficial effect of DCP on the dispersion and interfacial adhesion of ER/PDMS and ER/VT-PDMS blends was examined by the investigation of the dynamic mechanical properties of the blends.

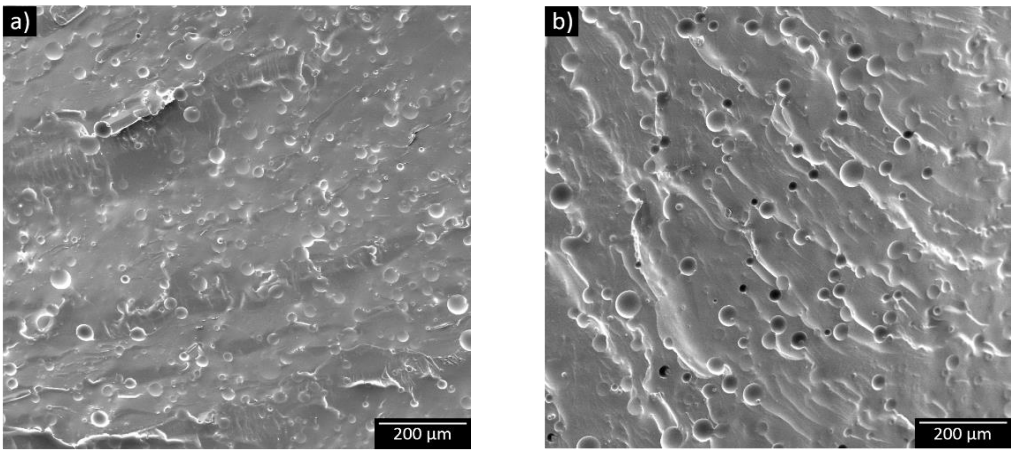

Fig. 13. SEM micrographs for ER modified by polysiloxane and DCP (2 wt. %): a) ER/PDMS 10/DCP2 and b) ER/VT-PDMS10/DCP2.

b)

3.1.3 Dielectric properties

Epoxy resin exhibits four relaxations processes – alpha, beta, gamma and delta (Figure 14 a). Precise identification of relaxation mechanisms was carried out on the basis of the temperature shift of the observed peaks (Figure 15a). While the beta, gamma and delta relaxations follow the Arrhenius equation rather well with linear dependence of ln f_{max} on $1/T$, the alpha relaxation shows considerable bending in agreement with the Vogel–Fulcher–Tamman (VFT) model (Fig. 15b). Fitting experimental data to the Arrhenius model allows one to determine the activation energy of the observed relaxation process, which are following beta= 326.0 kJ mol^{-1}, gamma = 55.5 kJ mol^{-1}, and delta 21.5 kJ mol^{-1}. The VFT model does not explicitly contain activation energy as a parameter for alfa relaxation process.

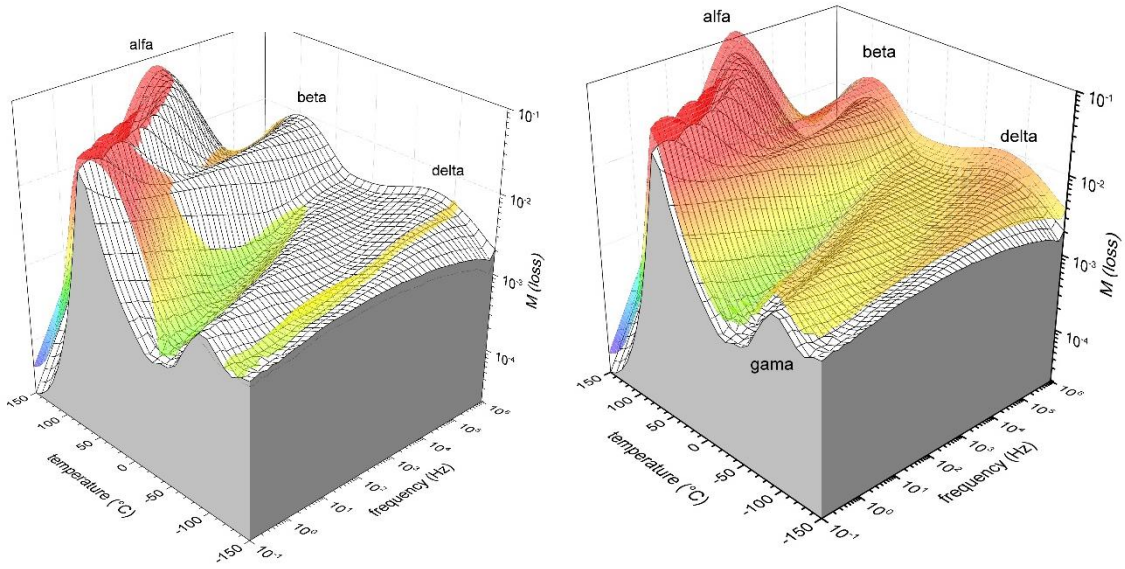

Fig. 14 Dielectric spectra comparison of ER/PDMS10 (a) and ER/VT-PDMS10/DCP2 (b); white surface in both figures shows pure ER spectrum for easier comparison.

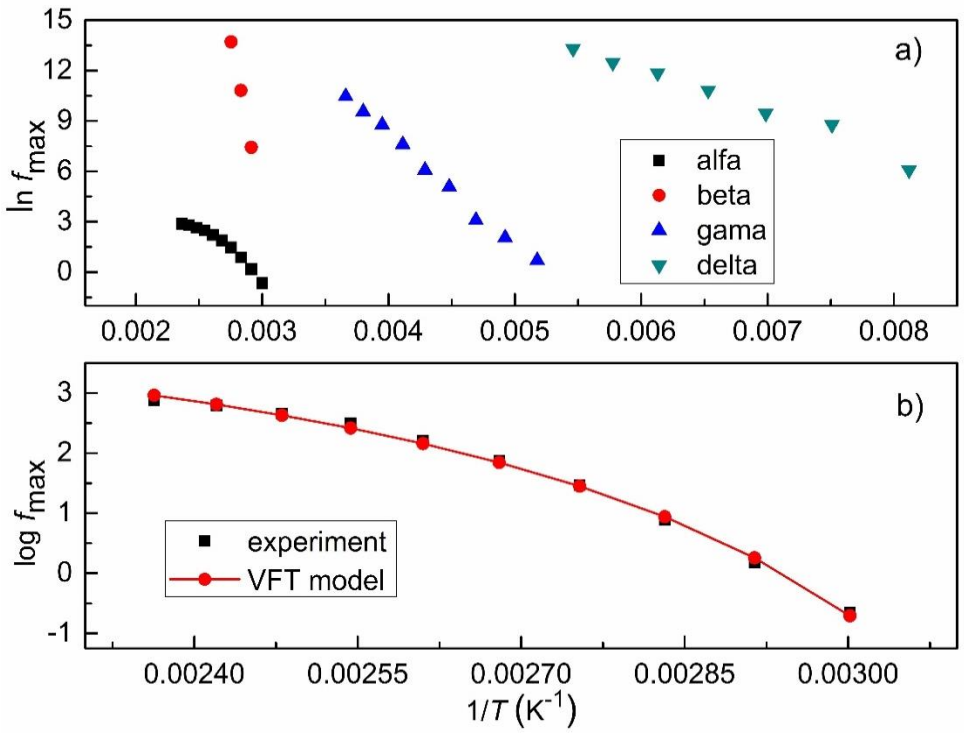

Fig. 15 Relaxation map observed processes (a) and alfa relaxation data approximated by VFT model (b).

On the contrary, an ER/PDMS blend (Fig. 14a) exhibits significant differences from ER spectrum which means there is no chemical bonding between PDMS and ER as in the previous case, which is mainly down to non-presence of compatibilizator.

3.1.4 Rheological properties

Rheological measurements were carried out at different isothermal temperatures to characterize physical transformations such as gelation that take place during curing. Figure 16 depicts the typical rheological behaviour at 80°C through polymerization of neat ER and ER with DCP (ER/DCP2) with the time evolution of *G′* and *G′′* of the developing gel.

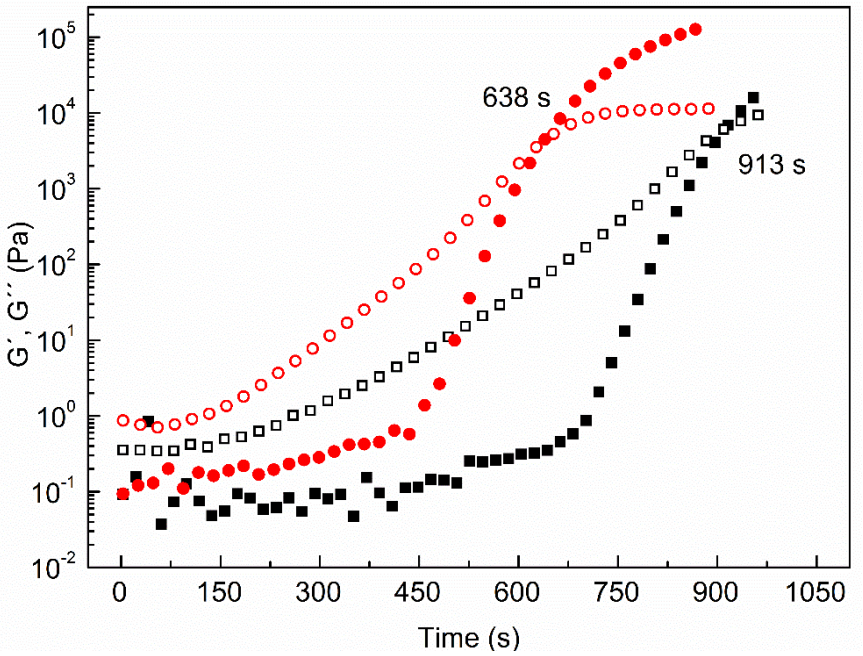

Fig. 16 Storage, G′, (solid) and loss, G′′, (open) moduli as a function of time for: ER(■, □), ER /DCP2 (●,○) at 80°C.

Initially, the system is in the liquid state with low stiffness and with *G′′* dominating over *G′*, both almost constant in time. This zone represents the state of the system before the start of the curing process. However, as the curing and the resulting cross-linking progress, both viscoelastic moduli increase until a crossover of *G′/G′′* occurs. This point shows that the gelation of the system is approximately 913 s for neat ER, while, for ER with DCP, it is only 638 s.

The results obtained show that DCP speeds up the curing of ER as far as it plays the role of a compatibilizing agent in polymer systems at all temperatures investigated (60-100) °C as indicated in Table 8. The compositions with DCP have also significantly lower curing time compared with the corresponding compositions without DCP for the systems ER modified by polysiloxane. It should also be noted that the curing time of resin generally modified by polysiloxane decreases with increasing polysiloxane content. The curing time

variation is determined by the dissimilarity between the crosslinking density and the size of rubber domains [100]. As can be also seen in Table 6, a slight difference in *G′/G″* at the crossover point was observed in samples ER/VT-PDMS10/DCP2 (612 s) and ER /VT-PDMS10 (632 s), while samples ER /PDMS10/DCP2 (690 s) and ER /PDMS10 (815 s) exhibited a significant difference at this crossover point. Both of these shifts confirm that the addition of DCP speeds up the curing process and more significantly for ER systems modified by PDMS compared with its analogue modified by VT-PDMS. Furthermore, an increase in the curing temperature leads to a decrease in the curing time, which indicates that the curing process is thermally activated.

The results of a single-frequency test represent only an approximate gelation point since, as the transient gel network structure forms, stress relaxation also takes place.

Tab. 6 Rheological gelation times at T_{cure} of 60, 80, and 100 C for given polymers.

Samples	**T (°C)**	**Single frequency test**	**Multiwaves test**
ER	60	2642	2047
ER	80	913	782
ER	100	279	210
ER/DCP2	60	2292	2002
ER /DCP2	80	638	447
ER /DCP2	100	212	167
ER /VT-PDMS5	80	660	570
ER /VT-PDMS10	80	632	420
ER /VT-PDMS15	80	695	700
Ee/VT-PDMS10/DCP2	80	612	449
ER /PDMS5	80	850	500
ER /PDMS10	80	815	453
ER /PDMS15	80	665	367
ER /PDMS10/DCP2	80	690	500

So, unless measurements on the gelling system are made extremely rapidly, the exact time of gelation is obscured by changes due to stress relaxation [101] that is why the stress relaxation is precisely captured in a multiwave test. Apart from the discussion related to the single-frequency test, Table 3 summarizes also rheological gelation times for systems under investigation obtained via multiwave tests. Evidently, a variation in the gelation time measured by two methods shows the same tendency, namely, the curing time decreases with DCP presence within the system as well as with incorporation of polysiloxane into the system.

Fig. 17 depicts complex viscosity versus time at 80 °C for epoxy resin modified by polysiloxane and its composition with DCP. The compositions with DCP have a significantly lower curing time compared with the corresponding compositions without DCP. It should also be noted that the curing time of resin generally modified by polysiloxane decreases with increasing polysiloxane content. According to [101], the curing time variation is determined by the dissimilarity between the crosslinking density and the size of rubber domains.

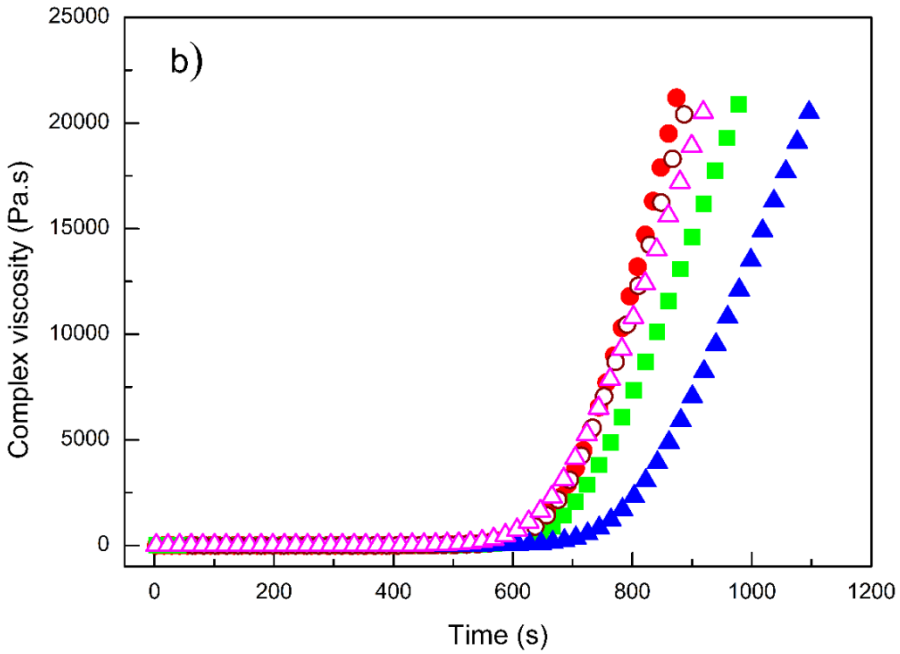

Fig. 17: Complex viscosity vs time for: ER/DCP2 (●), ER/VT-PDMS10 (■), ER/VT-PDMS10/DCP 2 (○), ER/PDMS10 (▲), ER/PDMS10/DCP 2 (△) at 80 °C.

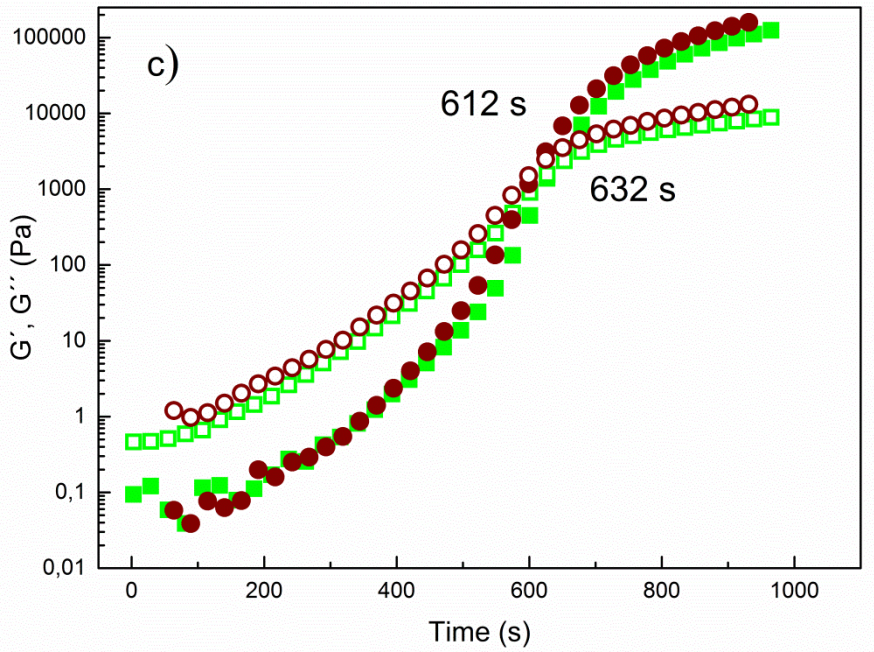

Fig. 18: Storage, G′, (solid) and loss, G′′, (open) moduli as a function of frequency, f, for:ER/VT-PDMS10 (■, □), ER/VT-PDMS10/DCP 2 (●,○) at 80 °C.

For polymer systems of epoxy with 10 wt.% of VT-PDMS (Fig. 18c) and epoxy with 10 wt.% PDMS (S) (Table 8) tested by a single frequency method at 80°C, where DCP is added, a slight difference in *G′/G″* at the crossover point was observed in samples ER/VT-PDMS10/DCP2 (612 s) and ER/VT-PDMS10 (632 s), while samples ER/PDMS10/DCP2 (690 s) and ER/PDMS10 (815 s) exhibited a significant difference at this crossover point. Both of these shifts confirm that the addition of DCP speeds up the curing process and more significantly for ER systems modified by PDMS compared with its analogue modified by VT-PDMS.

In Fig 19, the complex viscosity versus time is plotted at different isothermal curing temperatures (60, 80, and 100 C) for polymer systems ER, ER/VT-PDMS5 and ER/PDMS5 cured without DCP. An increase in the curing temperature leads to a decrease in the curing time, which indicates that the curing process is thermally activated. It was found that addition of VT-PDMS decreases the curing time, while PDMS increases the curing time. This effect was found at all temperatures.

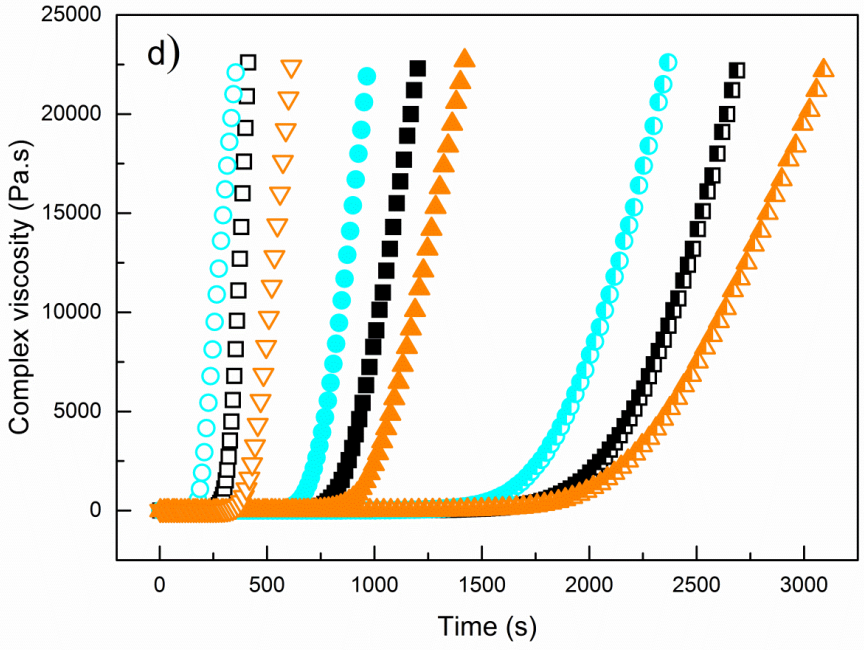

Fig. 19 Complex viscosity vs time at temperature 60 °C (half open, half solid), 80 °C (solid) and 100 °C (open) for: ER (black square), ER/VT-PDMS5 (blue ring) and ER/PDMS5 (orange triangle).

The results of a single-frequency test represent only an approximate gelation point since, as the transient gel network structure forms, stress relaxation also takes place. So, unless measurements on the gelling system are made extremely rapidly, the exact time of gelation is obscured by changes due to stress relaxation [102]. That is why the stress relaxation is precisely captured in a multiwave test. Apart from the discussion related to the single-frequency test, Table 3 summarizes also rheological gelation times for systems under investigation obtained via multiwave tests. Evidently, a variation in the gelation time measured by two methods shows the same tendency, namely, the curing time decreases with DCP presence within the system as well as with incorporation of polysiloxane into the system.

3.1.5 Mechanical properties

Dynamic mechanical properties

Dynamic mechanical analysis is a powerful technique for the investigation of viscoelastic properties of polymer blends and composites as a function of the temperature and modified interfacial compatibility between different phases as well as for the determination of the glass transition temperatures (T_g). Storage moduli *E'* and loss factors tan δ of neat epoxy, epoxy with DCP and ER/polysiloxane blends with or without DCP are shown in Figures 20 and 21.

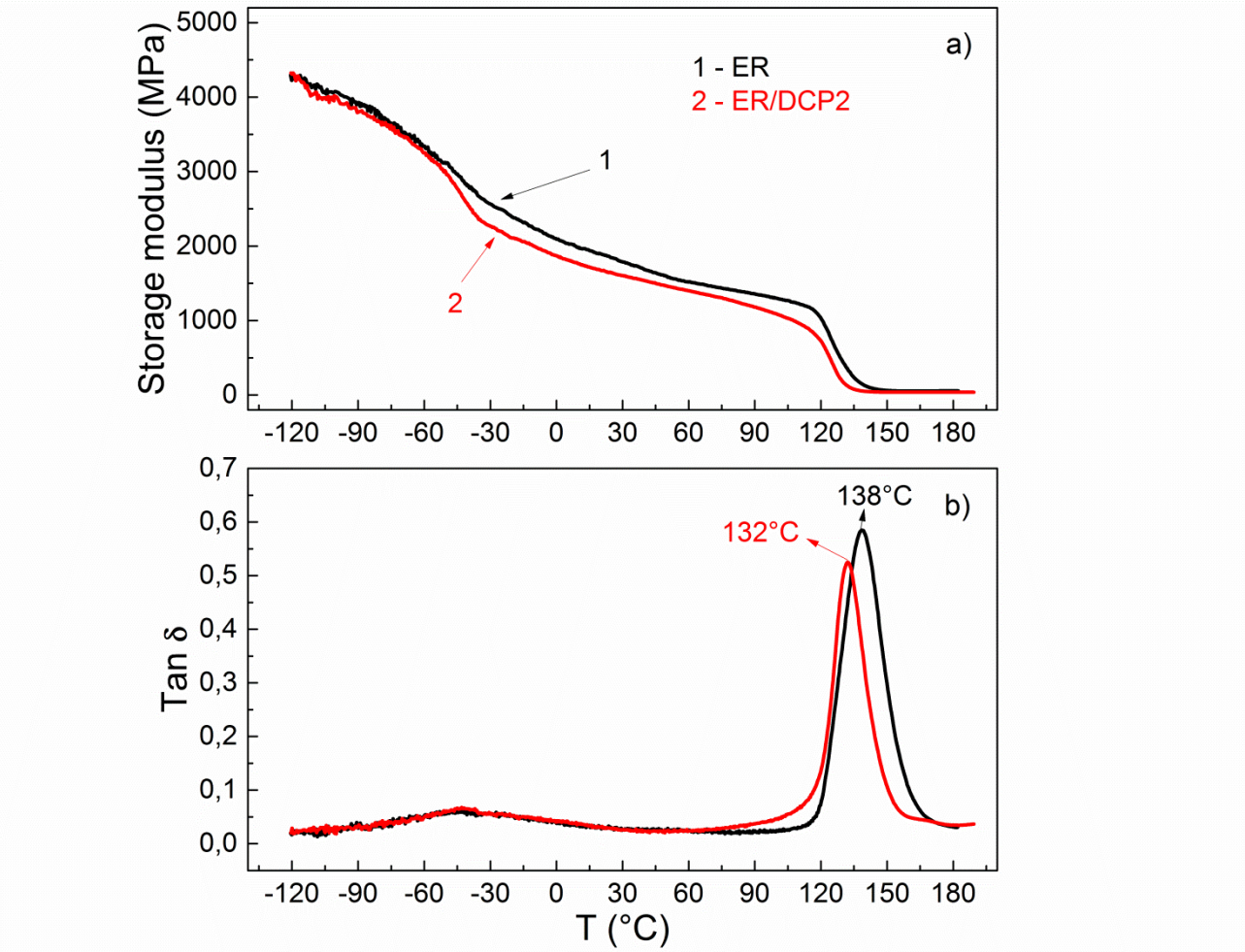

Fig. 20. Storage modulus (a) and loss factor (b) as a function of temperature for 1- ER, 2 - ER/DCP2.

As seen in Figure 20a, the neat ER at -120 C exhibits a storage modulus of 4300 MPa; however, around -40°C, there is a first decrease in the storage modulus (2600 MPa), which corresponds to the movement of the side groups of the polymer chain (gamma-relaxation). A significant temperature drop of *E'* at 140°C can be related to the segmental motion of polymer chains (alpha-relaxation) in epoxy resins, which is in good agreement with the dielectric spectroscopy data (Figure 14). Typically, as the temperature approaches the T_g, the storage modulus markedly drops. The T_g was determined from as the maximum value of the tan δ peak. The neat epoxy resins showed T_g at 138°C. DCP (2 wt. %) was added to ER to improve the curing process.

The addition of DCP decreased the storage modulus of the epoxy sample about 20% and shifted its T_g to lower temperatures about 6°C, which indicates changes upon the molecular structure.

Storage modulus and tan d of ER modified by VT-PDMS at 5, 10 and 15 wt. %, are shown in Figure 21. As was observed for VT-PDMS modified ER, storage

modulus before the main transition (T_g) decreased with increasing concentration of VT-PDMS. This decrease is due to the presence of VT-PDMS, and it affects T_g which decreases (from –139°C to –135°C) with rubber content. Moreover, it is apparent that 5 and 10 % temperature dependence of E´ have qualitatively very similar behaviour while 15 % exhibits less sharp relaxation of storage modulus with temperature. These findings are in good agreement with sample structure, where first two concentrations, despite obvious differences in rubber particle concentrations, have otherwise almost identical morphology (rubber particles with cracks), while 15% exhibits damage (plastic) zones around rubber inclusions without any clear cracks (Fig. 12 f). These changes indicate transition between two different mechanisms of energy absorption in this system making the composite less brittle. In other words we have observed ductile brittle transition shifting to larger particle size as the rubber content is increased over 10 wt. % [97] .Thus addition of rubber over 10 wt. % (optimum rubber content with maximal impact strength) does not lead to further increase in the impact strength of the composite.

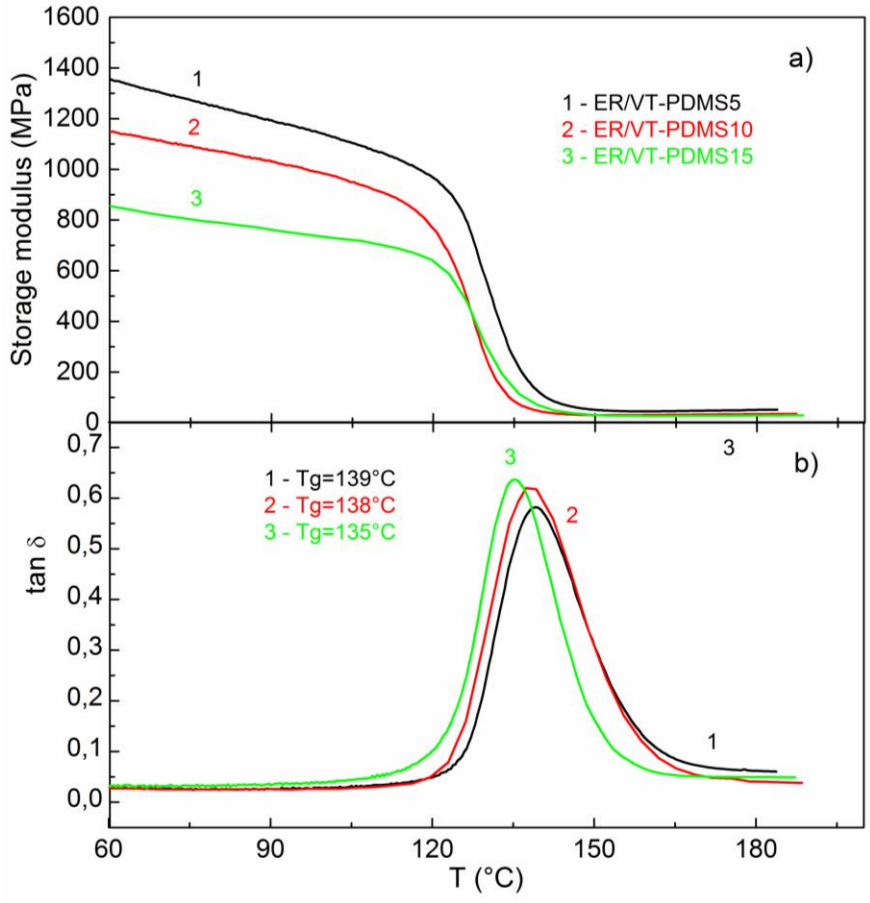

Fig. 21 Storage modulus (a) and tan d (b) on temperature for ER modified by VT-PDMS.

Thus addition of rubber over 10 wt. % (optimum rubber content with maximal impact strength) does not lead to further increase in the impact strength of the composite.

Figure 22 shows storage moduli and tan δ curves of epoxy resins blended with 10 wt. % of VT-PDMS and PDMS. The addition of VT-PDMS and PDMS influenced viscoelastic properties of epoxy resins differently. Both polysiloxanes admixed with epoxy resins caused a formation of two phase systems. VT-PDMS decreased T_g of epoxy resins about 3°C and PDMS increased T_g of epoxy resins about 10°C. These differences may correspond with different end-functional groups of polysiloxanes, which control their dispersion in epoxy resins as well as viscoelastic properties.

The addition of DCP into epoxy resins/polysiloxane blends slightly increased stiffness, which can indicate the improvement in the compatibility between epoxy resins and polysiloxane due to the new chemical interactions. Moreover, the lower values of T_g indicate that DCP could reduce a crosslinking density of epoxy resins/polysiloxane.

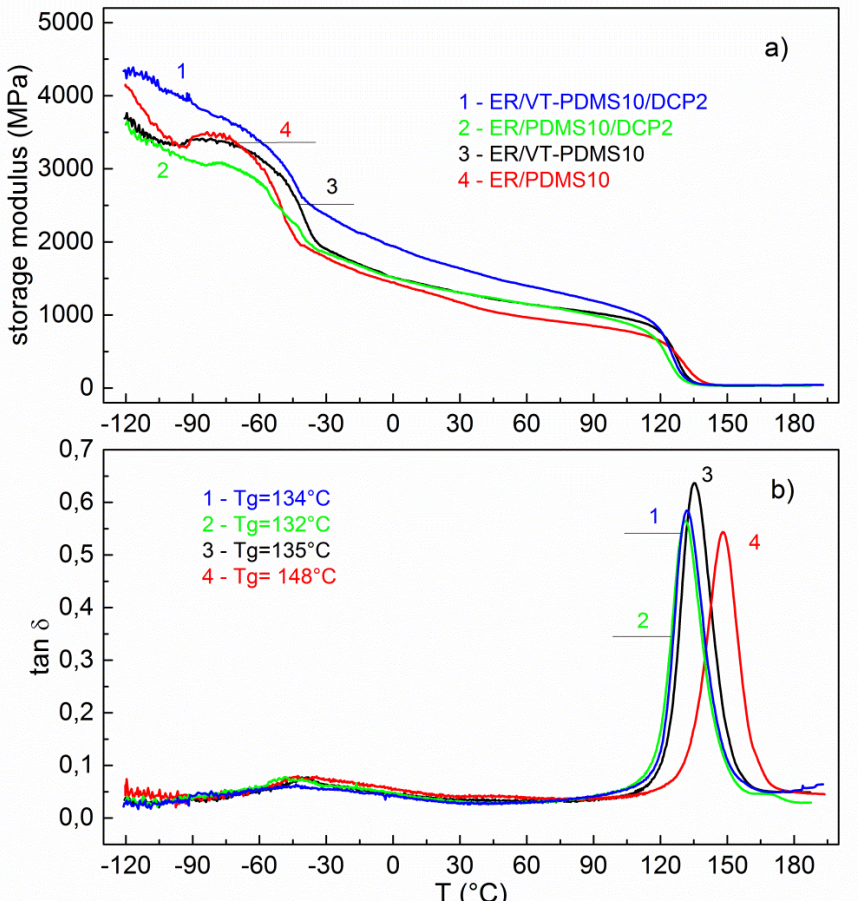

Fig. 22 Storage modulus (a) and loss factor (b) as a function of temperature for 1 ER /VT-PDMS10, 2 - ER /PDMS10. 3 - ER /VT-PDMS10/DCP2, 4 ER/PDMS10/DCP2.

Impact strength

The highest impact strength was recorded in ER/VT-PDMS10/DCP2 with value of 17 ± 2 kJ/m^2, which equals a 70 % improvement. The enhancement of impact strength in the DCP modified blends is due to the higher density of the network and inter-chain bonds in ER. The formation of inter-chain bonds is supposed to take place during the melt blending.

The improvement in the toughness of the polysiloxane systems stems from the reduction in the crosslinking density and, to a lesser extent, from flexibilization. The increase in the impact strength toughness behaviour of ER/VT-PDMS samples showed a better energy-transfer mechanism because of the excellent interfacial adhesion and bonding with the matrix.

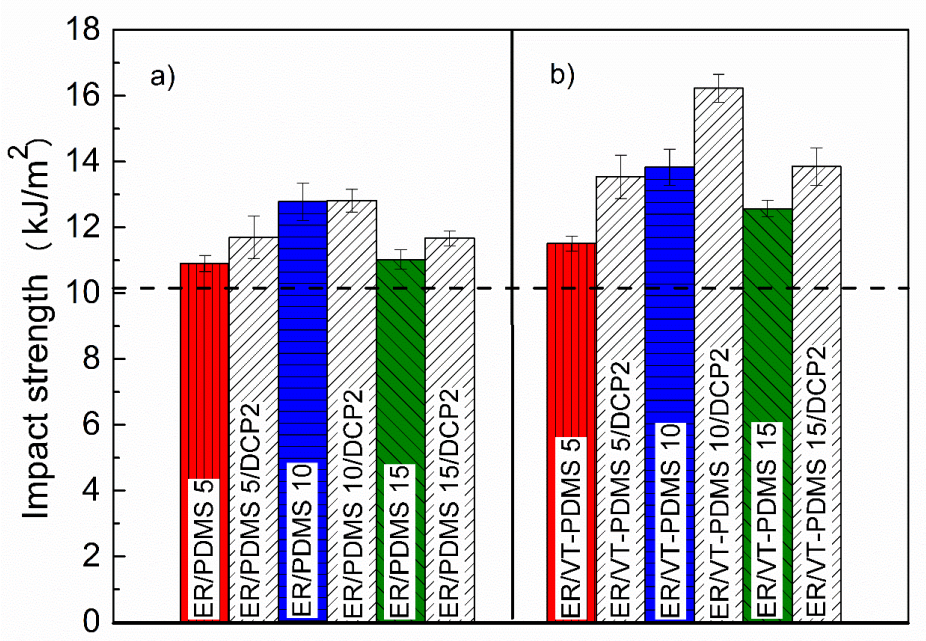

Fig. 23 Impact strength of epoxy polymer blends with (a) PDMS and (b) VT-PDMS polymer. Dashed line is for neat epoxy.

.

Lap shear strength

Adhesive bonding properties of ER and its polymer blends with polysiloxane and DCP were investigated on metal plates. Samples with polysiloxane without DCP show lower values (379±22 kgf) than the neat resin (417±31 kgf). The maximum value of lap shear strength was observed for 10 wt% of VT-PDMS in the presence of 2 wt.% of DCP (431 ± 27 kgf). This result shows that peroxide improves the interfacial adhesion between ER and polysiloxane.

Optimal composition leading to a considerable increase in ER toughness without significant reduction of polymer system modulus, glass transition temperature and interfacial adhesion was found. This composition comprising ER filled with

10 wt. % of VT-PDMS and 2 % of DCP has following physical-mechanical properties: storage modulus is 2000 MPa (at 20 °C), Tg = 138 C, lap shear strength is of 430 kgf and impact strength is of 17 kJ/m2, which equals 70% improvement over pure ER. Transition from brittle to ductile fracture mechanism with increasing elastomer content above 10 wt. % in ER was registered by morphological (SEM) as well DMA investigations. It is responsible for observing maximum impact strength at this concentration. Not only rubber inclusions size and concentration but also compatibility between VT-PDMS and ER is crucial for achieving aforementioned properties. The compatibility between ER and VT-PDMS can be seen from the following results: i) the increase of storage modulus in the rubbery area (above glass transition), ii) the shift of the glass transition temperature to higher temperatures, iii) narrowing of tan δ peak. This means that, for higher amount of DCP (2 wt.%), the phase separated VT-PDMS elastomer at 10 wt. % leads to improved fracture toughness of the ER network and can be applied in immiscible polymer systems as a modifier.

3.2 Preparation of polysiloxane composites filled with CB and CNT

3.2.1. A solvents dispersion method for modification of carbon nanotubes

The CNTs (1 g) were dispersed in neat NMP (40 ml) by ultrasonic treatment. The ultrasonic treatment has been carried out at 40 % amplitude and 0.4 cycles for 1 hr. After sonication, the visual inspection confirmed the absence of aggregates in all dispersions. The dispersion was immediately vacuum-filtered through binder-free glass fiber filters with 125 μm porosity. After filtration, the CNT-NMP was dried in drying oven (Binder, ED, USA) at 200 °C from 2 hrs.' to 1 day. As can be seen from Fig.24 and Fig. 25 modified CNTs are dispersed better than raw CNTs.

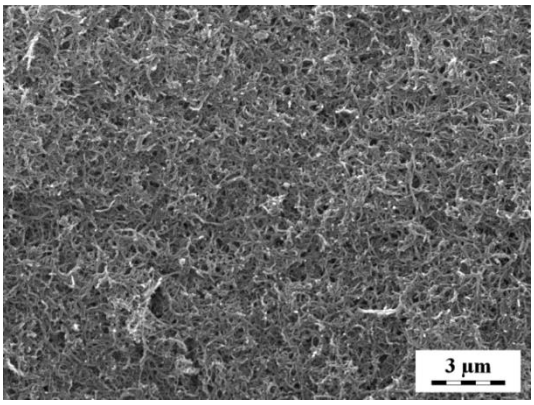

Fig. 24 SEM image of raw CNTs before surface modification

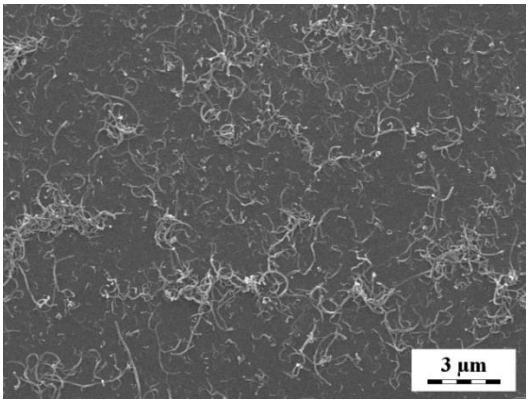

Fig. 25 SEM image of CNTs after modification by NMP

3.2.2. Current -Voltage characteristics

The current-voltage (I-V) dependencies of the composites with different amount of CNT, CNT-NMP and CB are shown in Figs. 26-28. A semiconducting character of the composites in transition area causes non-linearity of the current-voltage (I-V) characteristics. The non-linearity of I-V curves is quite pronounced for the composites with the low content of CNTs (~ 1–1.5 vol. %, Fig. 26) as well as for the composites containing 1–3.4 vol.% of CNT-NMP (Fig. 27) and 1–8 vol.% of CB (Fig. 28).

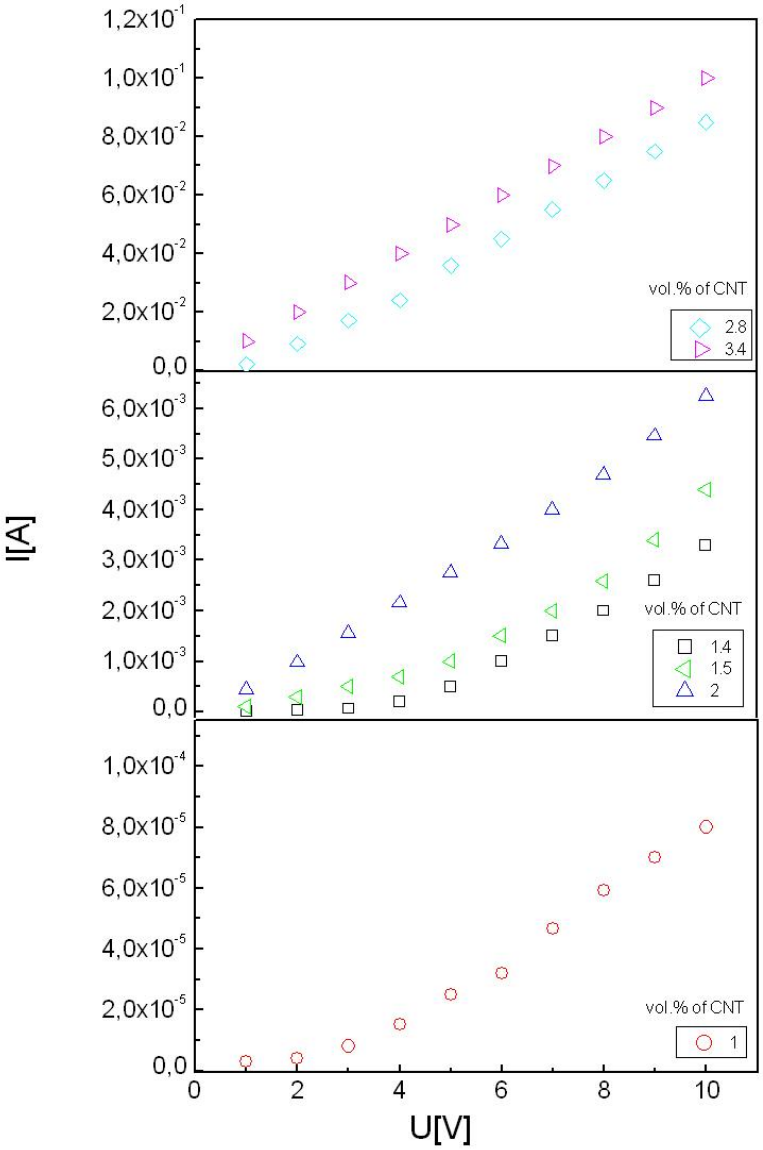

Fig. 26 I-V characteristic for the PDMS/CNT

This can be explained by an activation conductance mechanism, where the presence of a certain number of conducting paths determines the increase of conductivity with increase of voltage: more electrons are activated and hop over the non-conducting polysiloxane barriers between the conducting fillers islands/ clusters.

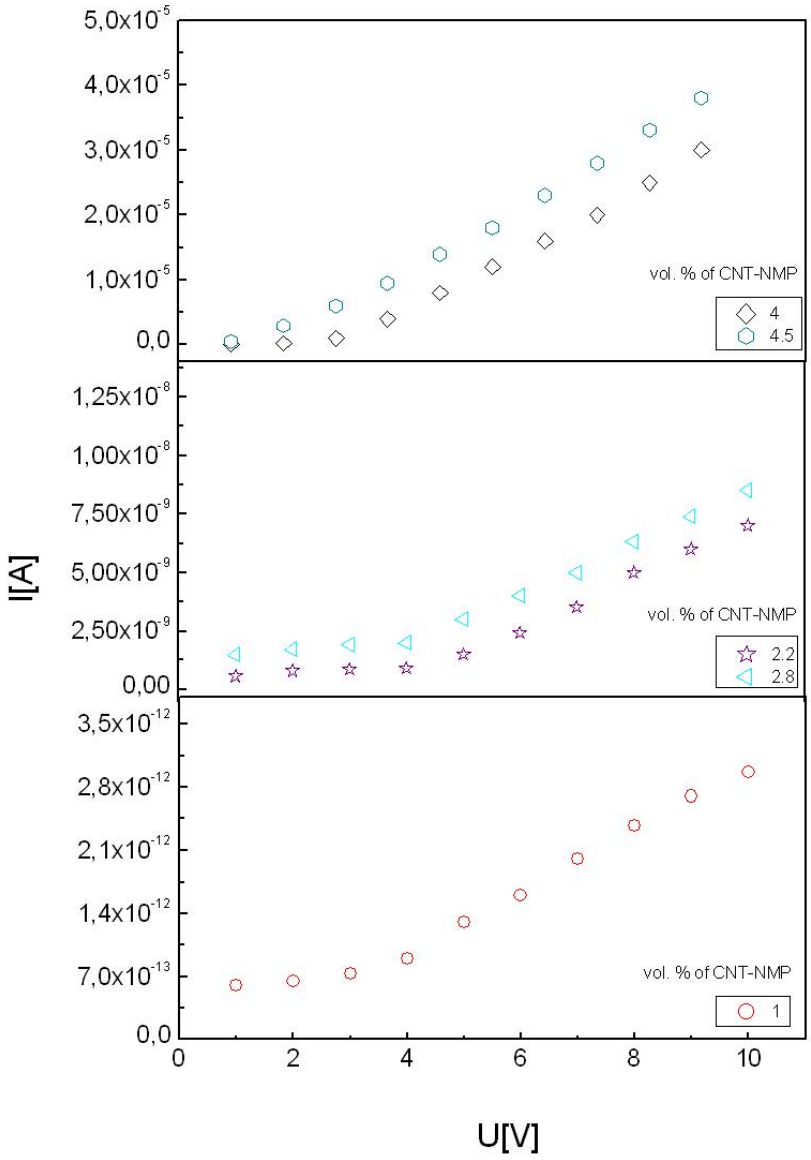

Fig. 27 I-V characteristic for the PDMS/CNT-NMP

With increasing content of filler (~ 2–3.4 vol.% of CNT (Fig. 26), 4–4.5 vol.% of CNT-NMP (Fig. 27) and 9– 12 vol.% of CB (Fig. 28) the I–V characteristics become linear. Thus, the ohmic charge transfer is given by direct contacts and the current increases with the voltage linearly

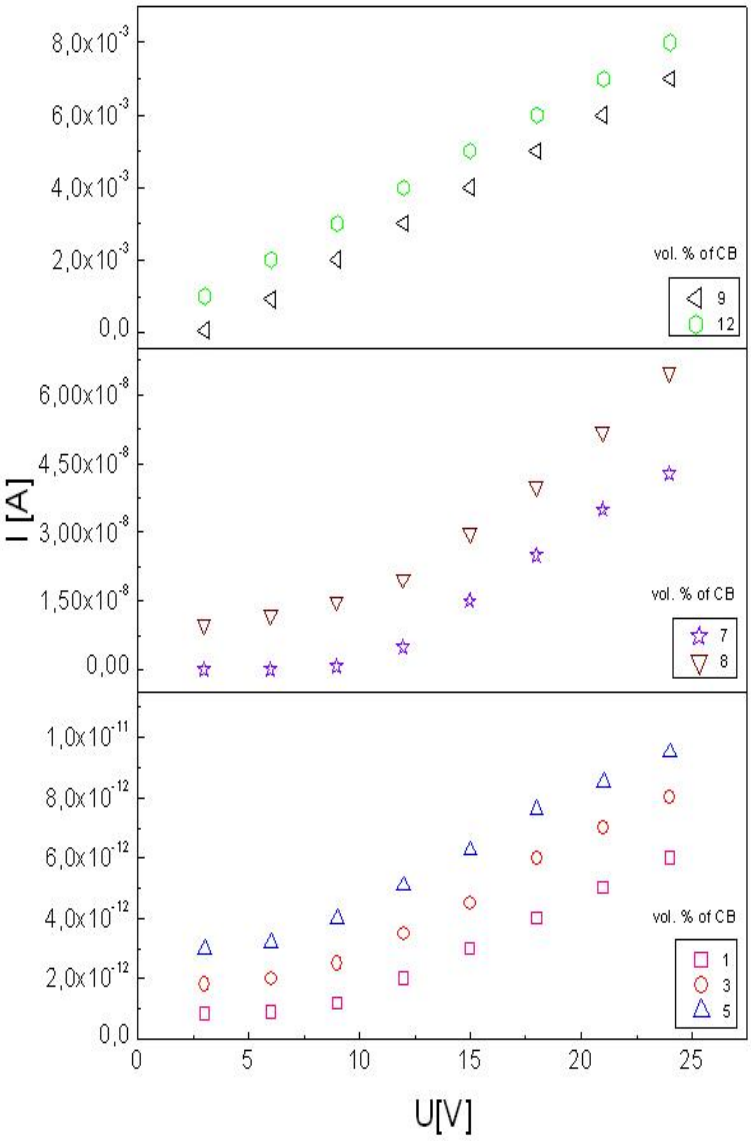

Fig. 28 I-V characteristic for the PDMS/CB

3.2.3. DC electrical conductivity

We presume that once the volume fraction of CNT reaches a critical value, i.e. the percolation threshold, the new conductive structure starts to form. This indicates a phase transition from insulator to conductor state. The electrical conductivity of silicone polymer composites depends on the concentration of conductive filler. Fig. 29 shows the dependence of DC specific conductivity against conductive filler content measured at laboratory temperature 25°C for PDMS/CNT, PDMS/CNT-acetone, PDMS/CNT-NMP and PDMS/CB composites. As regarding the pure polysiloxane matrix, it is an electrical insulator with very low value of conductivity ($\sigma_{DC} = 5 \cdot 10^{-12}$ S cm^{-1}).

In the Fig. 29 we can see comparison of electrical properties of polysiloxane

with the non-dispersive (CNT) and dispersive (CNT-acetone,CNT-NMP) carbon nanotubes. Further, we studied conductive systems with particle filler (CB) in polysiloxane. The electrical measurements carried out on samples (PDMS/CNT) revealed that conductivity starts to rise at the filler content of about 1 vol. %. The values of electrical conductivity of the PDMS/CNT increased by more than nine orders of magnitude, i.e. from 10^{-12} to 10^{-3} S cm^{-1} in the range of filler content of 1 to 3.4 vol. %. The electrical conductivity of PDMS/CNT showed slightly linear increase and reached 10^{-1} S cm^{-1} corresponding to conductive material when the CNTs content was 2.8 vol. %. The value of percolation threshold was reached at low content of conductive filler (φc ~ 1 vol. %), which is caused by poor dispersion and big bundles (agglomeration) where charge carriers are transported through conductive bundles of CNTs. A different behaviour is noted for the carbon nanotubes modified by N-methyl-2-pyrrolidon and acetone, which caused insulation and separation of CNTs and exerted influence on the shift of percolation threshold to higher value (φc ~ 4 vol. %, 2,5 vol. %). This value of percolation threshold for CNT-NMP and CNT-acetone composite indicates good homogeneity and dispersion of CNTs in the polysiloxane. The separation of CNTs decreases the probability of percolation cluster formation but increases the area of the CNT-polymer matrix interface. As can be seen, the good dispersion of CNTs shifts φ_c to the higher value. The percolation threshold of polymer composites with CB amounts to 9 vol. %. Such a high value of percolation threshold is caused by low aspect ratio of filler. Generally, it is known that with an increase in the aspect ratio of filler the percolation threshold shifts to higher values.

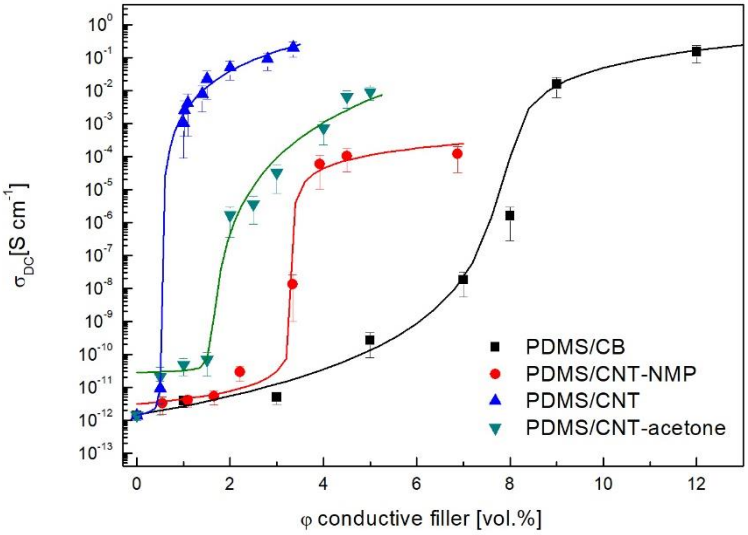

Fig. 29 The dependence of electrical conductivity σ_{DC} on the conductive filler content in the composite.

The percolation threshold of polymer composites with CB amounts to 9 vol. %. Such a high value of percolation threshold is caused by low aspect ratio of filler. Generally, it is known that with an increase in the aspect ratio of filler the percolation threshold shifts to higher values.

3.2.4. AC electrical conductivity

In Fig. 30 AC conductivity is presented as a function of applied frequency for all nanocomposites containing different conductive fillers (CNT, CNT-NMP, CB). AC conductivity for all systems has been calculated from the dielectric loss factor. For the composites AC conductivity is both frequency and CNT content dependent and increases by almost 8 orders of magnitude with increase in both frequency and volume content of fillers. AC spectra of specimens with filler concentrations below the percolation threshold display curve similarity and values proximity. For system, PDMS/CNT an abrupt increase of conductivity is observed (up to 6 orders of magnitude) in the specimens having CNT content in a range of 1.5 to 2 vol. %. This pronounced alternation is a first-hand indication that the percolation threshold has been already reached. AC conductivity spectra for the composites with 2.4 and 8 vol. % of filler (CNT, CNT-NMP and CB) content exhibit a wider plateau of the so called apparent DC conductivity. Fig. 30 shows the frequency dependence of σ_{AC} for the composites containing different conductive fillers (CNT, CNT-NMP, CB) measured at room temperature. It can be seen that σ_{AC} increases linearly with the frequency, showing a typical behaviour for non-conductive or semi conductive materials. Again, the increase of conductivity at low frequencies with the incorporation of nanotubes is observed with a percolation threshold between 2.8 and 4 vol. % of CNT-NMP at 100 Hz (considered to be the DC conductivity) at room temperature. The conducting state of the composites becomes very pronounced above the percolation threshold. Composites containing 4–4.5 vol. % of CNT-NMP are definitely above the percolation threshold as the power law regime is particularly shifted to higher frequencies and thus the material behaves as an ohmic conductor with conductivity almost independent of frequency. AC electrical conductivity of polysiloxane with varying content of carbon nanotubes is shown in Fig. 30a). The bulk electrical conductivity of polysiloxane filled with 1and 1.5 vol.% of CNTs increases with increase in frequency as expected for an insulating material with values of 10^{-12} S cm^{-1} and 10^{-11} S cm^{-1} at 10^{1} and 10^{2} Hz, respectively. A drastic increase in conductivity is observed for polysiloxane at 2 vol. % of CNT (10^{-6} S cm^{-1}) where the electrical conductivity is independent over a wide range of frequency indicating the formation of

percolating path of CNT. Polysiloxanes with 2, 2.8 and 3.4 vol. % of CNT exhibit a frequency independent plateau up to a critical frequency above which the conductivity dispersion is observed.

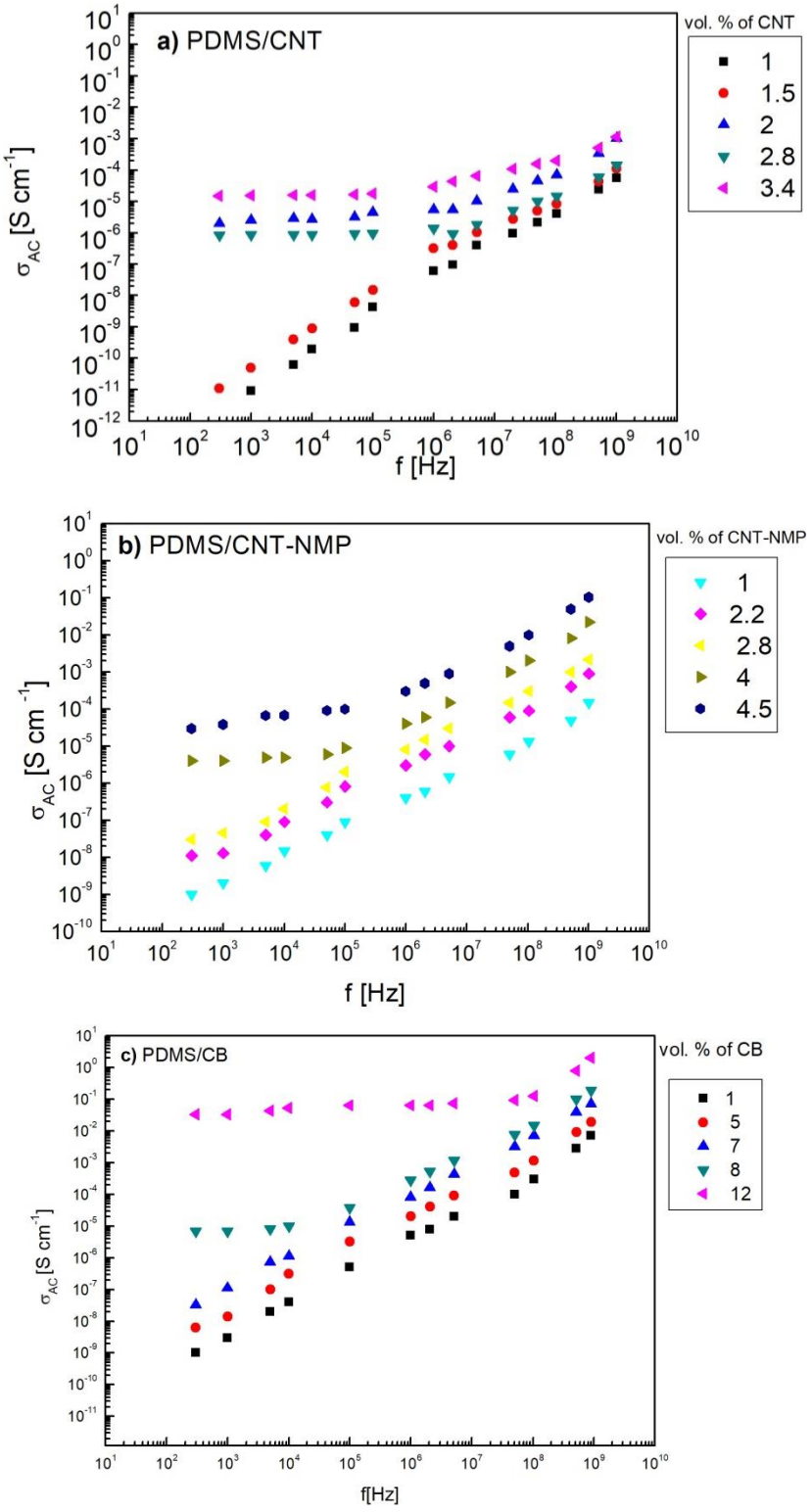

Fig. 30 The frequency dependence of electrical conductivity σ_{AC} for the: a) PDMS/CNT; b) PDMS/CNT-NMP; c) PDMS/CB

3.2.5. Dielectric properties

Additional frequency dependent measurements of the electrical properties are very useful for the investigation of the conduction mechanisms of polymer composites. Electrical properties can be determined at various frequencies. The frequency dependencies of the real part of the permittivity of conducting composites are shown in Fig. 31 characterizing the polarization of systems in an alternating field. With the increase in content of CNTs from 1 to 3.4 vol. % ε' increased. The highest value of ε' for the composite filled with 2.8 vol. % of CNT reached ~ 11^6. Real part of permittivity for PDMS/CNT-NMP composite is about 10 at approximately the same content of the filler (Fig. 31 b). With increasing, content of conductive filler this behavior changes. At low frequencies, permittivity significantly increases with the increase in filler content but at a certain frequency a relaxation processes take place resulting in a drop of the permittivity with increasing frequency. The difference in ε' between the PDMS/CNT and PDMS/ CNT-NMP composites increases rapidly, as the filler concentration increases. At 2.8 vol. % of filler ε' for PDMS/ CNT and PDMS/CNT-NMP is 116 and 10 respectively. However, at 3.4 vol. % of filler ε' of PDMS/CNT is about 270, whereas in PDMS filled with 4 vol. % of CNT-NMP ε'= 20. The systems of PDMS/CNT with poorly dispersed CNTs (with large bundles of CNTs) and those with well modified CNTs by NMP exhibit significant differences in the ε' caused by the difference in number of charge carriers. The lower values of ε' of materials (PDMS/CNT-NMP) were due to the organic solvent (NMP), which caused the insulation and separation of individual CNTs. It is reasonable that higher ε' can be obtained when the composites are filled with higher content of conductive filler due to the higher interfacial polarization at the conductive filler/ polysiloxane interface. The interfacial polarization can be more easily induced at lower frequency. Furthermore, the displacement current significantly lags behind the build-up potential as the frequency increased. Thus, it is reasonable that ε' decreased with increasing frequency and exhibited a visible frequency-dependent dielectric response. Fig. 31c shows dependencies of ε' on frequency for the composites with CB. The ε' is ~ 10 for polysiloxane filled with 5 vol. % of CB. It means that for composites filled with 5 vol.% of carbon black which is just a little higher than that for volume content of CNTs, the value of ε' is the same. It is caused by the shape of filler in particular form. Aspect ratio can significantly influence behaviour of polymer composites in AC electric field. The particular filler (CB) has L/D ≈ 1, on other hand, fibrous filler (CNT) has L/D ≈ 10^2 –10^3 , which can

significantly influence the concentration of charge carriers at the end of fibrous filler and change values of ε'.

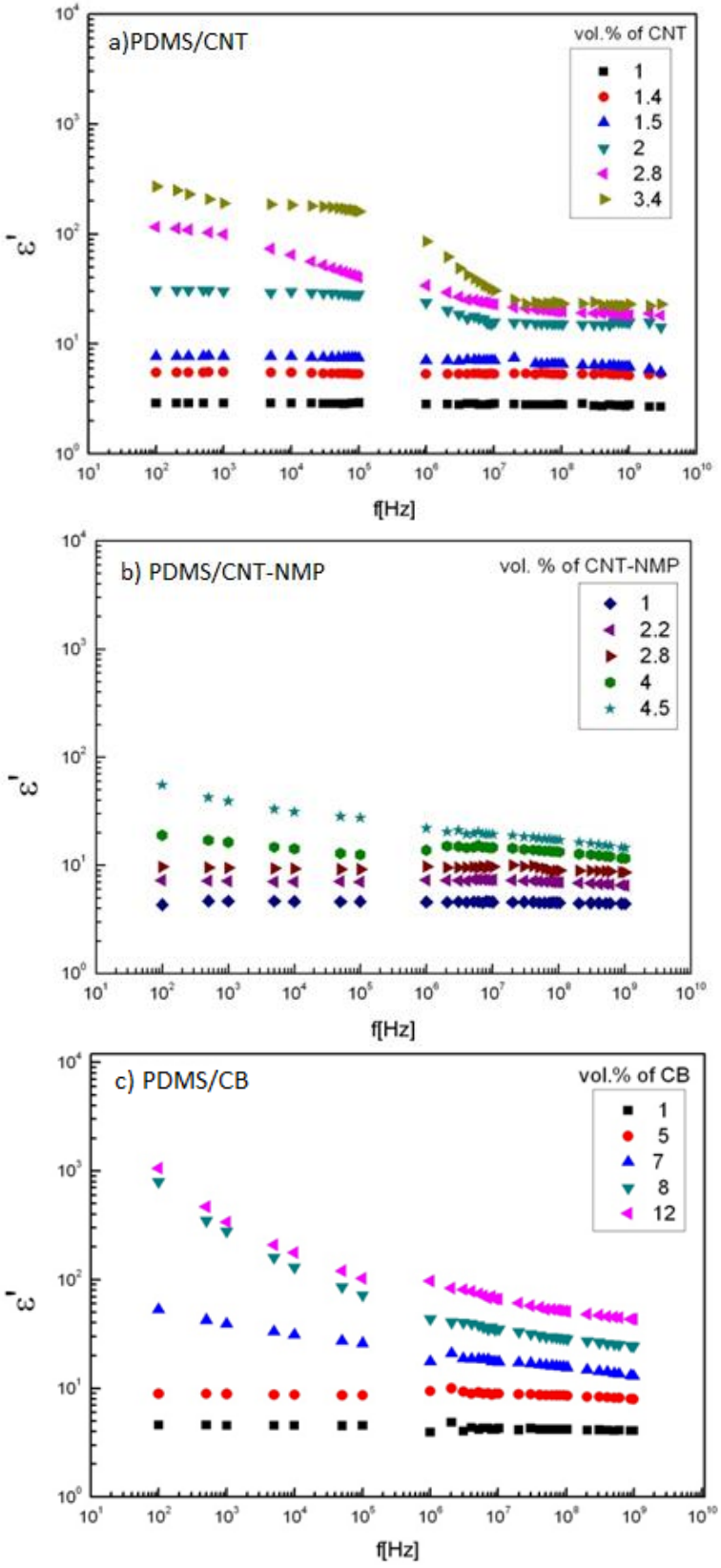

Fig. 31 The frequency dependence of real part of permittivity for the: a) PDMS/CNT; b) PDMS/CNT-NMP; c) PDMS/CB

Aspect ratio can significantly influence behaviour of polymer composites in AC electric field. The particular filler (CB) has L/D ≈ 1, on other hand, fibrous filler (CNT) has L/D ≈ 10^2 –10^3 , which can significantly influence the concentration of charge carriers at the end of fibrous filler and change values of ε'.

3.3 Effect of epoxy-polysiloxane blends microstructure on mechanical and electrical properties of nanocomposites.

CNT nanocomposites

Blending immiscible polymers is one of the most cost-effective methods to develop new materials with enhanced properties and performance than existing polymeric materials. It is well know that electrical conductivity of polymer blends filled with electrically conductive fillers depends on the percolation of the polymer phases and the percolation of the filler particles.

In the Fig. 32a we can see comparison electrical properties of three types of nanocomposites with polymer matrix (VT-PDMS, ER and SEF) and dispersive (CNT-aceton) carbon nanotubes (experimental data fitted by percolation model). CNT are strongly entangled forming aggregates due to Van der Waal's forces and to create polymer nanocomposites they have to be uniformly dispersed throughout the polymer matrix. CNTs were sonicated in solvent in order to achieve regular, homogenous distribution.

It can be seen that the percolation threshold has significantly shifted to lower concentration for SEF/CNT composite (0.6 vol. %) compared to 1.3 vol. % in the case of ER/CNT and VT-PDMS/CNT.

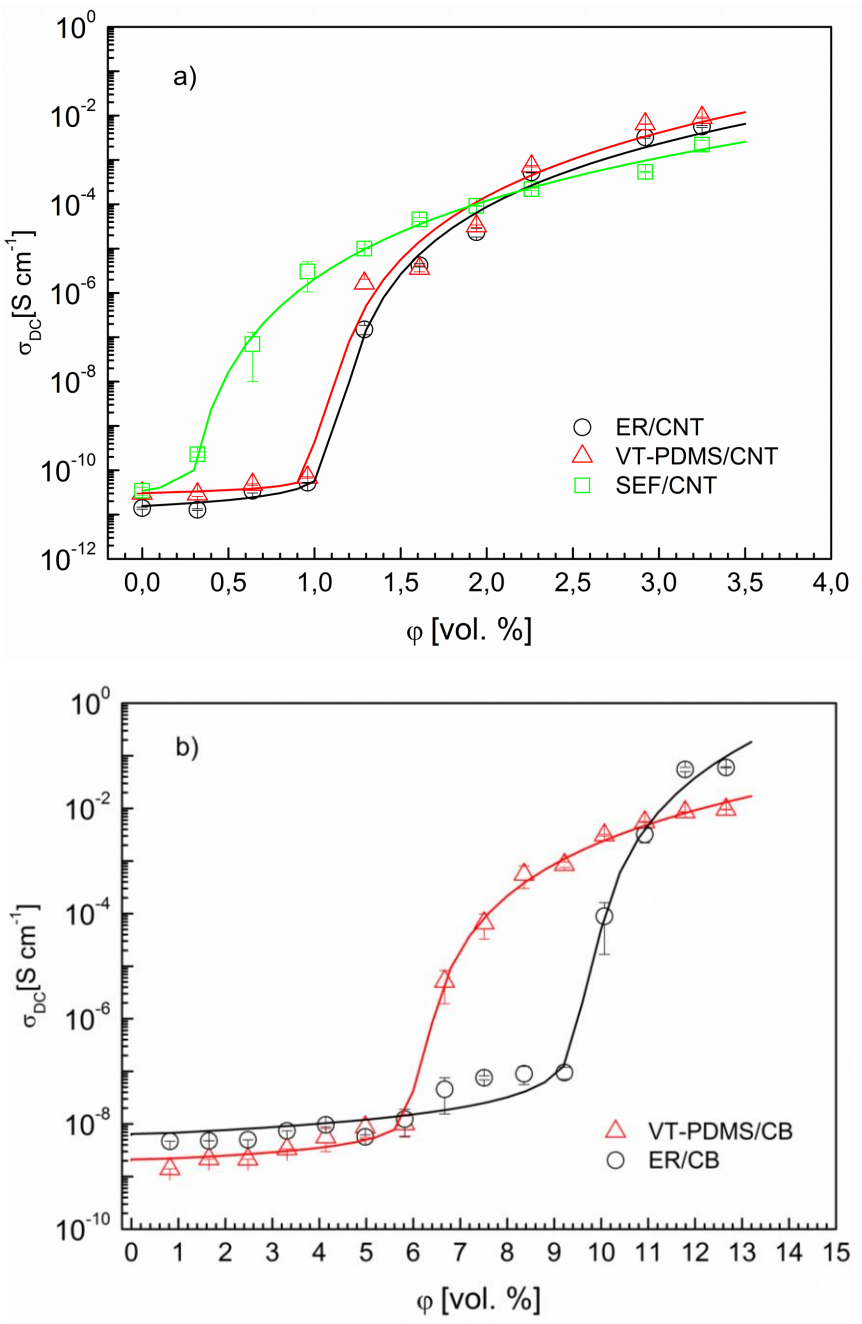

Fig. 32. The dependence of DC electrical conductivity on conductive filler a) CNT b) CB, content for polymer nanocomposites.

However, CB exhibited substantial difference in percolation threshold depending on the used polymer matrix (Fig. 32b). While ER/CB has a critical concentration of about 10 vol. %, CB mixed in VT-PDMS/CB shows decrease in percolation to 7 vol. %. This is probably due to different crystallinity of these two matrixes.

Comparing CNT and CB, it can be seen that CNT based composites have much lower percolation threshold (~1 vol.%) compared to CB (7 and 10 vol. % respectively; depending on matrix). This is a result of different aspect ratio of

each filler, where CNT clearly dominate.
Another way how to even further decrease the value of electrical percolation threshold is to utilize so called *double percolation*. The idea of double percolation introduces two polymers resulting in a polymer blend, which is subsequently filled with filler (Fig. 33). Such polymer blend must have co-continuous morphology so that both phases are said to be percolated. Finally, conductive filler has to be selectively dispersed in a continuous phase, which is ideally a minor component in order to get low percolation threshold.

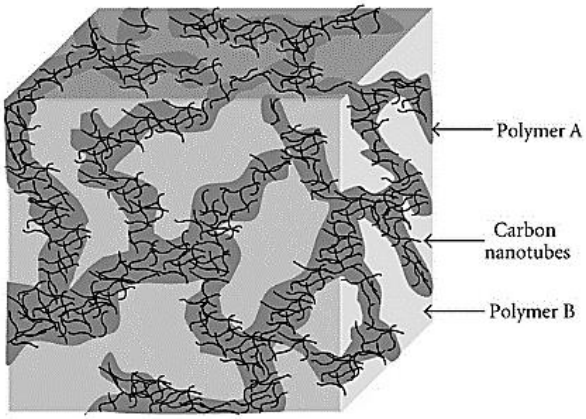

Fig. *33. Schematic illustration of the double percolation phenomenon.*

In the case of our blend only one of the phases is continuous (ER) while the other (polysiloxane) is present in the form of isolated inclusions creating so called "sea island" structure. Filler (CNT, CB) is then dispersed in the continuous phase.
Based on so obtained results of electrical percolation threshold, multicomponent systems (immiscible and partially miscible) with constant CNT content ~2 wt. % (1.3 vol. %) were prepared. The dependence of DC electrical conductivity on increasing volume ratio between polysiloxane (VT-PDMS and SEF) and ER (Fig. 34). The dramatic increase is registered at 5 wt. % PDMS and 20 wt. % SEF near the percolation threshold. The percolation threshold is reached at ER/VT-PDMS/CNT2 and ER/SEF/CNT2.

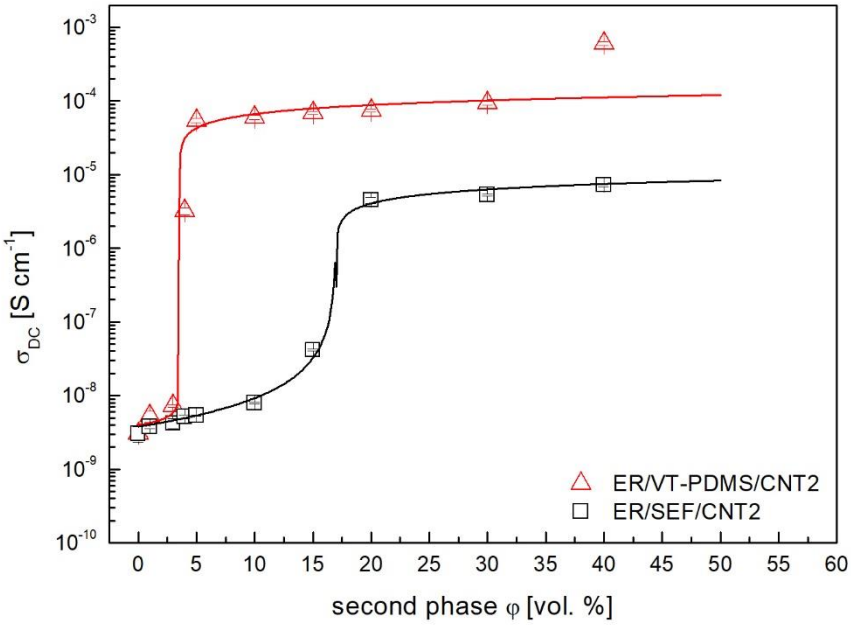

Fig. 34 The dependence of DC electrical conductivity on increasing content of PDMS and SEF in nanocomposites containing 2 wt.% of CNT. Experimental data is fitted by a percolation model vyhodit fitting (volume %)

It is established that the electrical properties of nanocomposites are influenced not only by the content of the CNT but also by the microstructure of the polysiloxane – epoxy resin system. Morphology was studied by scanning electron microscopy, in Fig. 35 we can see phase structure of nanocomposite ER/VT-PDMS/CNT2, for which jump change of electric conductivity (from 10^{-9} to 10^{-5} S cm^{-1}) was observed.

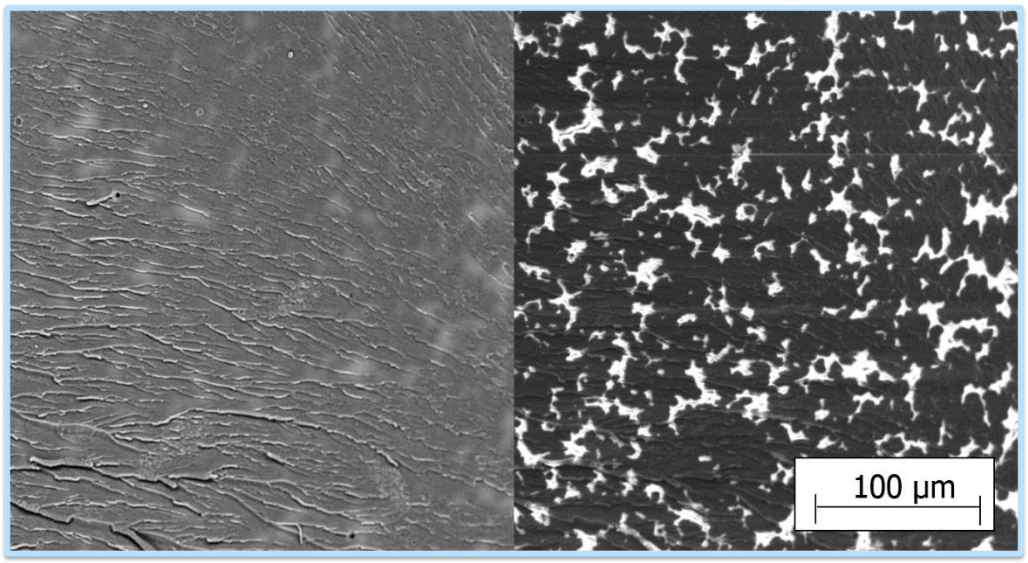

Fig. 35 SEM micrographs of multicomponent polymer nanocomposites (ER/VT – PDMS5/CNT2)

CNT are homogeneously dispersed in ER because its surface energy (50 mJ/m^2) is close to CNT value (54 mJ/m^2) while VT-PDMS exhibit values predominantly around 30 mJ/m^2, thus confirming our initial assumption of low affinity of CNT towards VT-PDMS.

On the other hand, multicomponent polymer nanocomposite ER/SEF20/CNT2 percolated only at 20 wt. % with conductivity of one order lower. The microstructure of this composite is shown in Fig. 36. For ER/VT-PDMS5/CNT2 we can observe a brittle structure of ER with VT-PDMS dispersed therein. ER/SEF20/CNT2 exhibits different structure with "sea islands" i.e. polysiloxane create integrated homogeneously dispersed particles of ER; thus, we can see miscibility between ER and SEF, however there is also a partial separation of polysiloxane component in the shape of anisometric droplets. Both systems created irregular droplets. This demonstrates that the systems are partially miscible. Both systems comprise homogeneously dispersed droplets of polysiloxane – a proof of an appropriate choice of preparation method.

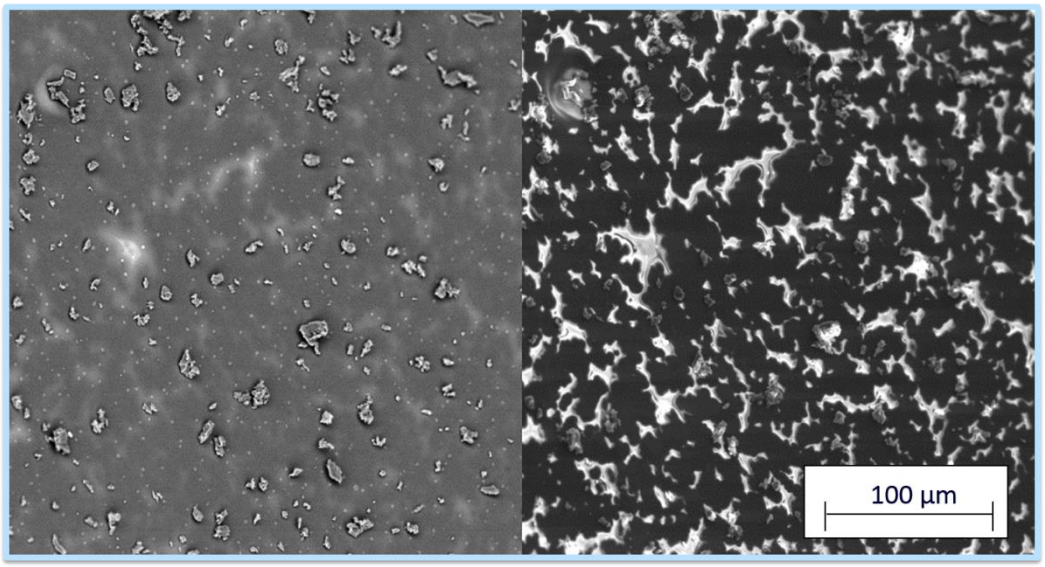

Fig. 36 SEM micrographs of multicomponent polymer nanocomposites (ER/SEF20/CNT2).

As can be seen, the change in morphology is small at low mixing ratios of components which results in big distance between individual nanotubes.

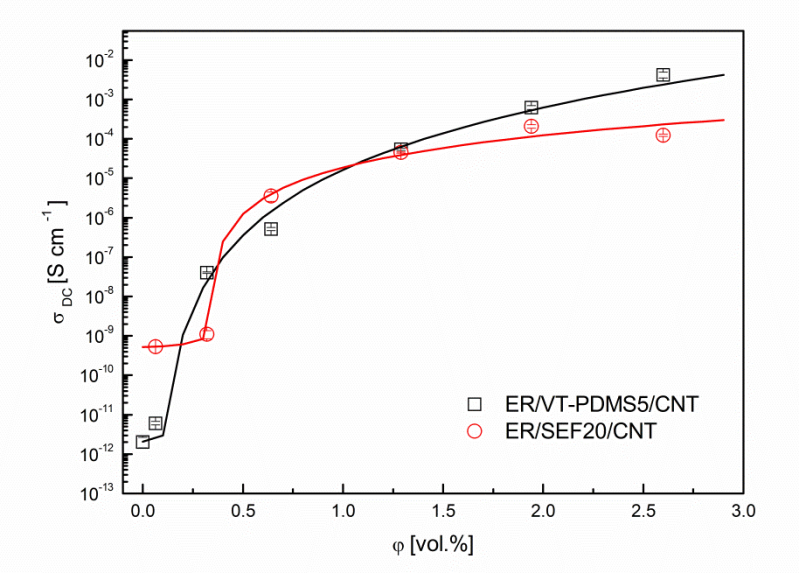

Fig. 37 The dependence of DC electrical conductivity on CNT content for ER/5 vol % of VT-PDMS (□) and ER/20 vol. % of SEF (Δ) in nanocomposites.

CB nanocomposites

CB particles are mixed with an immiscible matrix consisting of epoxy and polysiloxane, CB can be dispersed in epoxy or polysiloxane or at the interface between. Sumita et al [84] exposed that the localization of the CB is determined by the wetting coefficient (ω) that is defined by the following equation:

$$\omega = \frac{(\gamma_{CB-PDMS} - \gamma_{CB-ER})}{\gamma_{ER-PDMS}} \text{ [24]}$$

Where $\gamma_{CB\text{-}ER}$ is the interfacial tension between epoxy and carbon black, $\gamma_{CB\text{-}PDMS}$ is the interfacional tension between silicone and carbon black, $\gamma_{ER\text{-}PDMS}$ it the interfacial tension between epoxy and polysiloxane. The localization of CB particles is predicted by the following conditions: $\omega > 1$ CB particles are localized in ER; $-1 < \omega < 1$ CB are localized at the interface (where $\omega=0.85$); $\omega < -1$ CB particles are localized in VT- PDMS.

Tab. 7 Surface tension of uncured DGEBA, PDMS and CB.

Material	γ [dyn cm^{-1}]	Reference
CB	34,4	[84]
Uncured ER	50,6	
VT-PDMS	21,2	[105]

The location of conductive filler and the phase morphology of the composites could considerably affect the electrical properties of the polymer blends, and it is clear that the phase morphology can be changed by adjusting the CB concentration and the ER/VT-PDMS ratio.

Fig. 38 shows the electrical conductivity of ER/VT-PDMS/CB composites with and without DCP as a function of CB content. In both systems recorded percolation threshold (0.5 and 1.5 vol. % for with and without DCP respectively) is approximately ten times lower than for ER/CB (see Fig. 35b). This dramatic shift of percolation is most probably due to double percolation effect and the fact filler is dominantly located at phase interface (= 0.85). However even incorporated DCP affects blends percolation threshold and shifts it from 1.5 to 0.5 vol. %.

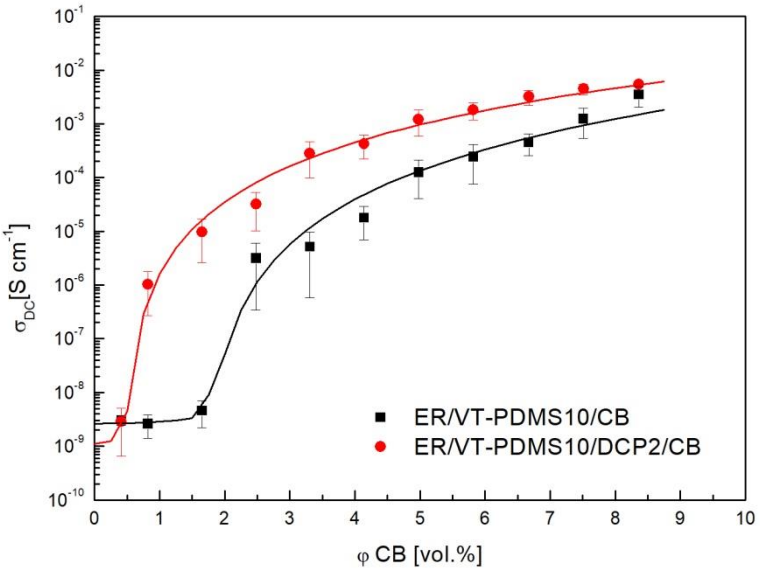

Fig. 38 The influence of DCP on percolation threshold of CB filled polymer blends.

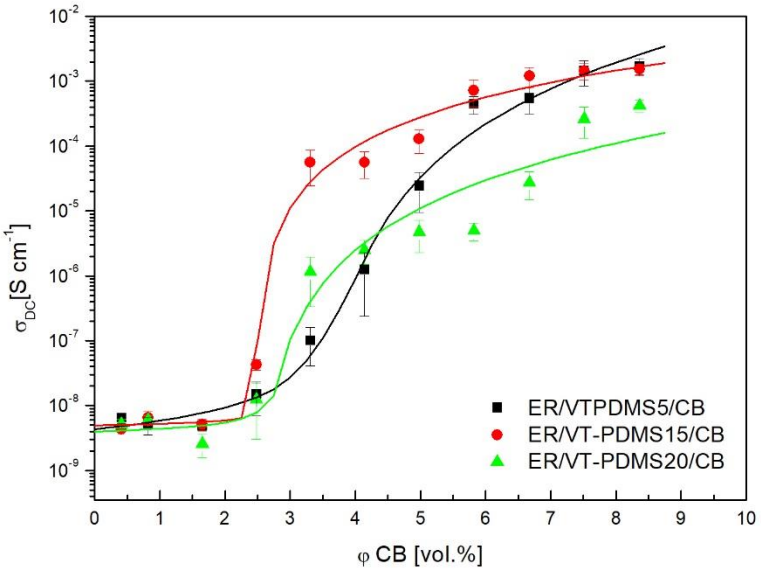

Fig. 39 Influence of elastomer phase on the percolation threshold.

The percolation threshold in polymer blends was also studied in relation to the polysiloxane content (Fig. 39). As can be seen there is no clear influence of polysiloxane on percolation threshold however the shape of the curve namely around the percolation threshold is altered for systems with polysiloxane content above 5 vol. %.

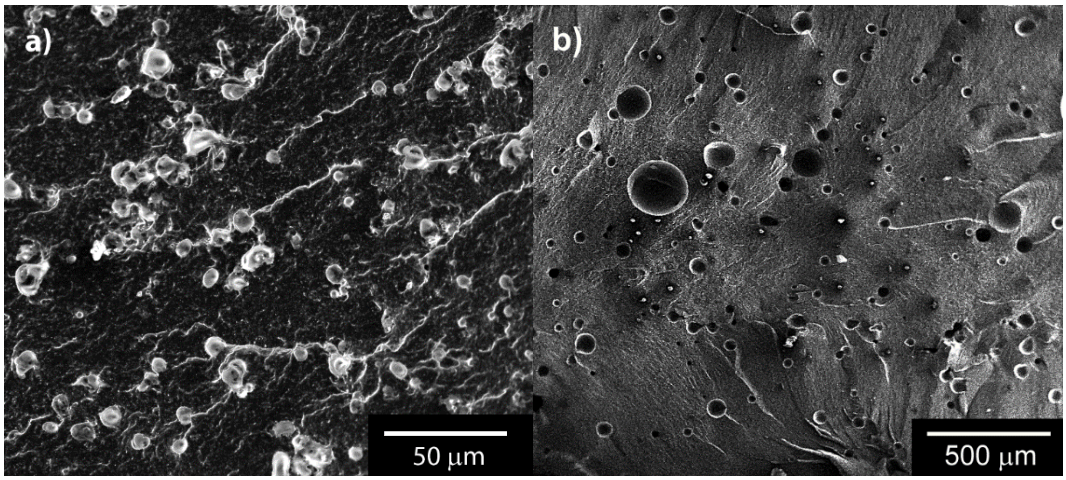

Fig. 40. SEM images of a) ER/VT-PDMS10 and b) PDMS10/DCP2/CB at 7 vol% CB.

Fig. 40 shows the morphology of the ER/VT-PDMS/CB and ER/VTPDMS/DCP2/CB. The ER/VT-PDMS/CB composite without DCP shows typical sea-island morphology, in which VT-PDMS irregular droplets

several micrometers (5-10 um) large are dispersed in the ER phase (Fig. 40 a). On the other hand, 2 vol. % of DCP in composites leads to the more regular spherical droplets however their size distribution is wider (Fig. 40 b). The regularity of polysiloxane spheres is due to the compatibilization efficiency of the DCP.

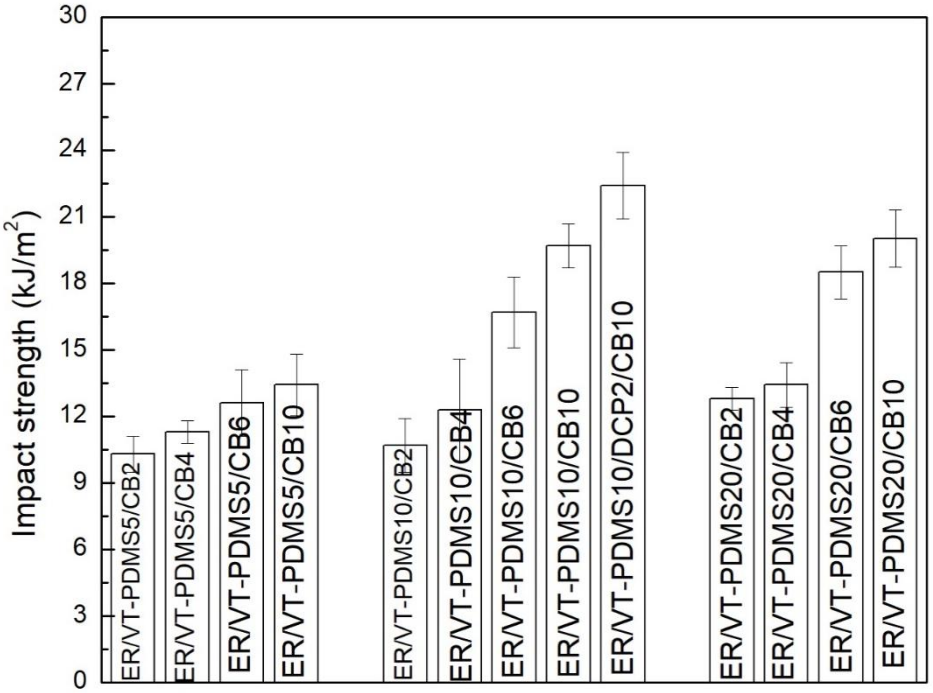

Fig. 41 Impact strength of epoxy-polysiloxane blends with CB.

To investigate the impact strength of the epoxy-silicone blends with carbon black we have conducted Charpy impact tests. The results are plotted in Fig. 41. It is verified that the increasing of CB content improves the impact strength. Although the error bars do overlap to some degree, the general trend is that the impact strength increases with VT-PDMS and CB content. Even though increasing concentration (2–10 wt.% equel to 1–7 vol. %) of CB enhances blend's toughness for all investigated systems, steepest dependence was recorded with ER/VT-PDMS10/DCP2 blend. In this case nanocomposite containing 7 vol. % of CB exhibited a remarkable improvement of the impact toughness by more than 23 % (from 17 to 22 kJ/ m^2) confirming the synergic effect of DCP (2 vol. %) and CB. We assume that CB acts as toughenning agent at the interface of ER and polysiloxane significantly affecting crack propagation (Fig. 42).

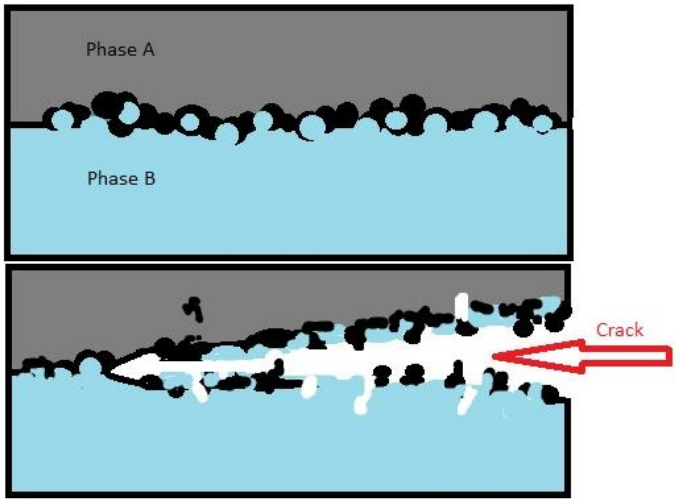

Fig. 42 Schematic representation of the selective distribution of CB at the interface between phases A and B (a) and the crack propagation along the interface plane.

CONCLUSIONS

- It is established that microstructure of epoxy-polysiloxane immiscible blends has great influence on the mechanical properties, namely whether or not there is compatibility between polymer phases. Therefore, the morphology of the blends was controlled through selection of elastomeric phase (PDMS, VT-PDMS) and its content together with the use of certain concentration of compatibilizator (DCP).
- Optimal composition leading to 70% enhancement of ER toughness (17 kJ/m^2) without significant reduction of polymer system modulus (2 GPa), glass transition temperature (138 °C) and interfacial adhesion (lap shear strength of 430 kgf) was found for ER filled with 10 wt. % of VT-PDMS and 2 % of DCP. This stemmed from transition from brittle to ductile fracture mechanism registered by SEM morphology and DMA investigations.
- In order to obtain electrically conductive systems, binary polymer matrix was filled with conductive filler (CNT, CB). Especially for CNT-based composites, special attention was paid to CNT surface modification and its distribution within polymer matrix. Value of percolation threshold was found to heavily depend on aspect ratio of filler and to some extent on used polymer matrix. Thus, depending on the matrix CNT percolated at about 0.5–1 vol. %, while CB only at 7–10 vol. %.

FUTURE PROSPECTS

We intend to apply our processing technology and experience with various ER-polysiloxane blends to create new materials with improved mechanical properties that would be achieved by the compatibilising effect of components in blends. In addition, we plan to use our technology for the design of efficient composite materials with controlled electrical properties for shielding of electromagnetic radiation that is required for many applications

CURRICULUM VITAE

Personal information:

Surname/First name:	Lenka Kutějová
Adress:	Hošťálková 342, 756 22, Czech Republic
Telephone:	+420 732 856 773
E-mail(s):	lenka.kutejova@pebal.cz
Date of birth:	23rd June 1986
Nationality:	Czech

Education and training:

Dates:	2010 – present
Title of qualification awarded:	Ph.D study
University:	Tomas Bata University in Zlin Faculty of Technology, Polymer Centre
Dates:	2008-2010
Title of qualification awarded:	Ing.
University:	Tomas Bata University in Zlin Faculty of technology, Chemistry and Chemistry and Materials Technology, Polymer Engineering
Dates:	2005-2008
Title of qualification awarded:	Bc.
University:	Tomas Bata University in Zlin Faculty of technology, Chemistry and Materials Technology

Work experience:

Dates:	2017- present
Position held:	Product manager/Technologist
Name of employer:	**Pebal s.r.o.**
Dates:	2015-2017
Position held:	Technologist
Name of employer:	**Invos, s.r.o**.
Dates:	2011 – 2014
Position held:	Research project staff
Name of employer:	Tomas Bata University in Zlin, Polymer Centre

Projects:

2012 **IGA/FT/2012/024** Development of multicomponent polymer systems on the base epoxy resin and silicone elastomer

2013 **IGA/FT/2013/024** Electrical and magnetic properties of filled multicomponent polymer systems

1/2015-12/2015 **TA03010548** Výzkum a vývoj pokročilých tenkovrstvých elementů pro přímé sledování časové proměnné pomocí přesně kalibrovatelné změny – technická koncepce řešení
1/2015-12/2015 **TA030010799** Využití nanomateriálů a přírodních extraktů jako funkčních látek ve vývoji aktivních obalových materiálů s barevným efektem, antimikrobiálním, protektivním a kyslík pohlcujícím efektem- technická koncepce řešení
1/2015-12/2015 **TA04010627** Vývoj biodegradabilních fólií – technická koncepce řešení
1/2015-12/2016 **TA03010544** Tištěné optické chemické sensory – technická koncepce řešení
1/2015-12/2016 **TA03010546** Bioaktivní obaly – technická koncepce řešení

Publications:

1. KUTĚJOVÁ, Lenka, VILČÁKOVÁ, Jarmila, MOUČKA, Robert, KAZANTSEVA, Natalia, WINKLER, Martin, BABAYAN, Vladimir Artur. A solvent dispersion method for the preparation of silicone composites filled with carbon nanotubes. *Chemické listy*, 2014, vol. 108, no. S1, p. 78-85. ISSN 0009-2770.

2. Užitný vzor: VILČÁKOVÁ, Jarmila, KUTĚJOVÁ, Lenka, BABAYAN, Vladimir Artur, KAZANTSEVA, Natalia, SÁHA, Petr: Blend for anticorrosive composite coating and layers with controlled conductivity, Document no. PUV 2014-30163, (Industrial Property Office CR).

3. VILČÁKOVÁ, Jarmila, KUTĚJOVÁ, Lenka, JURČA Marek, MOUČKA Robert, VÍCHA Robert, SEDLAČÍK Michal, KOVALČÍK Adriana, MACHOVSKÝ Michal, KAZANTSEVA, Natalia. Enhanced Charpy impact strength of epoxy resin modified with vinyl-terminated polydimethylsiloxane. *Journal of Applied Polymer Science*. Accepted for publication in 2017, DOI: **10.1002/app.45720.**

Presentation at conferences:

1. BENÍČEK, L., HUSÁR, B., KUTĚJOVÁ, L., VERNEY,V., MELICHÁRKOVÁ, P., COMMEREUC, S., ČERMÁK, R.; Rheological behavior of poly(1-butene)/wood composites. ANTEC 2010 – Society of plastic Engineers, Orlando, Florida, USA, May 16-20
2. KUTEJOVA, L. VILCAKOVA, J., KAZANTSEVA, N. E., MOUCKA, R.: Epoxy – elastomer polymer system: Regulation of physico – mechanical properties. In: Plastko 2012, April 11th-12th 2012, Zlin, Czech Republic, ISBN 978-80-7454-1357-7.
3. KUTEJOVA, L. VILCAKOVA, J., KAZANTSEVA, N.: Morphology and miscibility of epoxy – elastomer polymer system as a matrix for conductive

composites. In: BYPOS 2012, October 1st-5th 2012, Liptovsky Jan, Low Tatras, Slovakia. ISBN 978-80-970923-2-0.

ABBREVIATIONS AND SYMBOLS

CNT	Carbon nanotubes
PVA	Polyvinylalcohole
DGEBA	Diglycidyl ether bisphenol A
DBSA	Dodecylbenzensulfonic acid
PDMS	Polydimethylsiloxane
CVD	Chemical vapor deposition
DETA	Diethylentriamine
MPS	Multiphase Polymer Systems
p	Aspect ratios
DMA	Dynamic Mechanical Analyze
DSC	Differential Scanning Calorimetry
SWNT	Single-wall carbon nanotubes
CB	Carbon black
MWNT	Multi-wall carbon nanotubes
σ	Electrical conductivity
DCP	Dicumyl peroxide
ER	Epoxy resin
T	Temperature
TGMDA	Tetraglycidyl methylene dianiline
TTT	Triethylentriamine
TGDDM	Tetraglycidyl- 4,4''-diaminodiphenylmethane
DEAPA	Diethylaminopropylamine
T_g	Glass transition temperature
ΔGm	Gibbs free energy of mixing
T_{cure}	Curing temperature
ΔGm	Gibbs free energy of mixing
TTT	Time-Temperature-Transition
ΔGm	Gibbs free energy of mixing
ΔHm	Enthalpy of mixing
ΔSm	Entropy of mixing
CTBN	Carboxyl terminated butadiene acrylonitrile copolymers
R	Universal gas constant
ATBN	Amine terminated butadiene acrylonitrile copolymers
CTAB	Cetyltrimethylammonium bromide
HTBN	Hydroxyl terminated butadiene acrylonitrile copolymers
DMF	N,N-dimethylformamide

NMP	N-methyl-2-pyrrolidone
CI	Carbonyl iron
T_{curie}	Curie temperature
CPC	Conductive polymer composites
DC	Direct current
AC	Alternating current
φ_c	Volume fraction of filler at PC
PC	Percolation threshold
SEM	Scanning Electron Microscopy
VT-PDMS	Polydimehtyl siloxane vinyl terminated
ER	Epoxy resin
MEK	Methyl ethyl ketone peroxide
BP	Benzoyl peroxide
NMR	Nuclear magnetic resonance spectroscopy
VFT	Vogel–Fulcher–Tamman
SEF	Silikopon EF

LIST OF FIGURES

LIST OF TABLES

REFERENCES

[1] ETIENNE, S.; STOCHMIL, C.; BESSEDE, J. L. Dielectric properties of polymer-based microheterogeneous insulator. *Journal of alloys and compounds*, 2000, 310.1: 368-373.

[2] PAN, T.; HUANG, J. P.; LI, Z. Y. Optical bistability in metal/dielectric composite with interfacial layer. *Physica B: Condensed Matter*, 2001, 301.3: 190-195.

[3] GUBBELS, Frederic, et al. Kinetic and thermodynamic control of the selective localization of carbon black at the interface of immiscible polymer blends. *Chemistry of materials*, 1998, 10.5: 1227-1235.

[4] MATHEW, Viju Susan, et al. Epoxy resin/liquid natural rubber system: secondary phase separation and its impact on mechanical properties. *Journal of materials science*, 2010, 45.7: 1769-1781.

[5] CAMPBELL JR, Flake C. (ed.). *Manufacturing processes for advanced composites*. Elsevier, 2003.

[6] KUMAR, Hemant, et al. Synthesis, characterization and application of coatings based on epoxy novolac and liquid rubber blend. *Journal of Chemistry*, 2009, 6.4: 1253-1259.Newez HA. U.S. Patent, 1958. 775:2264.

[7] BRADLEG, T. F. Epoxy curing by Polyacid. *US Patent*, 1950, 449: 2500.

[8] CASTON, P. Epoxy Curing by Anhydride. *US Patent*, 1943, 483: 2324.

[9] UTRACKI, Leszek A. *Two-phase polymer systems*. Munich et al.: Hanser Verl., 1991.

[10] CALBERG, Cédric, et al. Electrical and dielectric properties of carbon black filled co-continuous two-phase polymer blends. *Journal of Physics D: Applied Physics*, 1999, 32.13: 1517.

[11] HUANG, Jan-Chan. Carbon black filled conducting polymers and polymer blends. *Advances in Polymer Technology*, 2002, 21.4: 299-313.

[12] AVILA, Antonio F., et al. A dual analysis for recycled particulate composites: linking micro-and macro-mechanics. *Materials characterization*, 2003, 50.4: 281-291.

[13] GLATZ-REICHENBACH, J., et al. Feature article conducting polymer composites. *Journal of Electroceramics*, 1999, 3.4: 329-346.

[14] THOMAS, Sabu, et al. Physical, thermophysical and interfacial properties of multiphase polymer systems: state of the art, new challenges and opportunities. *Handbook of multiphase polymer systems*, 2011, 1-12.

[15] URBANIAK, Magdalena; GRUDZIŃSKI, Karol. Time-temperature-transformation (TTT) cure diagram for EPY epoxy system. *Polimery*, 2007, 52.2.

[16] THOMAS, Raju, et al. Cure kinetics, morphology and miscibility of modified DGEBA-based epoxy resin–Effects of a liquid rubber inclusion. *Polymer*, 2007, 48.6: 1695-1710.

[17] *Process for curing polyepoxides by amine adducts and resulting products*. U.S. Patent No 2,864,775, 1958.

[18] MAY, Clayton (ed.). *Epoxy resins: chemistry and technology*. CRC press, 1987.

[19] OLEINIK, Eduard F. Epoxy-aromatic amine networks in the glassy state structure and properties. In: *Epoxy resins and composites IV*. Springer, Berlin, Heidelberg, 1986. p. 49-99.

[20] COLEMAN, Michael M.; PAINTER, Paul C.; GRAF, John F. *Specific interactions and the miscibility of polymer blends*. CRC Press, 1995.

[21] NOLL, Walter. *Chemistry and technology of silicones*. Elsevier, 2012.

[22] YILGÖR, İskender; MCGRATH, James E. Polysiloxane containing copolymers: a survey of recent developments. In: *Polysiloxane Copolymers/Anionic Polymerization*. Springer, Berlin, Heidelberg, 1988. p. 1-86.

[23] GRAFFIUS, Gabriel; BERNARDONI, Frank; FADEEV, Alexander Y. Covalent functionalization of silica surface using “inert” poly (dimethylsiloxanes). *Langmuir*, 2014, 30.49: 14797-14807.

[24] YILGÖR, Emel; YILGÖR, Iskender. Silicone containing copolymers: synthesis, properties and applications. *Progress in Polymer Science*, 2014, 39.6: 1165-1195.

[25] ZHAO, Feng, et al. Preparation and properties of polydimethylsiloxane-modified epoxy resins. *Journal of applied polymer science*, 2000, 76.11: 1683-1690.

[26] RIFFLE, J. S., et al. Elastomeric polysiloxane modifiers for epoxy networks: Synthesis of functional oligomers and network formation studies.

[27] SOBHANI, Sarah; JANNESARI, Ali; BASTANI, Saeed. Effect of molecular weight and content of PDMS on morphology and properties of silicone-modified epoxy resin. *Journal of Applied Polymer Science*, 2012, 123.1: 162-178.

[28] YILGOR, Emel; YILGOR, Iskender. 1, 3-bis (γ-aminopropyl) tetramethyldisiloxane modified epoxy resins: curing and characterization. *Polymer*, 1998, 39.8-9: 1691-1695.

[29] PAUL, D. R. Interfacial agents ("compatibilizers") for polymer blends. *Polymer blends*, 1978, 2: 35-62..

[30] UTRACKI, L. A. Thermodynamics of polymer blends. In: *Polymer blends handbook*. Springer Netherlands, 2003. p. 123-201.

[31] NESTEROV, Anatoly E.; LIPATOV, Yuri S. *Thermodynamics of polymer blends*. CRC Press, 1998.

[32] TOMOVA, D.; KRESSLER, J.; RADUSCH, H.-J. Phase behaviour in ternary polyamide 6/polyamide 66/elastomer blends. *Polymer*, 2000, 41.21: 7773-7783.

[33] PEACOCK, Andrew J.; CALHOUN, Allison. *Polymer Chemistry: Properties and Application*. Carl Hanser Verlag GmbH Co KG, 2012.

[34] UTRACKI, Leszek A. *Commercial polymer blends*. Springer Science & Business Media, 2013.

[35] UTRACKI, Leszek A.; FAVIS, B. D. *Polymer alloys and blends*. Marcel Dekker: New York, 1989.

[36] UTRACKI, Leszek A. Compatibilization of polymer blends. *the Canadian journal of chemical Engineering*, 2002, 80.6: 1008-1016

[37] TANJUNG, Faisal Amri; HASSAN, Azman; HASAN, Mahbub. Use of epoxidized natural rubber as a toughening agent in plastics. *Journal of Applied Polymer Science*, 2015, 132.29. [38]

BAKER, Warren E., et al. *Reactive polymer blending*. Munich: Hanser, 2001.

[39] AJJI, Abdellah; UTRACKI, L. A. Interphase and compatibilization of polymer blends. *Polymer Engineering & Science*, 1996, 36.12: 1574-1585.

[40] LIU, N. C.; BAKER, W. E. Reactive polymers for blend compatibilization. *Advances in Polymer Technology*, 1992, 11.4: 249-262.

[41] XANTHOS, M.; DAGLI, S. S. Compatibilization of polymer blends by reactive processing. *Polymer Engineering & Science*, 1991, 31.13: 929-935.

[42] XANTHOS, M. Interfacial agents for multiphase polymer systems: recent advances. *Polymer Engineering & Science*, 1988, 28.21: 1392-1400.

[43] HU, Guo-Hua; SUN, Yi-Jun; LAMBLA, Morand. Devolatilization: A critical sequential operation for in situ compatibilization of immiscible polymer blends by one-step reactive extrusion. *Polymer Engineering & Science*, 1996, 36.5: 676-684.

[44] EICHHORN, J. Synergism of free radical initiators with self-extinguishing additives in vinyl aromatic polymers. *Journal of Applied Polymer Science*, 1964, 8.6: 2497-2524.

[45] TRIPATHI, Garima; SRIVASTAVA, Deepak. Studies on blends of cycloaliphatic epoxy resin with varying concentrations of carboxyl terminated butadiene acrylonitrile copolymer I: Thermal and morphological properties. *Bulletin of Materials Science*, 2009, 32.2: 199-204.

[46] THOMAS, Raju, et al. Influence of carboxyl-terminated (butadiene-co-acrylonitrile) loading on the mechanical and thermal properties of cured epoxy blends. *Journal of Polymer Science Part B: Polymer Physics*, 2004, 42.13: 2531-2544.

[47] HORIUCHI, S., et al. Fracture toughness and morphology study of ternary blends of epoxy, poly (ether sulfone) and acrylonitrile-butadiene rubber. *Polymer*, 1994, 35.24: 5283-5292.

[48] MATHEW, Viju Susan, et al. Epoxy resin/liquid natural rubber system: secondary phase separation and its impact on mechanical properties. *Journal of materials science*, 2010, 45.7: 1769-1781.

[49] YORKGITIS, E. M., et al. Siloxane-modified epoxy resins. In: *Epoxy Resins and Composites I*. Springer, Berlin, Heidelberg, 1985. p. 79-109.

[50] SOBHANI, Sarah; JANNESARI, Ali; BASTANI, Saeed. Effect of molecular weight and content of PDMS on morphology and properties of silicone-modified epoxy resin. *Journal of Applied Polymer Science*, 2012, 123.1: 162-178.

[51] VAZQUEZ, A., et al. Rubber-modified thermosets: prediction of the particle size distribution of dispersed domains. *Polymer*, 1987, 28.7: 1156-1164.

[52] ALTAWEEL, Abdullah Mohammed Ali Mohammed; RANGANATHAIAH, C.; KOTHANDARAMAN, B. Mechanical properties of modified epoxies as related to free volume parameters. *The Journal of Adhesion*, 2009, 85.4-5: 200-215.

[53] BASFAR, A. A.; SILVERMAN, Joseph. Improved ozone resistance of styrene-butadiene rubber cured by a combination of sulfur and ionizing radiation. *Polymer degradation and stability*, 1994, 46.1: 1-8.

[54] MIWA, Minoru, et al. Volume fraction and temperature dependence of mechanical properties of silicone rubber particulate/epoxy blends. *Composites*, 1995, 26.5: 371-377.

[55] VILČÁKOVÁ, Jarmila, et al. Electrical properties of composites of hard metal carbides in a polymer matrix. *Polymer composites*, 2002, 23.5: 942-946.

[56] DONNET, Jean-Baptiste; BANSAL, Roop Chand. *Carbon fibers*. CRC Press, 1998.

[57] DONNET, Jean-Baptiste (ed.). *Carbon black: science and technology*. CRC Press, 1993.

[58] HUANG, Jan-Chan. Carbon black filled conducting polymers and polymer blends. *Advances in Polymer Technology*, 2002, 21.4: 299-313.

[59] MEDALIA, Avrom I. Electrical conduction in carbon black composites. *Rubber Chemistry and Technology*, 1986, 59.3: 432-454.

[60] GUBBELS, Frédéric, et al. Design of electrical composites: determining the role of the morphology on the electrical properties

of carbon black filled polymer blends. *Macromolecules*, 1995, 28.5: 1559-1566.

[61] SAITO, Riichiro; DRESSELHAUS, Gene; DRESSELHAUS, Mildred S. *Physical properties of carbon nanotubes*. World scientific, 1998.

[62] BIN, Y., et al. Electrical properties of polyethylene and carbon black particle blends prepared by gelation/crystallization from solution. *Carbon*, 2002, 40.2: 195-199.

[63] QIN, F.; BROSSEAU, Christian. A review and analysis of microwave absorption in polymer composites filled with carbonaceous particles. *Journal of applied physics*, 2012, 111.6: 4.

[64] BREUER, Orna; SUNDARARAJ, Uttandaraman. Big returns from small fibers: a review of polymer/carbon nanotube composites. *Polymer composites*, 2004, 25.6: 630-645.

[65] KUTĚJOVÁ, Lenka, et al. A solvent dispersion method for the preparation of silicone composites filled with carbon nanotubes. *Chem. Listy*, 2014, 108: s78-s85.

[66] YU, Rongqing, et al. Platinum deposition on carbon nanotubes via chemical modification. *Chemistry of Materials*, 1998, 10.3: 718-722.

[67] WANG, Yao; WU, Jun; WEI, Fei. A treatment method to give separated multi-walled carbon nanotubes with high purity, high crystallization and a large aspect ratio. *Carbon*, 2003, 41.15: 2939-2948.

[68] CUI, S., et al. Characterization of multiwall carbon nanotubes and influence of surfactant in the nanocomposite processing. *Carbon*, 2003, 41.4: 797-809

[69] WONG, Stanislaus S., et al. Covalently functionalized nanotubes as nanometre-sized probes in chemistry and biology. *Nature*, 1998, 394.6688: 52.

[70] VALENTIN, Emmanuel, et al. High-density selective placement methods for carbon nanotubes. *Microelectronic Engineering*, 2002, 61: 491-496.

[71] VILČÁKOVÁ, Jarmila, et al. Effect of surfactants and manufacturing methods on the electrical and thermal conductivity of carbon nanotube/silicone composites. *Molecules*, 2012, 17.11:

13157-13174.
[72] ZHANG, Sam; ALI, Nasar (ed.). *Nanocomposite thin films and coatings: processing, properties and performance*. Imperial college press, 2007.

[73] NARKIS, M.; RAM, A.; FLASHNER, F. Electrical properties of carbon black filled polyethylene. *Polymer Engineering & Science*, 1978, 18.8: 649-653.

[74] PONOMARENKO, A. T.; SHEVCHENKO, V. G.; ENIKOLOPYAN, N. S. Formation processes and properties of conducting polymer composites. In: *Filled Polymers I Science and Technology*. Springer, Berlin, Heidelberg, 1990. p. 125-147.

[75] CELZARD, A., et al. Critical concentration in percolating systems containing a high-aspect-ratio filler. *Physical Review B*, 1996, 53.10: 6209.

[76] FOULGER, Stephen H. Reduced percolation thresholds of immiscible conductive blends. *Journal of Polymer Science Part B: Polymer Physics*, 1999, 37.15: 1899-1910.

[77] FENG, Jiyun; CHAN, Chi-Ming. Electrical properties of carbon black-filled polypropylene/ultra-high molecular weight polyethylene composites. *Conductive polymers*, 1999, 219.

[78] SUMITA, Masao, et al. Dispersion of fillers and the electrical conductivity of polymer blends filled with carbon black. *Polymer bulletin*, 1991, 25.2: 265-271.

[79] ELIAS, L., et al. Morphology and rheology of immiscible polymer blends filled with silica nanoparticles. *Polymer*, 2007, 48.20: 6029-6040.

[80] ZHU, M., et al. High-performance transparent solvent-free silicone resins with stable storage and low viscosity based on new hyperbranched polysiloxanes. *High Performance Polymers*, 2013, 25.5: 594-608.

[81] PONNAMMA, Deepalekshmi; SADASIVUNI, Kishor Kumar; THOMAS, Sabu. NMR Studies of Natural Rubber Composites from Macro-to Nanoscales–A Review. In: *Natural Rubber Materials*. 2013. p. 683-702.

[82] KOHLI, Rajiv; MITTAL, Kashmiri L. (ed.). *Developments in Surface Contamination and Cleaning, Vol. 1: Fundamentals and Applied Aspects*. William Andrew, 2015.

[83] VAN DER PAUW, Leo J. A method of measuring specific resistivity and Hall effect of discs of arbitrary shapes. *Philips research reports*, 1958, 13: 1-9.

[84] KRESS-ROGERS, Erika; BRIMELOW, Christopher JB (ed.). *Instrumentation and sensors for the food industry*. Woodhead Publishing, 2001.

[85] POTHEN, L. A.; CHAN, C. Han; THOMAS, S. *Natural Rubber Materials, Volume 2-Composites and Nanocomposites*. Royal Society of Chemistry, 2013.

[86] HE, Yi. Thermomechanical and viscoelastic behavior of a no-flow underfill material for flip-chip applications. *Thermochimica acta*, 2005, 439.1: 127-134.

[87] NORMA, I. S. O. 179: 1993. *Plastics–Determination of Charpy Impact Strength*, 179-2.

[88] PASCAULT, Jean-Pierre; WILLIAMS, Roberto JJ (ed.). *Epoxy polymers: new materials and innovations*. John Wiley & Sons, 2009.

[89] WOODS, Rachel, et al. Epoxy silicone based matrix materials for two-photon patterning of optical waveguides. *Polymer*, 2011, 52.14: 3031-3037.

[90] KARGARZADEH, Hanieh; AHMAD, Ishak; ABDULLAH, Ibrahim. Mechanical Properties of Epoxy–Rubber Blends. *Handbook of Epoxy Blends*, 2016, 1-36.

[91] THOMAS, Raju, et al. Influence of carboxyl-terminated (butadiene-co-acrylonitrile) loading on the mechanical and thermal properties of cured epoxy blends. *Journal of Polymer Science Part B: Polymer Physics*, 2004, 42.13: 2531-2544.

[92] OZTURK, A.; KAYNAK, C.; TINCER, T. Effects of liquid rubber modification on the behaviour of epoxy resin. *European Polymer Journal*, 2001, 37.12: 2353-2363.

[93] MATHEW, Viju Susan, et al. Epoxy resin/liquid natural rubber system: secondary phase separation and its impact on mechanical properties. *Journal of materials science*, 2010, 45.7: 1769-1781.

[94] HODGKIN, J. H.; SIMON, G. P.; VARLEY, R. J. Thermoplastic toughening of epoxy resins: a critical review. *Polymers for Advanced Technologies*, 1998, 9.1: 3-10.

[95] VIJAYAN, P. Poornima, et al. Effect of organically modified nanoclay on the miscibility, rheology, morphology and properties of epoxy/carboxyl-terminated (butadiene-co-acrylonitrile) blend. *Soft Matter*, 2013, 9.10: 2899-2911.

[96] KAMAR, Nicholas T.; DRZAL, Lawrence T. Micron and nanostructured rubber toughened epoxy: A direct comparison of mechanical, thermomechanical and fracture properties. *Polymer*, 2016, 92: 114-124.

[97] BAGHERI, Reza; PEARSON, Raymond A. Role of particle cavitation in rubber-toughened epoxies: II. Inter-particle distance. *Polymer*, 2000, 41.1: 269-276.

[98] BUCKNALL, C. B. Applications of microscopy to the deformation and fracture of rubber-toughened polymers. *Journal of microscopy*, 2001, 201.2: 221-229.

[99] BUCKNALL, C. B.; PAUL, D. R. Notched impact behaviour of polymer blends: Part 2: Dependence of critical particle size on rubber particle volume fraction. *Polymer*, 2013, 54.1: 320-329.

[100] BAGHERI, R.; MAROUF, B. T.; PEARSON, R. A. Rubber-toughened epoxies: a critical review. *Journal of Macromolecular Science®, Part C: Polymer Reviews*, 2009, 49.3: 201-225.

[101] RUIZ-PEREZ, Lorena, et al. Toughening by nanostructure. *Polymer*, 2008, 49.21: 4475-4488.

[102] SANTIAGO, David, et al. Influence of the end groups of hyperbranched poly (glycidol) on the cationic curing and morphology of diglycidylether of bisfenol A thermosets. *Reactive and Functional Polymers*, 2011, 71.4: 380-389.

[103] VENKATARAMAN, Sundar K., et al. Critical extent of reaction of a polydimethylsiloxane polymer network. *Polymer*, 1989, 30.12: 2222-2226.

[104] NANDA, M.; TRIPATHY, D. K. Relaxation behavior of conductive carbon black reinforced chlorosulfonated polyethylene composites. *Journal of applied polymer science*, 2010, 116.5: 2758-2767.

[105] Kuo, Alex CM. "Poly (dimethylsiloxane)." *Polymer data handbook* (1999): 411-435.

ATTACHMENT

Tab. 2 **Composition of prepared blends.**

Samples	DGEBA+DETA [wt.%]	PDMS [wt.%]	DCP [wt.%]
ER	100	-	-
ER/DCP1	99	-	1
ER /DCP2	98	-	2
ER /DCP3	97	-	3
ER/VT-PDMS5	95	5	-
ER/VT-PDMS10	90	10	-
ER/VT-PDMS15	85	15	-
ER/VT-PDMS5/DCP1	94	5	1
ER/VT-PDMS5/DCP2	93	5	2
ER/VT-PDMS5/DCP3	92	5	3
ER/VT-PDMS10/DCP1	89	10	1
ER/VT-PDMS10/DCP2	88	10	2
ER/VT-PDMS10/DCP3	87	10	3
ER/VT-PDMS15/DCP1	84	15	1
ER/VT-PDMS15/DCP2	83	15	2
ER/VT-PDMS15/DCP3	82	15	3
ER/PDMS5	95	5	-
ER/PDMS10	90	10	-
ER/PDMS15	85	15	-
ER/PDMS5/DCP1	94	5	1
ER/PDMS5/DCP2	93	5	2
ER/PDMS5/DCP3	92	5	3
ER/PDMS10/DCP1	89	10	1
ER/PDMS10/DCP2	88	10	2
ER/PDMS10/DCP3	87	10	3
ER/PDMS15/DCP1	84	15	1
ER/PDMS15/DCP2	83	15	2
ER/PDMS15/DCP3	82	15	3

Tab. 3 List of composites on the based polymer blends ER/VT-PDMS and ER/SEF filled with CNT

Samples	ER/VT-PDMS [wt.%]	CNT [wt.%]
ER/VT-PDMS5/CNT2	95	2
ER/VT-PDMS10/CNT2	90	2
ER/VT-PDMS15/CNT2	85	2
ER/VT-PDMS20/CNT2	80	2
ER/VT-PDMS30/CNT2	70	2
ER/VT-PDMS40/CNT2	60	2
ER/SEF1/CNT2	99	2
ER/SEF2/CNT2	98	2
ER/SEF3/CNT2	97	2
ER/SEF4/CNT2	96	2
ER/SEF5/CNT2	95	2
ER/SEF10/CNT2	90	2
ER/SEF15/CNT2	85	2
ER/SEF20/CNT2	80	2
ER/SEF30/CNT2	70	2
ER/SEF40/CNT2	60	2
ER/VT-PDMS5/CNT02	95	0,2
ER/VT-PDMS5/CNT05	95	0,5
ER/VT-PDMS5/CNT1	95	1
ER/VT-PDMS5/CNT2	95	2
ER/VT-PDMS5/CNT3	95	3
ER/VT-PDMS5/CNT4	95	4
ER/SEF20/CNT02	80	0,2
ER/SEF20/CNT05	80	0,5
ER/SEF20/CNT1	80	1
ER/SEF20/CNT2	80	2
ER/SEF20/CNT3	80	3
ER/SEF20/CNT4	80	4

Tab. 4 List of composite on the based polymer blends ER/VT-PDMS filled with CB

Samples	ER/VT-PDMS [wt.%]	CB [wt.%]
ER/VT-PDMS5/CB05	95	0,5
ER/VT-PDMS10/CB05	90	
ER/VT-PDMS15/CB05	85	
ER/VT-PDMS20/CB05	80	
ER/VT-PDMS5/CB1	95	1
ER/VT-PDMS10/CB1	90	
ER/VT-PDMS15/CB1	85	
ER/VT-PDMS20/CB1	80	
ER/VT-PDMS5/CB2	95	2
ER/VT-PDMS10/CB2	90	
ER/VT-PDMS15/CB2	85	
ER/VT-PDMS20/CB2	80	
ER/VT-PDMS5/CB3	95	3
ER/VT-PDMS10/CB3	90	
ER/VT-PDMS15/CB3	85	
ER/VT-PDMS20/CB3	80	
ER/VT-PDMS5/CB4	95	4
ER/VT-PDMS10/CB4	90	
ER/VT-PDMS15/CB4	85	
ER/VT-PDMS20/CB4	80	
ER/VT-PDMS5/CB5	95	5
ER/VT-PDMS10/CB5	90	
ER/VT-PDMS15/CB5	85	
ER/VT-PDMS20/CB5	80	
ER/VT-PDMS5/CB6	95	6
ER/VT-PDMS10/CB6	90	
ER/VT-PDMS15/CB6	85	
ER/VT-PDMS20/CB6	80	
ER/VT-PDMS5/CB7	95	7
ER/VT-PDMS10/CB7	90	
ER/VT-PDMS15/CB7	85	
ER/VT-PDMS20/CB7	80	

The table continues from the previous page

Samples	**ER/VT-PDMS [wt.%]**	**CB [wt.%]**
ER/VT-PDMS10/CB8	95	8
ER/VT-PDMS10/CB8	90	
ER/VT-PDMS15/CB8	85	
ER/VT-PDMS20/CB8	80	
ER/VT-PDMS5/CB9	95	9
ER/VT-PDMS10/CB9	90	
ER/VT-PDMS15/CB9	85	
ER/VT-PDMS20/CB9	80	
ER/VT-PDMS5/CB10	95	10